

SKB

**TECHNICAL
REPORT**

92-06

**Characterization of nearfield rock –
A basis for comparison of repository
concepts**

Roland Pusch, Harald Hökmark

Clay Technology AB and Lund University of Technology

December 1991

SVENSK KÄRNBRÄNSLEHANTERING AB

SWEDISH NUCLEAR FUEL AND WASTE MANAGEMENT CO

BOX 5864 S-102 48 STOCKHOLM

TEL 08-665 28 00 TELEX 13108 SKB S

TELEFAX 08-661 57 19

CHARACTERIZATION OF NEARFIELD ROCK - A BASIS FOR
COMPARISON OF REPOSITORY CONCEPTS

Roland Pusch, Harald Hökmark

Clay Technology AB and Lund University of Technology

December 1991

This report concerns a study which was conducted for SKB. The conclusions and viewpoints presented in the report are those of the author(s) and do not necessarily coincide with those of the client.

Information on SKB technical reports from 1977-1978 (TR 121), 1979 (TR 79-28), 1980 (TR 80-26), 1981 (TR 81-17), 1982 (TR 82-28), 1983 (TR 83-77), 1984 (TR 85-01), 1985 (TR 85-20), 1986 (TR 86-31), 1987 (TR 87-33), 1988 (TR 88-32), 1989 (TR 89-40) and 1990 (TR 90-46) is available through SKB.

**Characterization of Nearfield Rock -
A Basis for Comparison of
Repository Concepts**

Lund, December 1991

**Roland Pusch
Harald Hökmark**

**Clay Technology AB and
Lund University of Technology**

CONTENTS

	Page
ABSTRACT	
SUMMARY	1
1 INTRODUCTION	3
2 STRUCTURE OF GRANITIC ROCK	3
2.1 <i>Discontinuities in crystalline rock</i>	3
2.1.1 Basic characterization principle	3
2.1.2 Origin of discontinuities	5
2.1.3 Formation of small-scale discontinuities	7
2.1.3.1 Fine rock structure	7
2.1.3.2 Fractures (joints)	10
2.2 <i>Complete discontinuity model of virgin, undisturbed and unweathered granitic rock</i>	11
2.2.1 General	11
2.2.2 1st order discontinuities	11
2.2.3 2nd order discontinuities	11
2.2.4 3rd order discontinuities	12
2.2.5 4th order discontinuities	13
2.2.6 5th order discontinuities	14
2.2.7 6th order discontinuities	16
2.2.8 7th order discontinuities	17
2.2.9 Summary	20
2.3 <i>Structural variations on a large scale</i>	21
2.3.1 Orientation of discontinuities	21
2.3.1.1 General	21
2.3.1.2 Strike	22
2.3.1.3 Dip	26
2.4 <i>Influence of mechanical disturbances on granite rock structure</i>	31
2.4.1 Introduction	31
2.4.2 Influence of excavation on rock structure	31
2.4.2.1 Blasting	31
2.4.2.2 Stress redistribution	36

2.4.2.3	Fragmentation	37
2.4.2.4	Thermomechanical effects	38
3	THE VDH CONCEPT	38
3.1	<i>General</i>	38
3.2	<i>Large-scale variation of virgin rock structure</i>	40
3.3	<i>Influence of disturbing components</i>	41
3.3.1	Load conditions	41
3.3.2	Mud penetrability	42
3.3.3	Influence of stress redistribution	44
3.3.3.1	Influence of existing, active fractures, wedge formation	44
3.3.3.2	Fracturing	50
3.3.3.3	Thermomechanical effects	52
3.4	<i>Structural model of VDH nearfield rock as influenced by disturbances</i>	54
3.4.1	Basic pattern	54
3.4.2	"Fine-rock structure"	54
3.4.3	Interaction with large structures	55
4	THE KBS3 CONCEPT	59
4.1	<i>General</i>	59
4.2	<i>Influence of excavation on the rock conductivity</i>	59
4.2.1	Blasting of tunnels	59
4.2.2	Fragmentation by drilling of deposition holes	60
4.2.3	Stress redistribution of rock around tunnels	60
4.2.3.1	Tunnels	60
4.2.3.2	Deposition holes	73
4.2.4	Influence of location and orientation of tunnels and deposition holes with respect to structural features	73
4.2.4.1	General	73
4.2.4.2	Tunnels	74
4.2.4.3	Deposition holes	90

4.3	<i>Thermomechanical effects</i>	92
4.3.1	General	92
4.3.2	Tunnels	92
4.3.3	Deposition holes	94
4.4	<i>Structural model of KBS3 nearfield rock as influenced by disturbances</i>	97
4.4.1	Basic pattern	97
4.4.2	"Fine-rock structure"	98
4.4.2.1	"Conservative" case	98
4.4.2.2	"Standard reference" case	102
4.4.2.3	Water-flow paths, channeling	103
4.4.2.4	Aspects on the applicability of the models	104
4.4.3	Interaction with large structures	105
5	THE VLH CONCEPT	107
5.1	<i>General</i>	107
5.2	<i>Influence of excavation on the rock conductivity</i>	107
5.2.1	Mechanical disturbances	107
5.2.1.1	General	107
5.2.1.2	Thrust	108
5.2.1.3	Fragmentation	109
5.2.2	Stress redistribution	110
5.2.2.1	General	110
5.2.2.2	Calculations	111
5.2.3	Internal pressure	118
5.2.4	Thermomechanical effects	120
5.2.5	Net effect of the influence of excava- tion, internal pressure and thermomechanics	124
5.3	<i>Structural model of VLH nearfield rock as influence by disturbances</i>	125
5.3.1	Basic pattern	125
5.3.2	"Fine-rock structure"	126
5.3.3	Interaction with large structures	128

6	DISCUSSION	129
6.1	<i>Scope</i>	129
6.2	<i>Summary of nearfield hydraulic properties</i>	130
6.3	<i>Interference with low-order structures</i>	131
6.4	<i>Rock stability aspects</i>	132
6.5	<i>Recommendations</i>	133
7	REFERENCES	135

ABSTRACT

The hydraulic conductivity of the nearfield rock controls the rate of wetting of adjacent buffer material, as well as the rate of degradation of its smectite content and of the transport of radionuclides from the buffer/rock interface.

Comparison of different repository concepts with respect to the function of the nearfield rock requires a common rock structure model, which is suggested in the report. Applying this model and 2D and 3D numerical calculations for evaluation of stress-induced structural changes, major differences between the three concepts VDH, KBS3 and VLH concerning the hydraulic conductivity of the nearfield have been identified. The importance of the orientation of the excavations turns out to be particularly obvious.

Further development of the rock structure model is concluded to offer ways of quantifying more accurately the damaging effects of blasting and TBM-drilling.

SUMMARY

The hydraulic conductivity of the nearfield rock is a determinant of the wetting rate of the canister-embedding clay and of the transport of radionuclides from leaching canisters. It is a function of the fracture network of the virgin rock and the changes that it undergoes due to "disturbing" effects caused by the excavation technique, i.e. blasting or drilling, by stress changes, and by heat caused by the radioactive decay. Although the virgin rock structure varies in a rock mass and is not the same in rock of different age and origin, one can define a basic, generalized structural pattern that is related to actually observed fracture networks and recorded bulk hydraulic conductivities, and which can be applied for evaluating changes in conductivity due to disturbances, particularly for comparing the effect on the nearfield of different repository concepts.

Such a rock structure model of "fractal"-type, i.e. with equally oriented substructures forming orthogonal networks, is proposed in the report. It comprises discontinuities of seven orders; 1st and 2nd order structures representing large-scale fracture zones with several hundred meter spacings, and 3rd order zones with about 50 m spacing. 4th order breaks with 5 m spacing represent discrete fractures of very long extension, while higher order breaks are not continuous, narrow fractures and fissures. The transport capacity of water-bearing structures is controlled by channels which are assumed to be regularly distributed and of standard size in the generalized structure model. Regular variation in structure orientation in the form of sinusoidal undulation is assumed to be characteristic of both steep and flat-lying structures.

Using this basic rock structure model and applying relevant 2D and 3D numerical calculations, the nearfield rock constitution and hydraulic properties have been evaluated for the three concepts VDH, KBS3, and VLH with respect to the influence of excavation damage and heating. The study shows that the nearfield of the lower part of KBS3 deposition holes exhibit minimum disturbance, while maximum disturbance is caused in the upper part of these holes. VLH and VDH are expected to give similar disturbance that is intermediate to that of the two KBS3 extremes. For all the concepts it was found that the orientation of the holes (and tunnels) with respect to the strike of major fractures is very essential for the axial conductivity. This matter needs further consideration but a tentative conclusion is that a very consider-

able reduction in axial flow is obtained if the deviation is larger than about 15° . A matter of considerable importance is that the combined effect of disturbances yields highly pervious zones at the crown and floor of KBS3 tunnels.

The study led to the conclusion that further development of the rock structure model would yield both a more realistic basic pattern of discontinuities, and a possibility to simulate the damaging effects of blasting and TBM drilling.

The rock in the immediate proximity of deposition holes containing clay-embedded HLW canisters, controls the transport of radionuclides that escape from the holes and is therefore of profound importance for the isolating function of the nearfield. The near-field rock inherits its structure and physical properties from the virgin rock but they are altered because of the stress and temperature changes that are caused by the excavation and heat dissipation from the radioactive waste. We will consider crystalline rock, primarily granite, in this study which aims at forming a basis of functional analyses of the integrated system of rock/buffer/canisters of the three basic concepts KBS3, VLH, and VDH.

2 STRUCTURE OF GRANITIC ROCK

2.1 *Discontinuities in crystalline rock*

2.1.1 **Basic characterization principle**

Fig.1 serves to show the major types of discontinuities that can easily be discerned when viewing a granitic rock mass. We identify (cf.1):

- * Fractures (joints) which are the most common structural features. They tend to form sets of mutually parallel units and are discontinuous in their own planes and extend over relatively short distances

- * Fracture zones, defined as zones of closely spaced and interconnected discrete breaks. They are tectonically induced disturbances of long extension and range in width from meters to tens of meters but need not be continuous throughout the rock mass

- * Shear zones can extend for kilometers and result from large-scale shear that usually has resulted in intense crushing of the rock. They are of similar width as fracture zones and often contain clay formed from attack of hydrothermal solutions

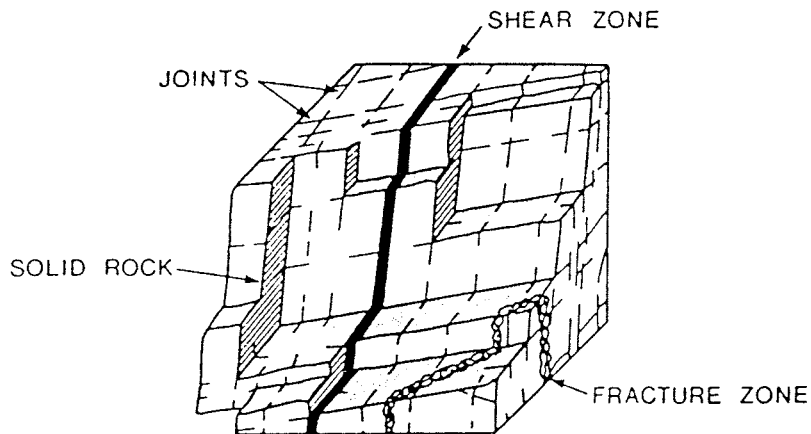


Fig.1 Major, directly discernible structural features in a granitic rock mass (After Gale and Witherspoon)

While these types of structural features are of wide use in characterizing rock masses, their origin is not fully known, nor is the associated structural impact on the virtually intact rock material that forms the rest of the mass. The present study aims at a complete description of the structure of granitic rock in an attempt to explain the influence of rock excavation and to give a concrete picture of its flow paths.

2.1.2 Origin of discontinuities

Discontinuities in rock formed from molten semi-solid magma stem from overstressing due to numerous processes, like thermal effects, subsidence, erosion and uplift, plutonic injections, metasomatic expansion, and plate tectonics due to magma convection. The build-up of high anisotropic, tectonically induced regional stresses caused creep in weak spots by which accumulation of strain-induced structural defects and weakening led to macroscopic failure of the Mohr/Coulomb-type (Fig.2). Megascopic slip zones oriented oblique to the major principal stress resulted from large strain, leaving less strongly affected rock material in between (Fig.3).

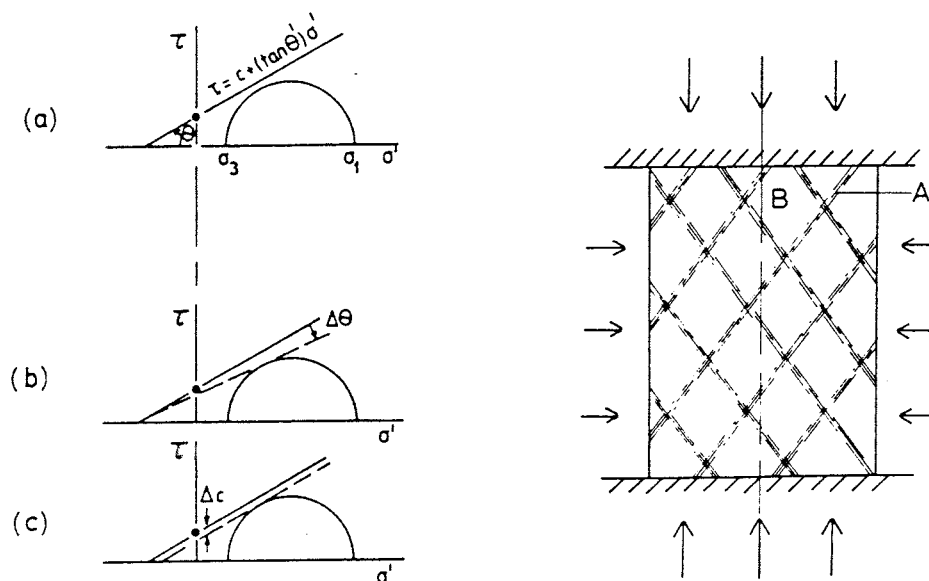


Fig.2 Left: Mohr/Coulomb stress circle with failure envelope. a) Stable conditions, b) Failure due to strain-induced drop in internal friction, c) Failure due to strain-induced drop in cohesion.

Right: Mohr/Coulomb failure mode at large strain in slip zones (A) with apparently intact material retained in between (B)

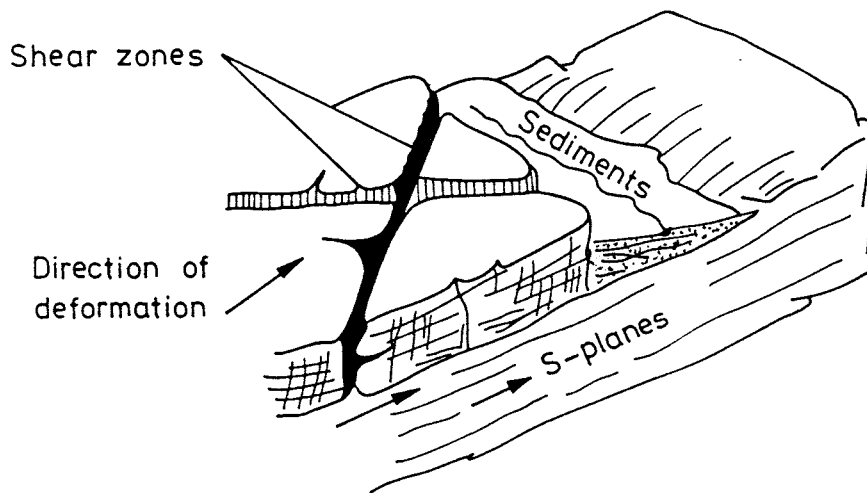
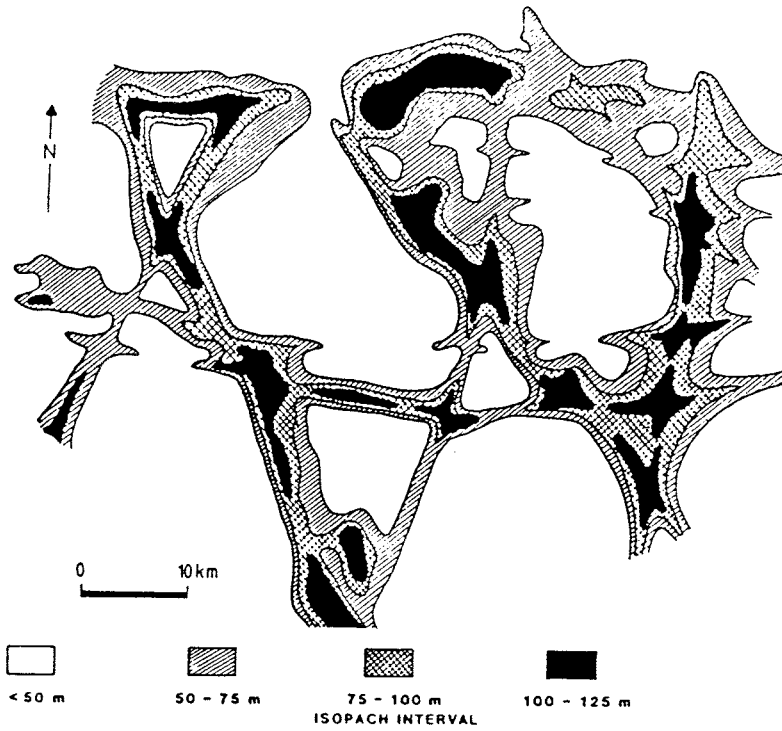


Fig.3 Large-scale deformation patterns. Upper: Anomalous thickness of upper Silurian carbonate deposits in salt dissolution cavities, the depth of which indicates the location of major fracture zones (After Sanford & Thompson).

Lower: Integrated post-crystallization large-scale deformation model (After Larsson)

While such large-scale structures appear to represent failure in the Mohr-Coulomb mode and are very significant for the performance and location of repositories, the discontinuities occurring on a smaller scale seem to have a different origin and nature. They are represented by breaks ranging from major shear zones to fractures (joints) and various embryotic features, which all stem from ancient or prevailing critical stresses. Fracture theory and basic rock mechanics offer the background of the generation and nature of these discontinuities as outlined below.

2.1.3 Formation of small-scale discontinuities

2.1.3.1 Fine rock structure

Plane discontinuities in the crystal matrix arise from tension and shear stresses that initiate fissures. Following Griffith, Gramberg, Paul & Gangal and many others, failure of brittle material like crystalline rock with microstructural defects in the form of elongated voids is initiated by fissure growth from the edges of critically oriented voids in the direction of the major principal stress when the deviator stress is sufficiently high (Fig.4).

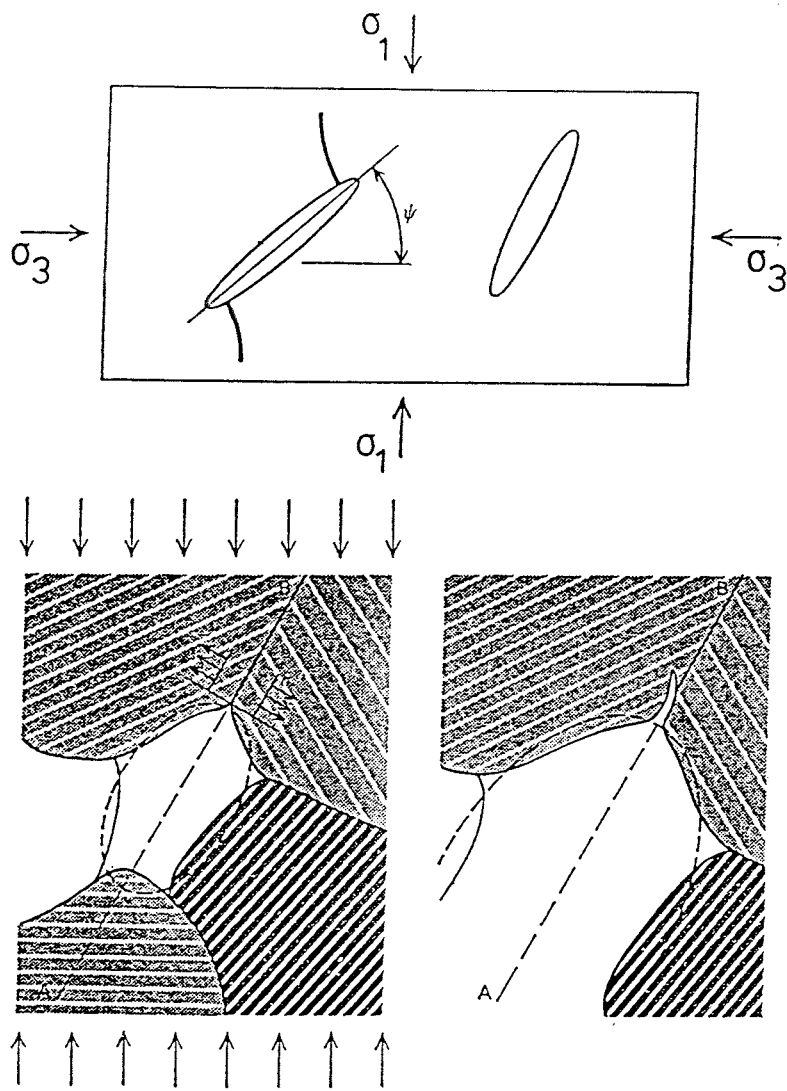


Fig.4 Fissure growth from elongated void. Natural voids exist where several crystals join, and where the crystal contacts are incomplete (After Gramberg)

Primary failure takes place when the stress path reaches the critical state (C in Fig.5) and fracture propagation yielding "secondary failure" occurs on further stress increase (D in Fig.5). This yields macroscopic failure in the form of axial cleavage at low lateral support (Fig.6).

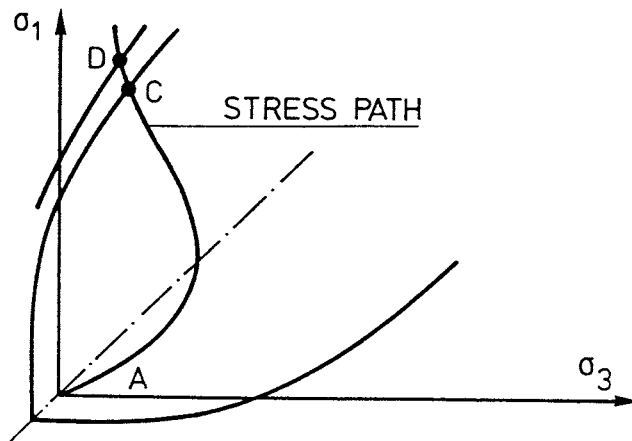
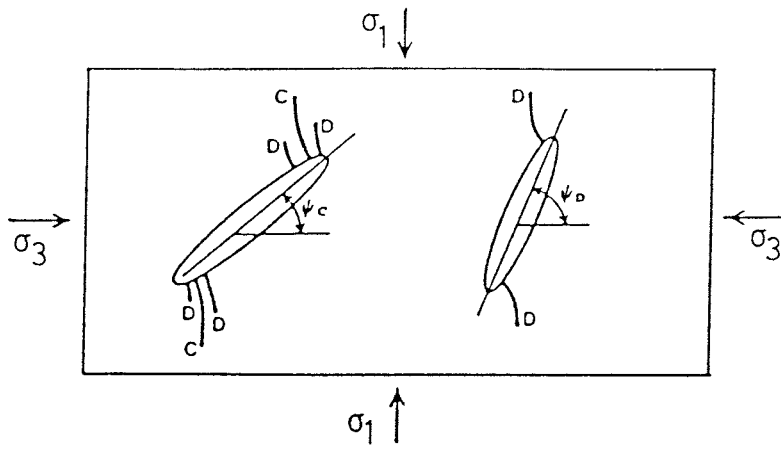


Fig.5 Primary (C) and secondary (D) failure with fissure propagation in the direction of the major principal stress according to Paul & Gangal

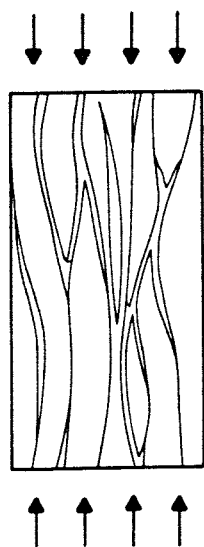


Fig.6 Axial cleavage

2.1.3.2 Fractures (joints)

In this report we will refer to fractures as being small-scale discontinuities that serve as joints between adjacent rock blocks and along which displacements have been very small or negligible. They are supposed to have originated from fissures and to have propagated mainly because of thermal effects and very slight tectonics. As suggested by Fig.1 and supported by numerous observations, fractures usually form more or less orthogonal patterns with a small number of erratic discontinuities. The distribution of fracture lengths, widths and apertures vary in a roughly log-normal fashion and it has become popular to depict the system of interacting fractures of varying size as a 3-dimensional pattern of ultrathin ellipsoids (Fig.7).

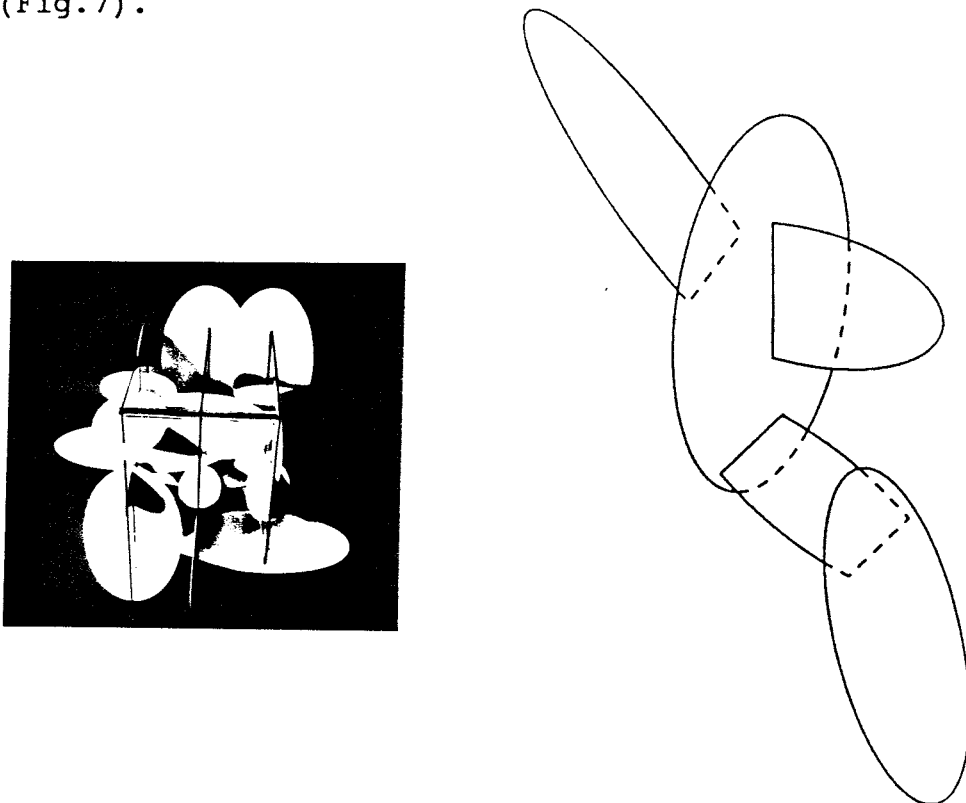


Fig.7 Schematic orthogonal-type fracture pattern. Left: Physical model with white discs simulating fractures.

Right: Random grouping of interacting fractures (After Dershowitz et al)

2.2 *Complete discontinuity model of virgin, undisturbed and unweathered granitic rock*

2.2.1 **General**

Various attempts have been made to integrate most of the described types of discontinuities into one model but it appears that they do not cover the fine rock structures, which actually control the properties of the nearfield rock by undergoing changes related to the quickly altered stress field due to excavation and thermal effects. The present report introduces a complete model, which is very much in line with common characterization schemes for large-scale structures* and which proposes fine rock structures that would result from the application of the cited rock failure theories and that can commonly be observed.

2.2.2 **1st order discontinuities**

The 1st order discontinuities correspond to regional fracture zones with a spacing of one to a few kilometers, ranging in width from meters to tens of meters. They have an extension of many tens of kilometers and usually form a more or less distorted orthogonal pattern. They contain closely spaced and interconnected breaks, yielding an average hydraulic conductivity of around 10^{-6} m/s. In the presently applied version of the model the spacing of the usually steeply oriented zones is set at 3 km.

2.2.3 **2nd order discontinuities**

The 2nd order discontinuities represent local, usually steeply oriented fracture zones that are common-

* Pers. communic. Kaj Ahlbom, Conterra AB

ly seen at 100 to several hundred meters intervals. They may extend for several thousand meters and have a width and character and an organization that are similar to those of the 1st order discontinuities and represent a hydraulic conductivity of around 10^{-7} m/s. In the present version of the model the spacing is set at 500 m.

2.2.4 3rd order discontinuities

The 3rd order discontinuities, which serve as major transmissive fracture zones in repositories because of their frequency and conductivity, may extend for several hundred meters in their own plane. They often form an orthogonal-type subsystem conformous to the large-scale structures and usually consist of several discrete, not always interacting breaks. Their width is typically a few decimeters, and their spacing is 50 to 150 m, the lower figure being used in the presently applied version of the model. The average hydraulic conductivity is set at 10^{-8} m/s. A practical example of this type of structure is the so-called J-zone which supplies the eastern arm of the 3D cross in Stripa with water (Fig.8).

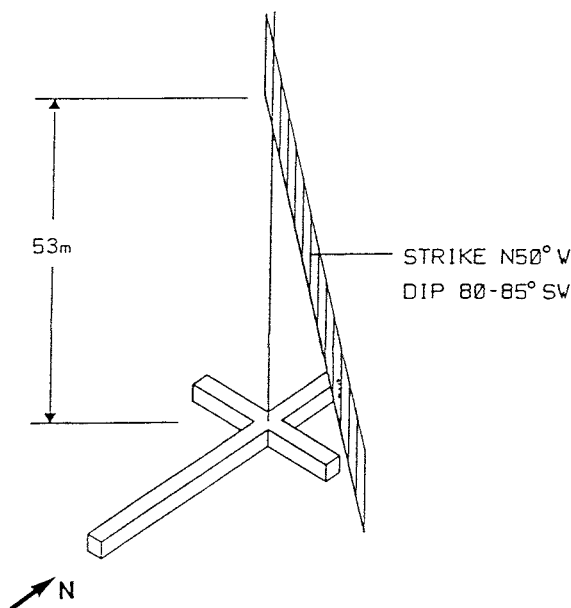


Fig.8 The J-zone in the 3D Cross area in the Stripa mine

The 4th order discontinuities correspond to the hydraulically active members of the basic fracture pattern. Literature offers a huge supply of information concerning such fractures, and although there are different views respecting their spacing and character there seems to be some consensus. Putting together the information from extensive studies of granitic rock at SFR, Finnsjön and Stripa, it is concluded that the idea of virtually orthogonal systems of water-bearing fractures, being responsible for the bulk conductivity of granitic rock, applies in principle. It is also concluded that the spacing of the fractures forming these sets is relatively large, i.e. on the order of 2 - 7 m, which is also their persistence. Looking closer at the connectivity of the fractures it seems reasonable to apply an average spacing of interacting members of the network in *virgin* granite of around 5 m, which is therefore applied in the present version of the model.

A very important fact is that the water-transmissive fractures in granitic rock do not act as plane parallel slots, but let water through in channels. It is believed that the permeable parts of conductive fractures are archipelago-like, with channels of varying width and aperture, and it is assumed that the most conductive passages consist of channels formed where fractures intersect. Taking these channels as being passages that control the bulk hydraulic conductivity of virgin, undisturbed rock, the model implies that the water flows through a regular network of continuous channels formed at the intersection of the orthogonal fracture system in such rock. The validity of this model can be estimated by applying typical cross sections of channels, a reasonable average shape being a rectangular shape with 100 μm aperture and 1 cm width. Applying this to rock characterized by only 4th order discontinuities one finds that a 25

m² section holds only one channel yielding an average bulk hydraulic conductivity of around 10^{-11} m/s, which applies fairly well to the Stripa rock. Ongoing studies in Stripa indicate that the actual shape of channel cross sections can be generalized to have a rhomboidal shape with a width of 10-100 mm and a maximum aperture of 50-100 μ m. This yields a rather wide range of bulk conductivities, approximately corresponding to the interval 10^{-11} to 10^{-10} m/s.

Fig.9 illustrates an orthogonal pattern of 4th order fractures containing a KBS3 deposition hole. Fractures or fracture changes induced by stress or thermal effects are not considered.

2.2.6 5th order discontinuities

In the extensive fracture surveys that were conducted at SFR, Finnsjön and Stripa, it was found that one can define a substructure of 5th order discontinuities, that is largely conformous to the orthogonal-type network of fractures that constitute the 4th order discontinuities. The fractures forming the 5th order breaks are not hydraulically active in undisturbed, virgin granite since they are closed either by creep or precipitations or by "mechanico/chemical" processes (2). The average spacing of the 5th order discontinuities seems to be around 1/10 of that of the 4th order breaks and the present version of the model therefore specifies a spacing of the first-mentioned ones of 0.5 m. Their tensile and shear strength is estimated to be low, which suggests that they easily become activated and let water through when the stress is significantly altered by excavation or exposure to non-uniform heating. This is concluded to be due to dilatancy and to breakage, i.e. fissuring of the fracture coatings, on shearing. Fig.10 illustrates the general character of 5th order discontinuities.

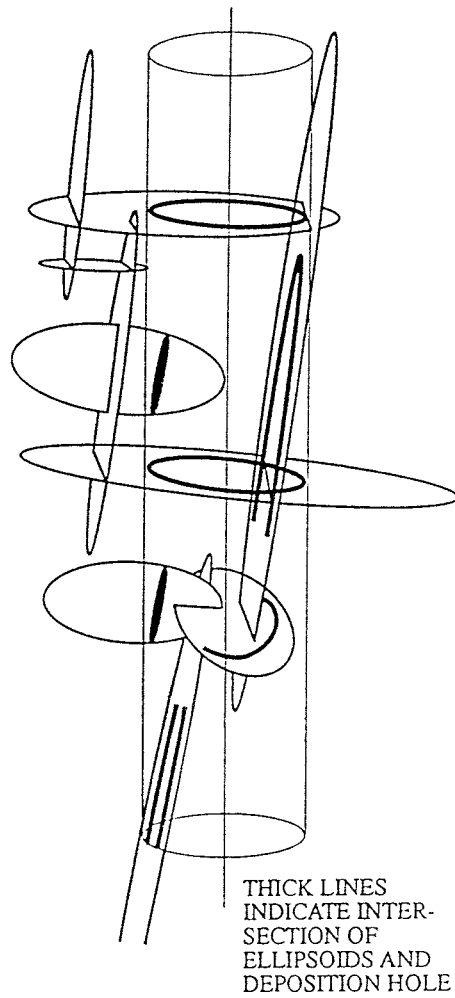
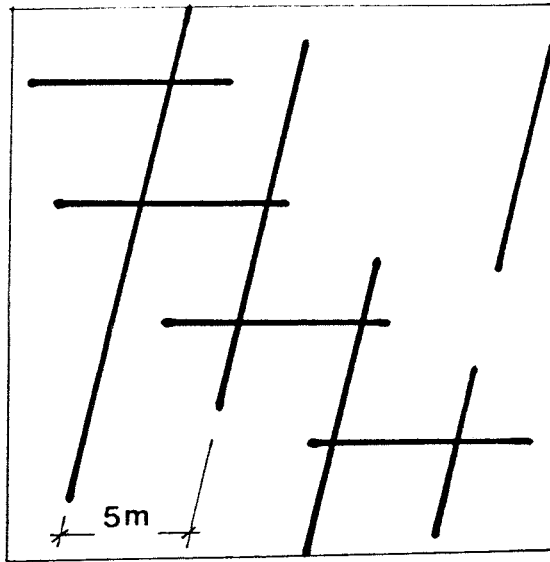


Fig.9 4th order discontinuities. Upper: 2D view of nearly orthogonal fracture system.

Lower: Application to KBS3 deposition hole

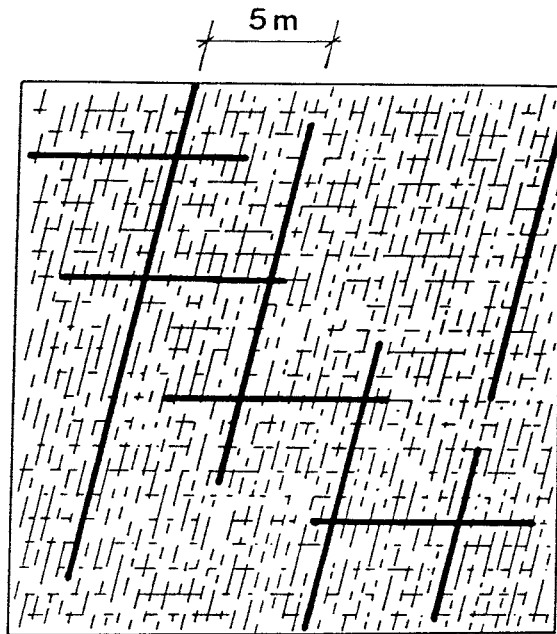


Fig.10 5th order discontinuities integrated in a 4th order break network

2.2.7 6th order discontinuities

The 6th order discontinuities are naturally occurring fissures representing embryotic breaks. They are assumed to have been generated by the same stress fields that created the 4th and 5th order discontinuities and are therefore more or less aligned with these fractures. They represent potential planes of weakness and are wellknown to stonecutters who make use of them in the preparation of cubical paving-stones from virtually isotropic granite.

Fig.11 schematically illustrates such features grown from Griffith cracks. In virgin, undisturbed granitic rock they have the form of plane fissures with a spacing and extension of 0.01 - 0.1 m and an aperture of 1 - 10 μm , yielding an average porosity and hydraulic conductivity of the rock matrix of 0.2 - 0.5 %, and 10^{-12} to 10^{-10} m/s, respectively. In the generalized model the 6th order discontinuities are taken to have the form of orthogonal systems of plane fissures with a spacing of 0.05 m and with two crossed hydraulically active 1 cm wide channels with an aperture of 1 μm at each fissure intersection. This yields an average hydraulic conductivity of larger blocks of virtually fracture-free rock of around 10^{-12} m/s.

2.2.8 7th order discontinuities

The smallest discontinuities of importance for the hydraulic conductivity of virtually homogeneous rock is concluded to be interconnected voids located at the junction points of several adjacent crystals, the interconnections having the form of incomplete crystal contacts. Fig.12 illustrates various sorts of microscopic "Griffith"-type discontinuities of which the largest ones tend to merge into more or less aligned 6th order discontinuities, while the smallest ones, forming embryotic fissures, can have any direction.

The 7th order discontinuities do not make up for the porosity of the crystal matrix but they control its hydraulic conductivity, which is on the order of 10^{-13} m/s to 10^{-12} m/s. In the present form of the model the 7th order breaks have the form of channels with 0.1 - 1 μm aperture and 100 μm width (Fig.13).

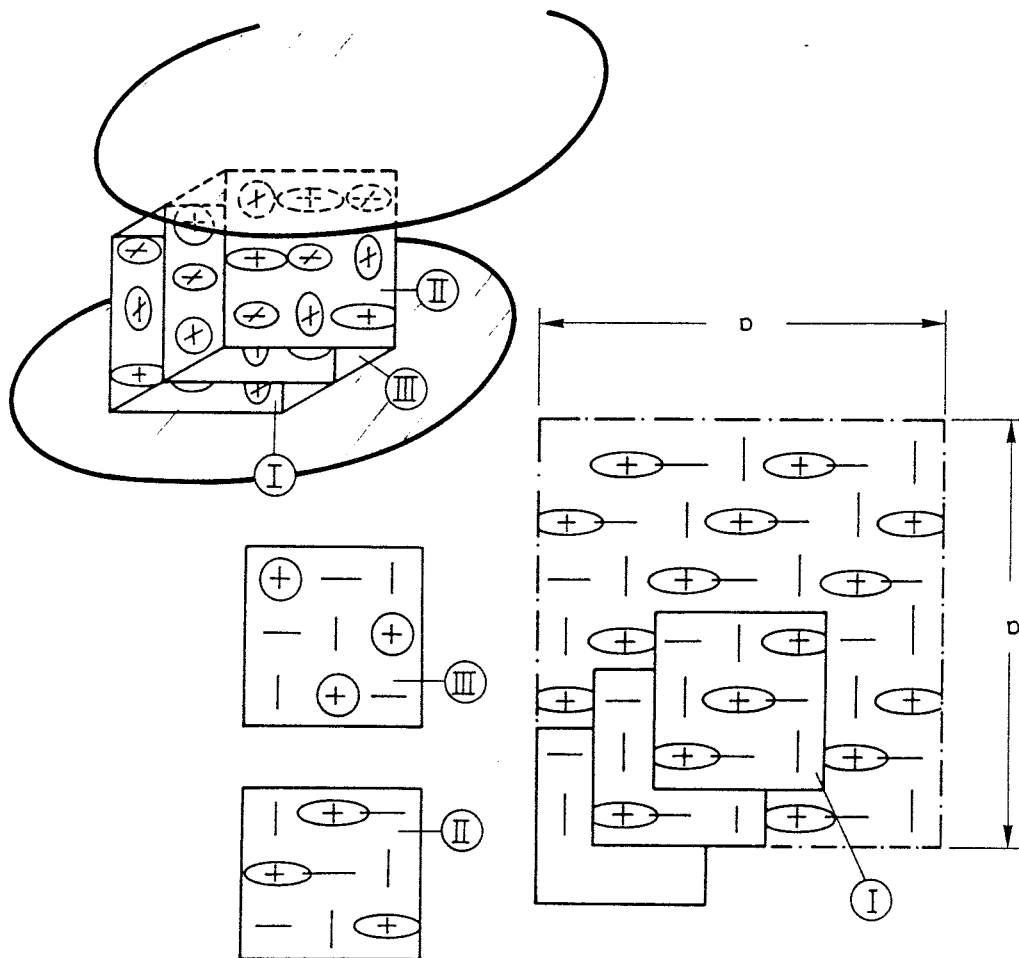


Fig.11 Fine rock structure. Upper picture shows sections of cubical element located between fissures (large ellipsoids) that have grown from activated "Griffith"-type cracks (small ellipsoids). Circles denote unactivated cracks

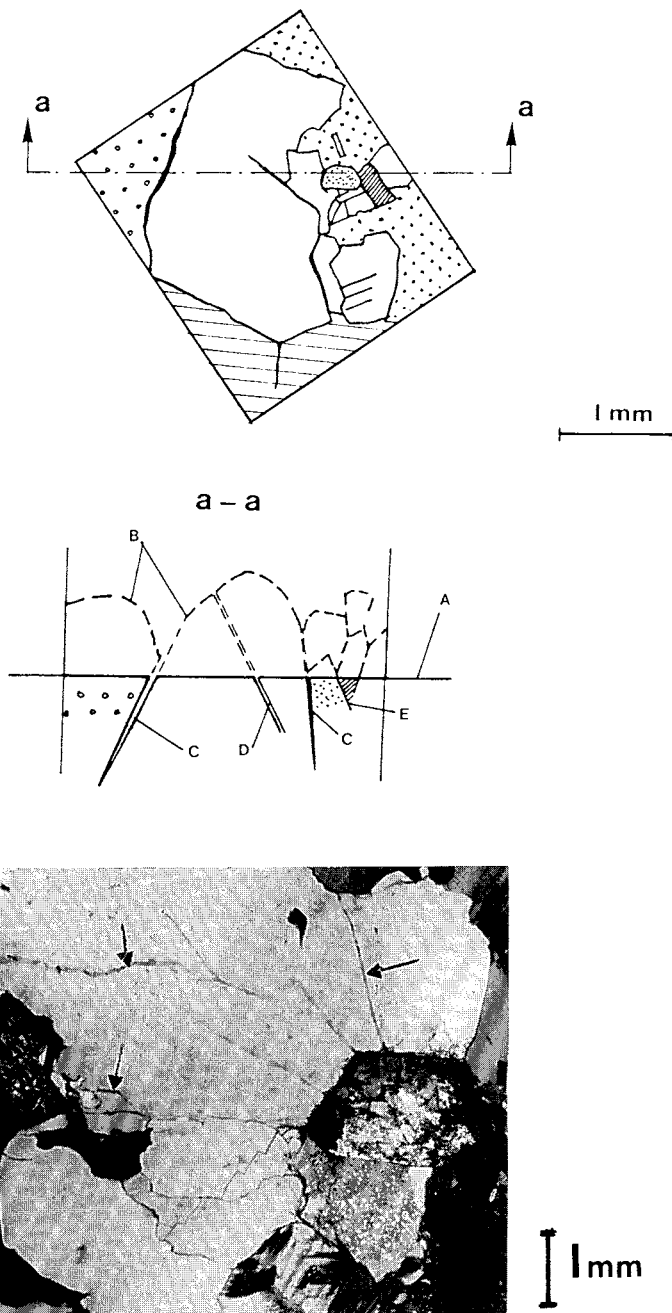


Fig.12 Incomplete crystals contacts and embryotic fissures representing 7th order breaks. Upper: Schematic microstructure as viewed in the microscope.

Central: Assumed actual structure before sectioning

Lower: Micrograph with arrows indicating fine fissures and incomplete crystal contacts

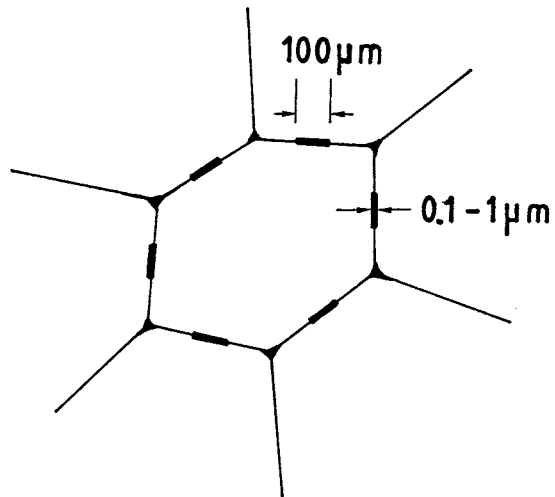


Fig.13 7th order discontinuities of the rock structure model

2.2.9 Summary

Putting together the spectrum of specified discontinuities we arrive at the condensed summary in Table 1, which also gives tentative information on their groutability.

Table 1 Structural features of virgin, unweathered granitic rock

Feature	Spacing m	Bulk conduct. m/s	Groutab.
1st order	3000	10^{-6}	Very good
2nd order	500	10^{-7}	Good
3rd order	50	10^{-8}	Possible
4th order	5	10^{-11}	None
5th order (closed)	0.5	0	None
6th order	0.05	10^{-12}	None
7th order	Any	10^{-13}	None

2.3 Structural variations on a large scale

2.3.1 Orientation of discontinuities

2.3.1.1 General

For nearfield considerations, 4th and higher order discontinuities are of major importance and we will confine ourselves to discuss such features. It is felt that the actual spread in spacing and mutual orientation of neighboring discontinuities of one and the same order is of less importance than large-scale

variations in orientation of the major sets of fractures. Thus, if one aims at orienting a straight deposition tunnel at a certain angle to one of the major fracture sets, which helps to reduce axial flow along it, it is possible only if this set has a constant strike and dip.

An attempt to identify large-scale variations in the horizontal plane as well as vertically has been made in conjunction with a general characterization of the Stripa granite as observed by inspecting blasted tunnels* and large boreholes. We will return to this characterization later and presently confine ourselves to describe large scale variations in strike and dip.

2.3.1.2 Strike

Several studies of the strike of major discontinuities have been made by various investigators, the most comprehensive ones being conducted by LBL** and reported in a number of papers. A major set of 4th and 3rd order (differently termed by LBL) fractures have been claimed to strike W to NW (dipping steeply to N or S) and a second one to strike N to NE (dipping 50-60° to W), i.e. approximately the same general pattern found in many other parts of Sweden.

The presently made determinations were made at 8 sites termed A,B,C,D,E,F,G and H located as indicated in Fig.14, i.e. along an approximately NE oriented line at 345 to 390 m depth. Table 2 gives a condensed description of the sites.

* "Tunnel" and "drift" are used interchangeably here

** Lawrence Berkeley Laboratory (Stripa field tests)

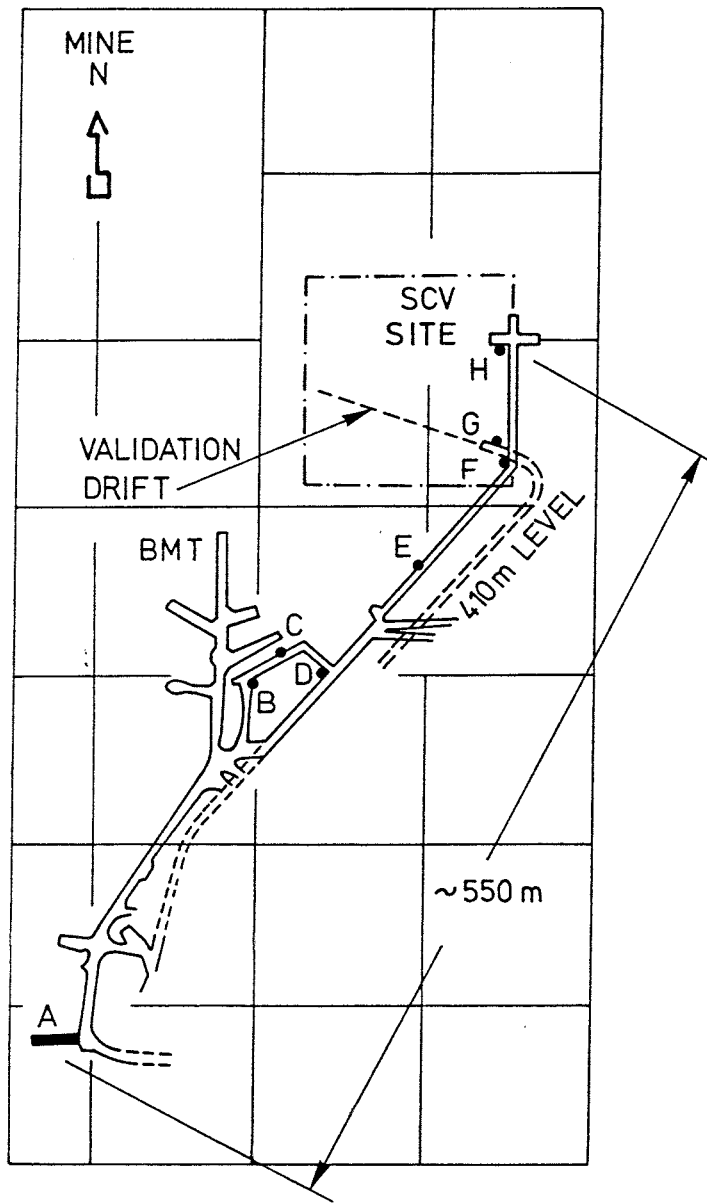


Fig.14 Location of sites for rock characterization in Stripa

Table 2 Sites selected for measurement of strike of 4th and 5th order discontinuities

Letter	Site	Depth (z)
A	Tunnel plug drift (HP)	380
B	Addit to Extensometer drift	365
C	Northern wall of Ext. drift	365
D	Staircase to SGU drift	360
E	Addit to 3D area	360
F	Long arm 3D area	360
G	390-410 m drift	390
H	Western arm of 3D area	360

The outcome of the measurements is given in Fig.15 which demonstrates that there is quite a variation in strike along the about 550 m long distance.

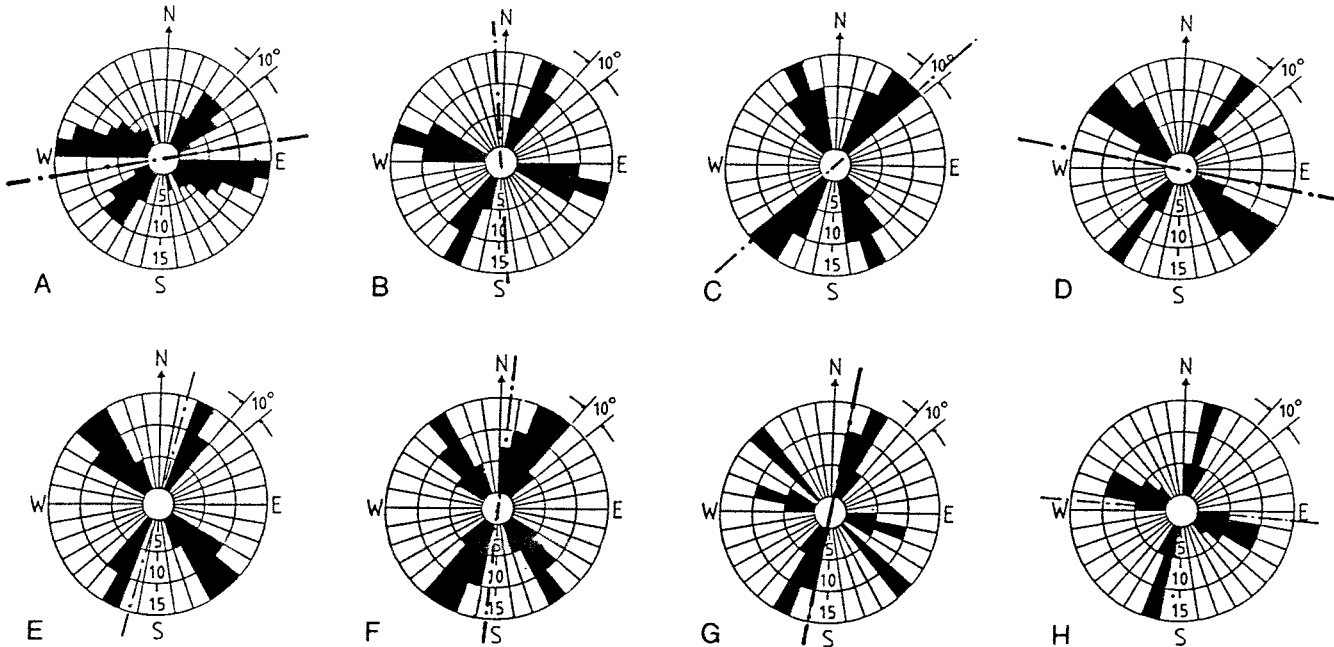


Fig.15 Compilation of strike recordings at sites A-H

A most interesting fact is that the variation in strike may not be at random. Thus, generalizing the patterns to represent one NW/SE oriented fracture set and one NE/SW directed one, and plotting the deviation (α) of the strike from the N-direction, the data tend to indicate that the two sets exhibit an undulating, sinusoidal-type pattern that may possibly be related to regional tectonics or variation in major stress fields (Fig.16). Assuming this pattern to be repetitive over larger distances it can be generalized as shown in Fig.17, from which one reads that the wavelength is around 500 m, i.e. about the spacing of the 2nd order discontinuities.

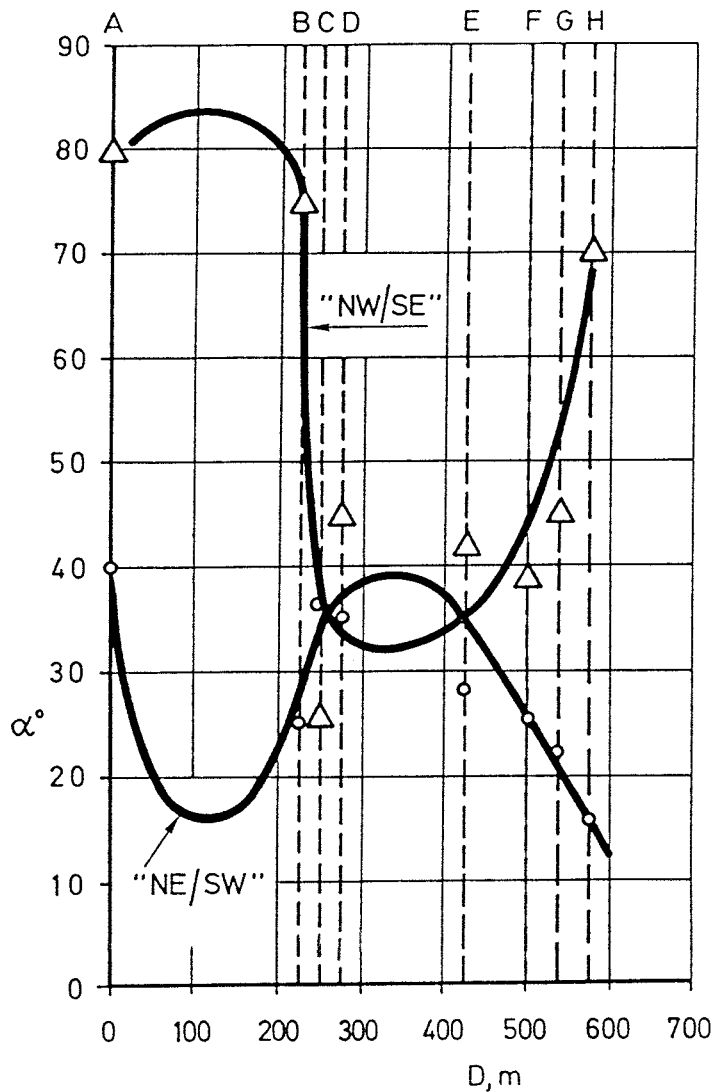


Fig.16 Deviation from N of major 4th order breaks

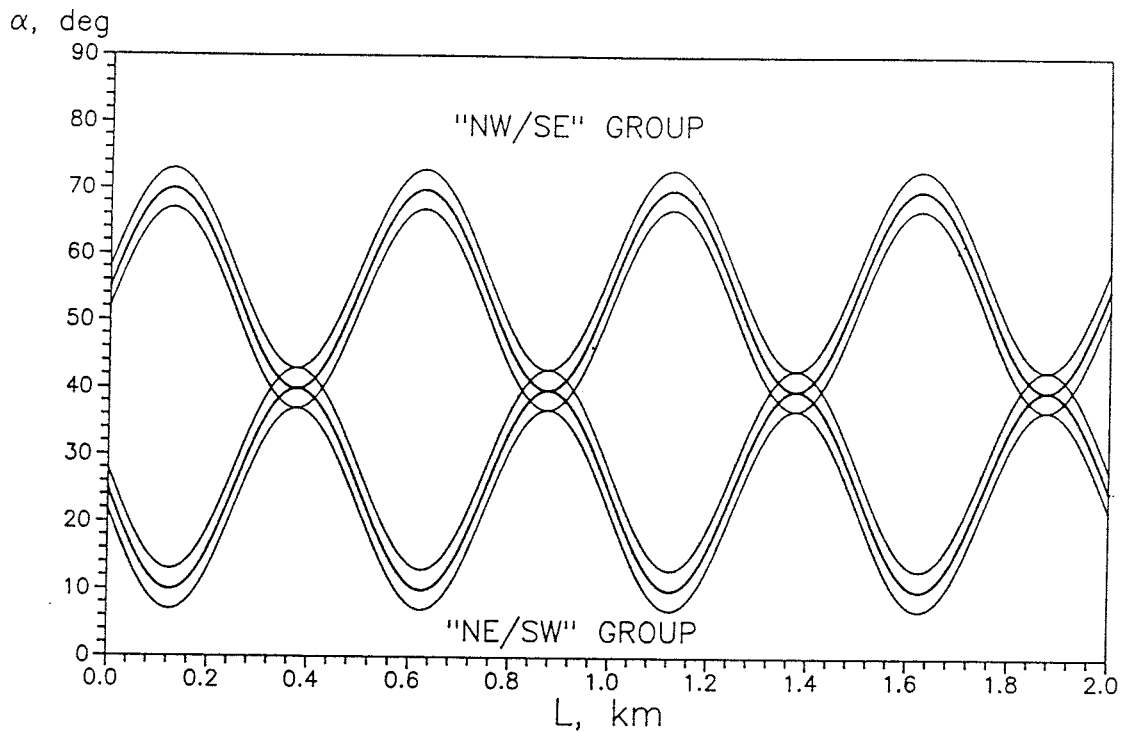


Fig.17 Generalized undulation pattern of major 4th order breaks. α shows deviation from N

The pattern in Fig.17 implies that "true" orthogonal, cubical symmetry of the fracture hierarchy is valid only over short distances. A phase shift by 250 m would yield a perfectly orthogonal system.

2.3.1.3 Dip

Large-scale variations in dip is particularly important to the nearfield rock of repositories of the VDH type. As in the case of strike a number of studies have been made and they tend to indicate that while fractures striking NW are usually very steeply oriented and dip towards N or S, NE fractures are not that steep. The presently conducted survey was made at the aforementioned 8 sites at 345 to 390 m depth, the result being shown in Fig.18. Only fractures with a steeper dip than 60° were included and for these one

finds that there are irregular, rather small variations in the range of no more than $\pm 15^\circ$ from the average inclination.

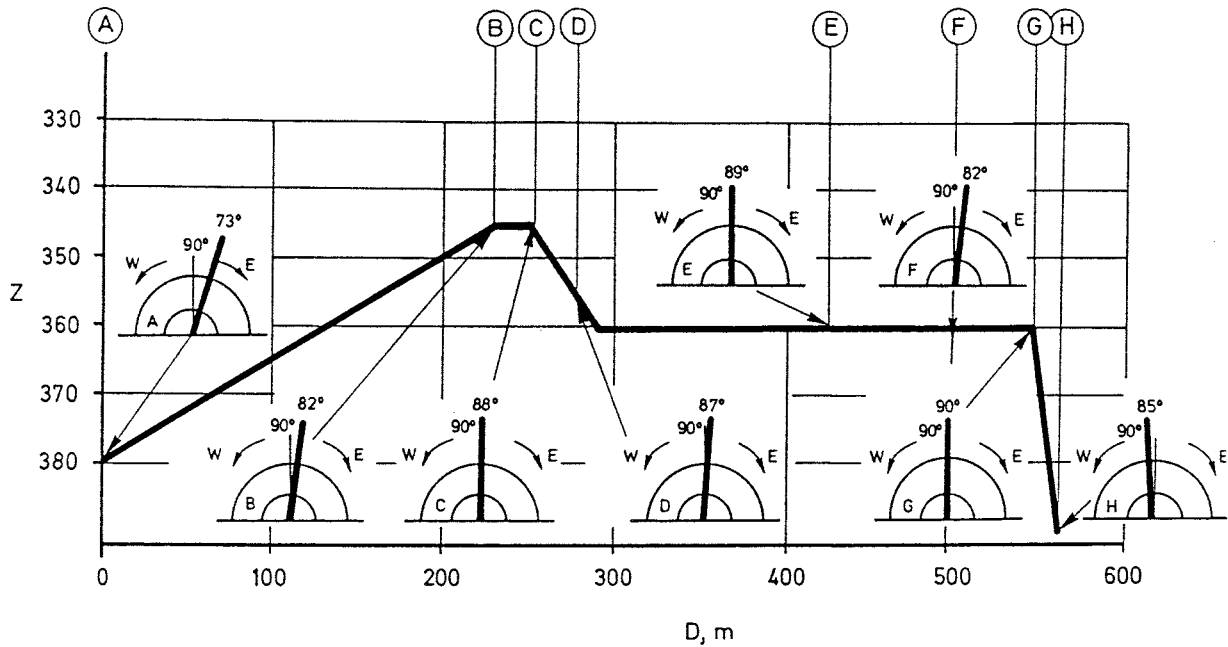


Fig.18 Schematic plot of average dip of 4th order fractures steeper than 60° in Stripa

Information on variations in dip along the vertical direction is not readily available but one valuable data source is LBL:s detailed plotting of fractures of the DBhV1 hole extending from 410 to 881 m depth. Considering only the population of fractures that have a dip steeper than 75° , one finds that there is a fairly regular variation in the frequency of intersection with the borehole. Thus, the number of intersected steeply oriented fractures tends to vary rather regularly along the hole in the fashion indicated in Fig.19, i.e from 0 to 1 per 10 m axial length to around 3 to 4 per 10 m length (Fig.19), some of the fractures being concluded to belong to the 5th order discontinuities.

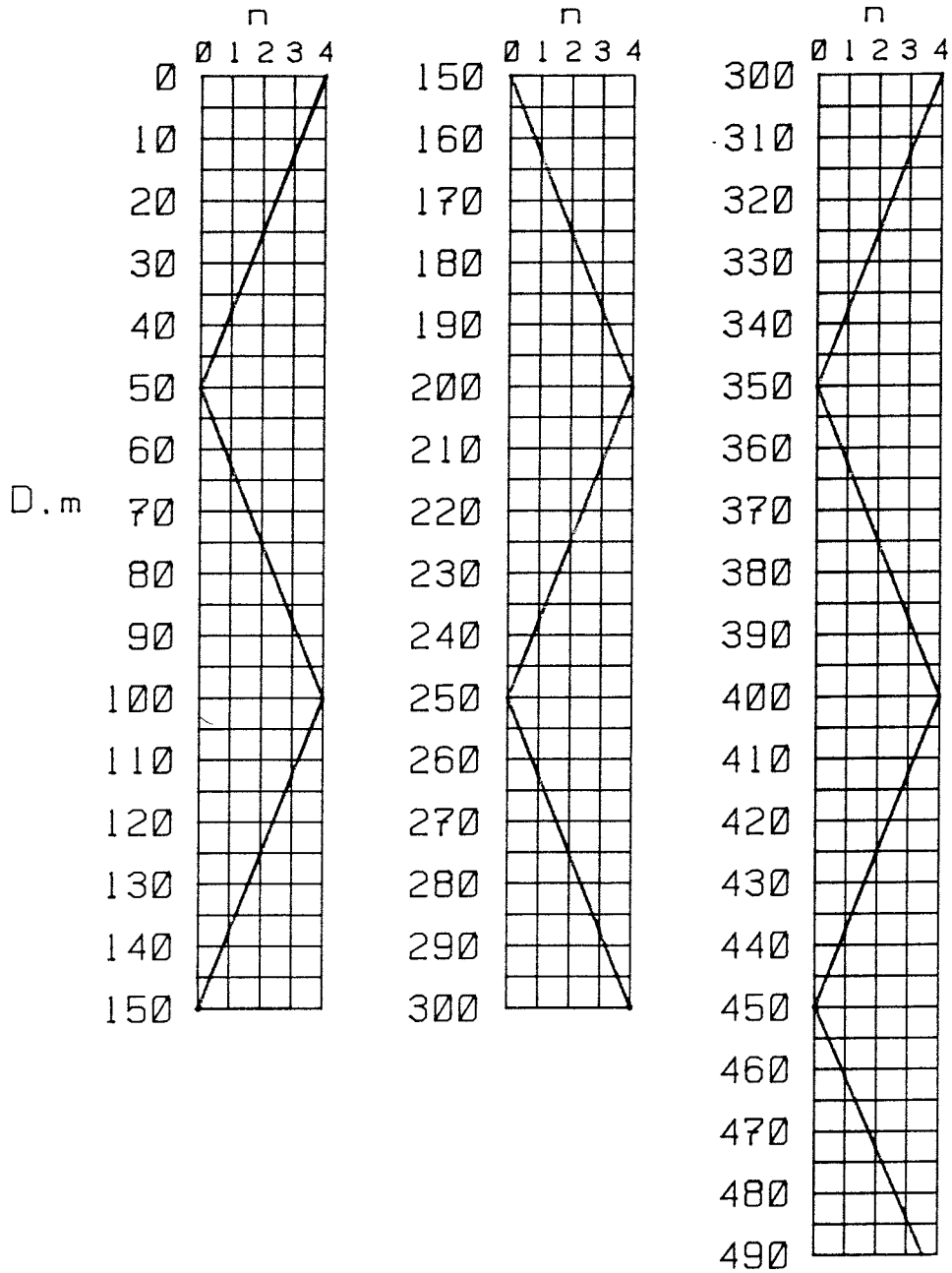


Fig.19 Schematic variation in intersected fractures dipping more than 75° along the 470 m long borehole DBhV1 drilled vertically

The variation in frequency of fracture intersection over the 470 m long borehole DBhV1 depicted in Fig.19 can be interpreted as a regular sinusoidal undulation of the form indicated in Fig.20, which also shows a generalized 2D projection of the same feature. The wavelength appears to be around 200 m and the minimum radius of curvature about 90 m, and one finds that approximately 20 m long parts with a spacing of about 100 m are oriented almost parallel to the hole, i.e. deviating less than 5° from the borehole axis. We will see later that these parts may be critical to the wall stability at certain fracture configurations.

The fact that two of the common three major fracture sets are usually steeply oriented in granite, makes it reasonable to assume that all vertically or very steeply drilled holes are characteristically intersected by fractures of 4th and 5th orders of nearly the same orientation and frequency as found in the present study. For holes drilled at an angle of 30 to 60° to the horizontal the frequency of fractures that form long wedges like the one indicated in Fig.20, is probably considerably lower.

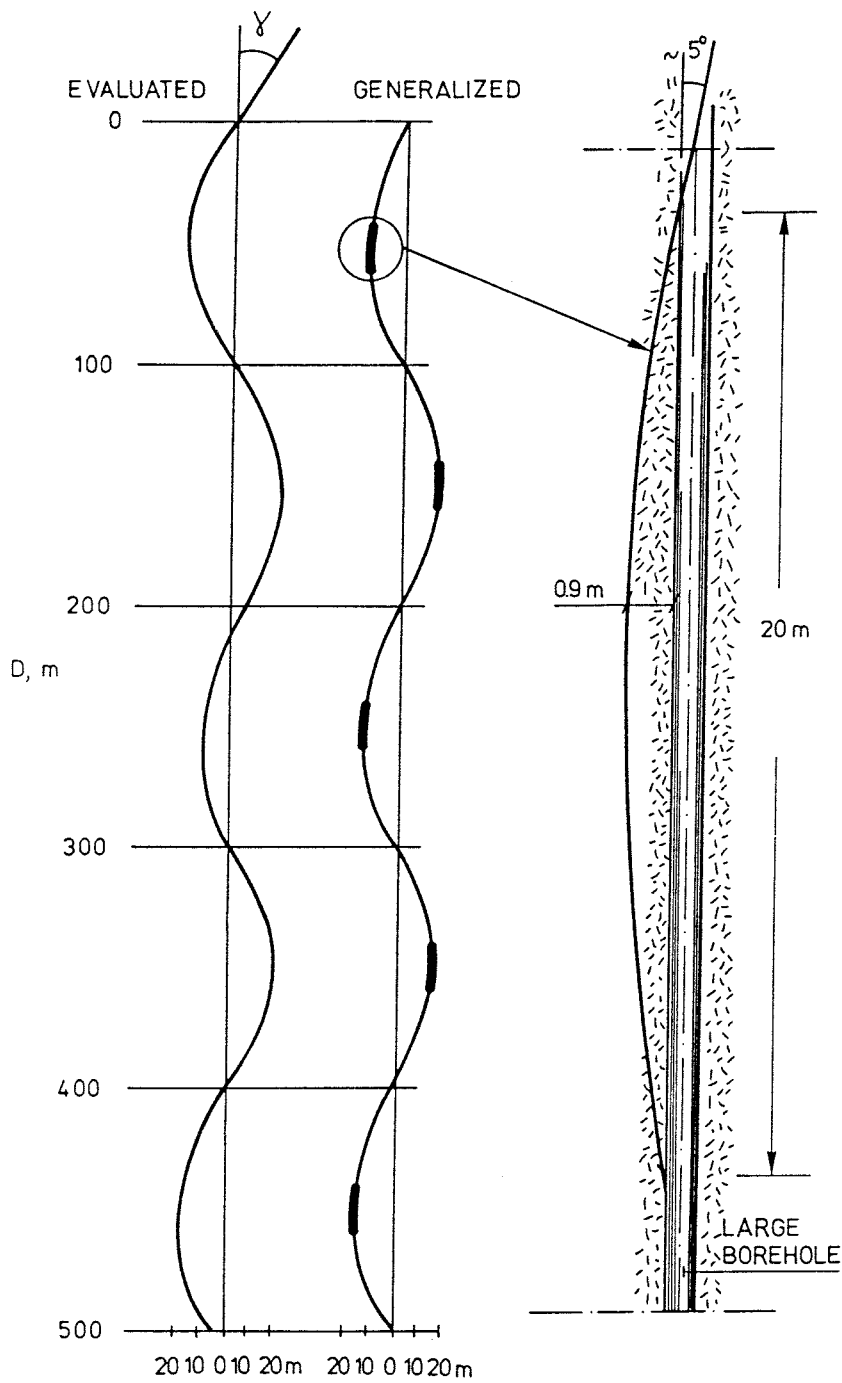


Fig.20 Model of presumed regular variation of the orientation of steep fractures with respect to the vertical direction. Right picture shows an example of possible wedge formation at the steepest part of fractures that intersect a vertical borehole

2.4 *Influence of mechanical disturbances on granite rock structure*

2.4.1 **Introduction**

We will be concerned here with effects of stress changes on the aperture and connectivity of hydraulically active discontinuities in granite, focussing primarily on the nearfield of deposition tunnels and boreholes of the three concepts KBS3, VDH and VLH. The study will comprise a condensed summary of the general influence of excavation techniques followed by an application to a generalized rock structure model derived from Stripa rock structure data.

2.4.2 **Influence of excavation on rock structure**

2.4.2.1 **Blasting**

Blasting yields very high gas overpressures of short duration and this breaks up rock by brittle failure. Fractures are formed extending radially from charged boreholes and prismatic blocks are loosened due to the tensile stresses that are set up by the reflection of the shock wave in the presence of free surfaces. The extension of radially oriented blasting-induced fractures can be roughly estimated by assuming that their volume is equal to the reduction in volume of the adjacent rock by compression, and such calculations yield penetration depths of a few decimeters if careful blasting is employed. Empirical rules based on subjective estimates of the structure-disturbing effects of blasting give a measure of the blasting-induced zone of disturbance that is related to the amount of explosives and that fits the results of the aforementioned theoretical derivation (2).

In general, fractures are generated in three ways (Fig.21 and 22):

- * Expansion and propagation of natural fractures that are intersected by charged holes
- * Formation of one or a few planar, radially oriented fractures along about 50 % of the length of charged holes
- * Formation of approximately spherical, richly fractured zones around the tip of the charged holes due to the extra "bottom" charge that has to be applied

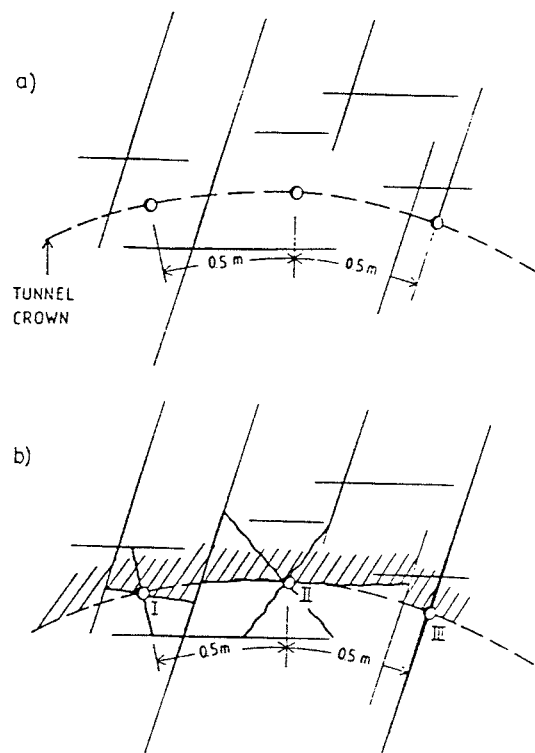


Fig.21 Schematic picture of influence of blasting. Upper: Natural pattern of 4th and 5th order fractures in virgin rock.

Lower: Neoformation of fractures and change of natural fractures

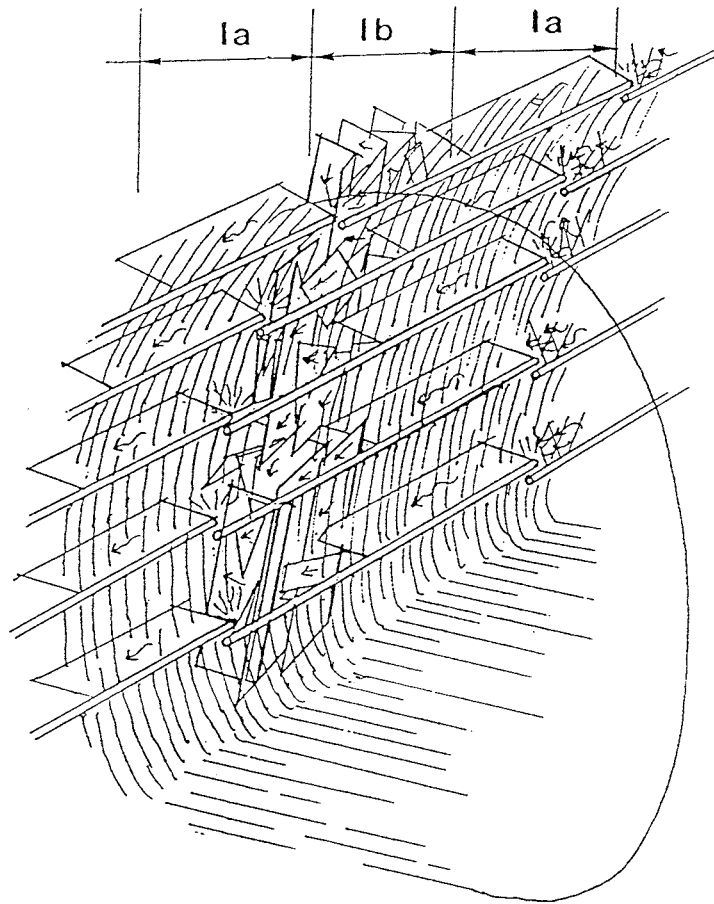


Fig.22 Blasting-induced defects. Upper: Zones of regular sets of plane fractures extending radially from the blast-holes (Ia). Strongly fractured zone at the tip of the holes.

Lower: Typical fracture of Ia type

Assuming an instant gas pressure of 100 MPa and a modulus of compression of 5×10^4 MPa, which are both on the actual order of magnitude, one finds that natural fractures of the III-type in Fig.21 get widened by at least 1 mm and under the primary stress conditions that usually prevail in Sweden, i.e. with a considerably higher horizontal than vertical stress, the low hoop stresses in the walls could make a large part of the expansion permanent. Rock debris enters the latter type of fractures and shear associated with the momentary expansion prevent such fractures from being effectively closed.

Radially oriented new fractures (I and II in Fig.21) extending from the blast-holes as represented by the rectangular, planes in zones Ia in Fig.22 are known to be very common. In the BMT drift in Stripa, where the average spacing of the contour holes was about 0.6 m and the charge being 0.3 kg/m Gurit over their entire length and using also 100 g Dynamex as "starter" at the tip of these holes, these blasting-induced fractures could be traced to about 1.5 m from the tips of the 3.6 m long holes, and core-drilling showed that they extended to about 0.3 m from the periphery. This means that these sets of fractures do not form continuous passages of uniform aperture along the entire drift. Hence, if the 2 m long intermediate Ib sections, separating the ones with regular fracture sets, were not affected at all, the net axial conductivity of the shallow rock would not be very different from that of the virgin rock. However, the high frequency of fractures close to the periphery over the entire wall area, as concluded from core-drilling and discussed in detail in conjunction with the analysis of the KBS3 concept, and the very rich fracturing around the tips of the blast-holes, suggest that the axial conductivity of the Ia zones may control the net axial conductivity of the entire blasting-affected nearfield rock. This would imply

the conductivity values given in Table 3, assuming the average hydraulic aperture to be 10-100 μm , the width 300 mm, and the spacing 0.5 m.

Table 3 Theoretical conductivity of Ia-zones in the nearfield of tunnels produced by careful blasting of the type used in Stripa BMT

Hydraulic aperture μm	Average bulk conductivity m/s
10	1.6×10^{-9}
20	1.3×10^{-8}
50	2.0×10^{-7}
100	1.6×10^{-6}

Experience shows that sufficient fragmentation for reasonably easy excavation of blasted tunnels requires extra charge in the blast-holes in the floor and although there is no defined model for the resulting fracturing, which is more extensive than in the walls and roof, it is commonly estimated to cause an average hydraulic conductivity that is 100 times that of the virgin rock down 1.5 m depth.

In summary, it is concluded that blasting-induced fractures may yield a very significant increase in the permeability of the rock, which, in combination with permanent expansion of natural fractures, may yield a net axial hydraulic conductivity of the first few decimeters of the rock adjacent to the periphery of 10^{-9} to 10^{-6} m/s when the conductivity of the virgin rock is about 10^{-10} m/s. The effect is particularly obvious in the floor where it extends deeper, and in the walls of tunnels located in primary stress fields of the usual type in Sweden, i.e. with significantly higher stresses in the horizontal than in the vertical direction (3,4).

2.4.2.2 Stress redistribution

One can distinguish between two major types of stress influence on nearfield rock that affect the porosity and thereby its hydraulic conductivity. One of them is the strain-induced change in aperture and extension of the hydraulically active part that will take place in existing, natural fractures, mainly of the 4th order type, while the other has the form of creation of new fractures and activation of pre-existing, sealed ones (5th order discontinuities).

I. Influence on existing, active fractures

Long-extending, intersecting fractures that have a strike that is not very different from that of a closely located tunnel or borehole may form wedges, which can be unstable if they are located in the roof of subhorizontally oriented excavations or in the walls of steeply oriented shafts or boreholes (cf. Fig.20). Even if they are maintained in position, the joints with the surrounding rock mass will undergo widening in conjunction with a tendency of the wedge to move towards the opening by which the axial hydraulic conductivity will be enhanced. The same effect appears where single, long-extending fractures intersect openings at a small angle.

A similar effect, which is usually less important, is the widening of fractures that do not intersect the periphery of tunnels, shafts and boreholes but are oriented more or less parallel to such openings and which are located so in the local stress field that they expand due to stress relaxation.

The influence of stress-induced changes of the aperture and connectivity of natural fractures in the nearfield will be dealt with in detail in conjunction with the discussion of each concept.

II Fracturing

New fractures will be formed where the rock strength is exceeded. This phenomenon takes place close to the periphery of blasted excavations where the hoop stresses are very high at the moment of detonation of the contour blast-holes, and at the front of the cutting head in large drilled holes. At the free surface where the lateral support is almost none, fracturing is expected to have the form of "axial cleavage" primarily developed from 6th order fissures oriented parallel to the free surface or from 7th order discontinuities. For a blasted tunnel with steep walls or the roof oriented more or less parallel to the major fracture sets, schistosity should be obvious to within a couple of decimeters from the free surface. The increase in fracture frequency and porosity of the rock close to the periphery naturally leads to reduced strength of the rock in this zone, which affects the stress conditions in the surrounding rock.

As in the case of blasting-disturbance, the axial hydraulic conductivity may undergo significant increase over a considerable distance due to stress changes, but the net conductivity over a long distance is expected to be strongly dependent on the rock structure.

2.4.2.3 Fragmentation

The mechanical impact when the drillbits of a rotating cutting-head shear off and break up the crystal matrix is known to cause fissuring and shattering on a small scale (2). Hereby, preexisting 6th order fissures will propagate and new fissures generated and propagated from 7th order discontinuities in directions that are controlled by the transient local stress field. Assuming the 6th order-type fissures to form a regular orthogonal pattern with 5 cm spacing

and 10 μm aperture, the average theoretical conductivity would be around 10^{-8} m/s, the activation of such fissures probably being confined to around 10 cm from the free surface. Activation of 7th order defects (Fig.13) to an extent corresponding to a largely disintegrated but still coherent matrix of cubical crystals with 1 mm side length separated by 1 μm wide space would cause an increase of the hydraulic conductivity from initially 10^{-13} to 10^{-7} m/s. The extension of this zone of more intense disturbance is expected to be in the range of millimeters at core-drilling, to 2-5 cm when TBM and other techniques with cutting-heads are used. Stress-induced microstructural degradation is very obvious in cores from 12 km depth in the Kola Superdeep Borehole, where the mechanism is stress release on overcoring.

2.4.2.4 Thermomechanical effects

Propagation of a heat front will induce successive expansion of blocks by which strain is caused that alters the aperture and extension of hydraulically active fractures and activates and connects previously sealed or isolated ones of all orders of magnitude. Such effects, which are strongly dependent on the generated thermal gradients and the rock structure and therefore different in the three repository concepts, may have a very important influence on the hydraulic conductivity of the nearfield rock.

3 THE VDH CONCEPT

3.1 *General*

VDH boreholes are taken to be drilled by use of a conventional "big hole" drilling assembly with a flat

bottom bit, the diameter of the upper 2 km of the hole being 1.3 m and 0.8 m of the lower 2 km. The bottom part of the last-mentioned "deployment zone" will be focused on here.

For the present purpose of characterizing the near-field rock we will make use of the previously derived rock structure model, which is taken to have the following features:

- * Basic pattern of interacting 4th order fractures in an approximately orthogonal network. It is generalized to have cubical symmetry with 5 m spacing of the parallel sets of fractures

- * The hydraulically active parts of the fractures are assumed to be channels formed at fracture intersections. In the present report, the channels in undisturbed, virgin granite are given "standard" dimensions with a width of 1 cm and an aperture of 100 μm forming crosses, disregarding the actual geometrical shape which is more or less rhomboidal (5). One such cross will be located at the center of each 25 m^2 square-shaped section, i.e. where 4th order fractures intersect, yielding an average bulk hydraulic conductivity of around 10^{-11} m/s of undisturbed granite

- * An equally oriented orthogonal network of 5th order discontinuities is integrated in the 4th order fracture network as indicated in Fig.10. The 5th order breaks are sealed and not hydraulically active or they may form isolated, partly open fractures

- * 6th and 7th order fissures and voids are homogeneously distributed in the virtually fracture-free rock mass, giving it a bulk conductivity of 10^{-12} m/s

3.2 *Large-scale variation of virgin rock structure*

The simple basic pattern of straight vertical and horizontal channels formed by intersection of 4th order discontinuities, has to be corrected with respect to the variation in orientation on a large scale. Hence, assuming the undulation identified in Stripa to be of general applicability and considering only cases where the statistical average dip is the same as that of the VDH holes one can apply the interpretation shown in Fig.23, i.e. one consisting of a regular, straight system of interconnected vertical and horizontal channels in cubical symmetry, in which a helical VDH hole is located. It affects a system of channels that has a horizontal extension of 40 x 40 meters.

Theoretically, the VDH hole makes one cycle per 200 m depth, thereby intersecting around 50 fractures but hitting 10 channels at maximum. Hence, there is direct hydraulic contact between the interior of the hole and the continuous channel system every 20 m. The average bulk hydraulic conductivity of the near-field rock due to the presence of 4th order discontinuities is 10^{-11} m/s *without considering any of the disturbing components which will be induced by stress changes or heat and which will be discussed in the subsequent text.*

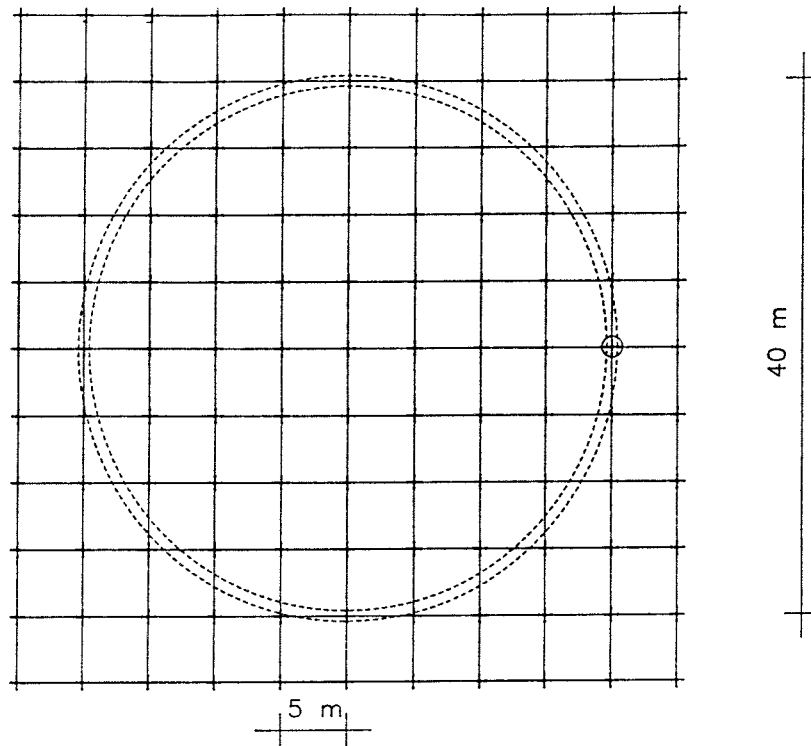


Fig.23 Theoretical model of straight system of channels (crosses) located where 4th order discontinuities (5 m spacing) of the basic orthogonal fracture pattern intersect. A helical 80 cm diameter VDH hole is winding through the channel system

3.3 *Influence of disturbing components*

3.3.1 **Load conditions**

The influence of the stress conditions on natural fractures and the possible activation of potentially expandable ones, as well as possible formation of new fractures, depend on the rock stress conditions and on the physical properties of the rock. In the case of VDH holes the rock stresses are strongly influenced by the internal pressure in the holes, ex-

erted by the drilling mud for a considerable period and by the deployment mud for their entire operative lifetime.

The most critical period with respect to the stability of the deep part of the 80 cm diameter holes is taken to be when they are filled with drilling mud since the deployment mud is stiffer and offers better support to the walls. The drilling mud is assumed to have a density of 1.3 g/cm^3 , either by use of Na bentonite mixed with 3.5 % NaCl solution, or by adding very finely ground barite to the bentonite slurry. The heavy mud exerts a pressure on the walls that increases linearly from an insignificant value at the ground surface to around 52 MPa at 4 km depth. The matter is in fact very complex since it is not known whether the mud will stiffen by consolidation or thixotropic action and stop acting as a heavy fluid. If so, wall support will only be offered by the effective pressure which is very much lower than the 52 MPa pressure at 4 km depth. Still, this pressure can be maintained by gentle pumping until emplacement of canisters will start since this involves sufficient mud movement to keep up the pressure at a high level.

3.3.2 Mud penetrability

The possibility of the drilling mud to enter channels and slot-shaped fractures is controlled by its fluidity and overpressure with respect to the water pressure in the fractures, and also by the possibility of displacing water in the fractures. The latter is assumed not to be critical while the viscosity of the mud is a determinant of how far it can get into the openings. Using the pattern in Fig.23 it is concluded that if mud can enter channels and slots to a depth

of 5 m, one would effectively seal off the entire nearfield with the exception of the permeable skin of mechanical damage due to the drilling. For 100 μm channel aperture at 3 km depth one finds that this criterion is fulfilled by the proposed drilling mud without adding barite, the water content of the slurry being around 160 %, i.e. about 1.6 times the liquid limit (w_L).

For more narrow openings one finds that the required compositions and densities are as shown in Table 3.

Table 4 Required properties of drilling mud to enter channels and slot-shaped fractures at 3 km depth from a VDH hole. w is the water content and w_L the liquid limit. ρ is the bulk density of the water saturated mud

Aperture μm	Mud data			Barite content
	w %	w_L %	ρ g/cm^3	%
100	160	100	1.32	0
50	180	100	1.30	0
25	190	95	1.30	12
10	200	90	1.30	25

We conclude from all this that mud, properly composed, has a potential to enter narrow openings and may help to seal at least wider channels. The hydraulic conductivity of the proposed muds is in the range of 10^{-8} to 10^{-6} m/s.

3.3.3 Influence of stress redistribution

3.3.3.1 Influence on existing, active fractures, wedge formation

Mechanical and thermomechanical simulations have been performed with the 2D distinct element code UDEC. The calculations concerned a horizontal cross section at 4 km depth through the 0.8 m borehole. The evaluation of the results was focused on changes in mechanical aperture for joints very close to the borehole periphery. Three different locations of the borehole relative to a generalized fracture system geometry were considered (Fig 24).

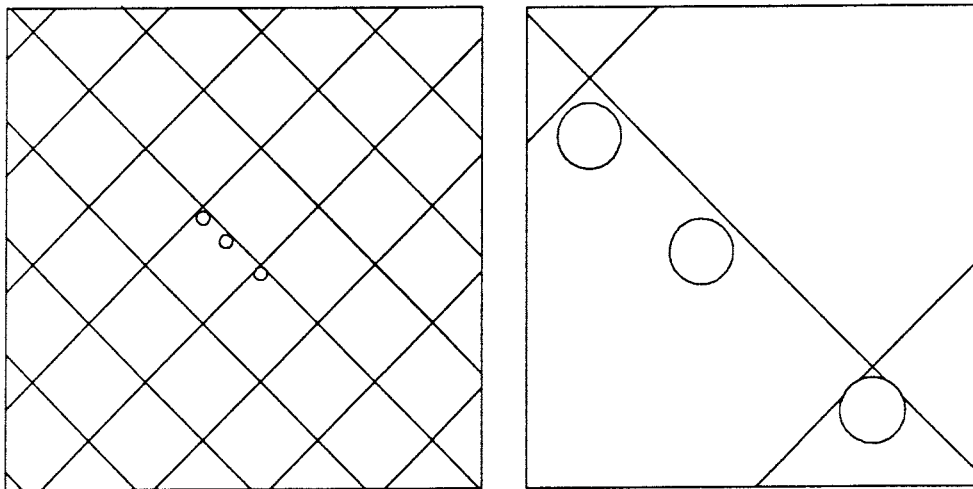


Fig.24 VDH borehole locations with respect to 4th order fracture sets

The dimensions of the model section were 100 m x 100 m with the 0.8 m borehole located in the central part. Joints were modeled only in a 30 m x 30 m region around the borehole. Two mutually orthogonal joint sets were modeled applying the geometrical data for the two sets given below:

Joint set	Spacing	Orientation relative to positive x direction
jset #1	5 m	45 deg
jset #2	5 m	135 deg

The intact rock, i.e. the material between joints, was assumed to be isotropic and homogeneous and to behave linearly elastically. The following values for the elastic properties, which are basically those of Stripa granite, were used:

$$\begin{aligned} \text{Density} &= 2.6 \text{ t/m}^3 \\ \text{Youngs modulus} &= 50 \text{ GPa} \\ \text{Poissons' ratio} &= 0.3 \end{aligned}$$

An elasto/plastic joint model with a non-linear stress-closure relation was used for the joints. Both the joint normal stiffness and the joint shear stiffness were assumed to depend on the joint normal stress according to a power law. This continuously yielding joint model also allows for peak/residual stress/displacement behavior for joints in shear. Figs.25 and 26 show the stress-strain relations used in this investigation. The parameter values were chosen so as to give close agreement with stress-strain relations obtained from laboratory tests on joint samples from the Stripa mine (6).

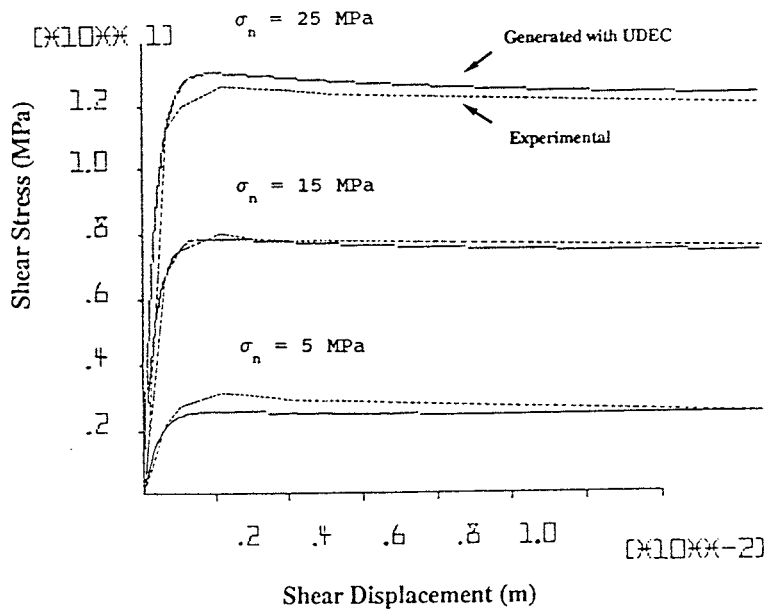


Fig.25 Shear stress vs shear displacement at three different constant normal stresses. Dotted lines represent laboratory results, while full lines represent UDEC approximations used in this investigation

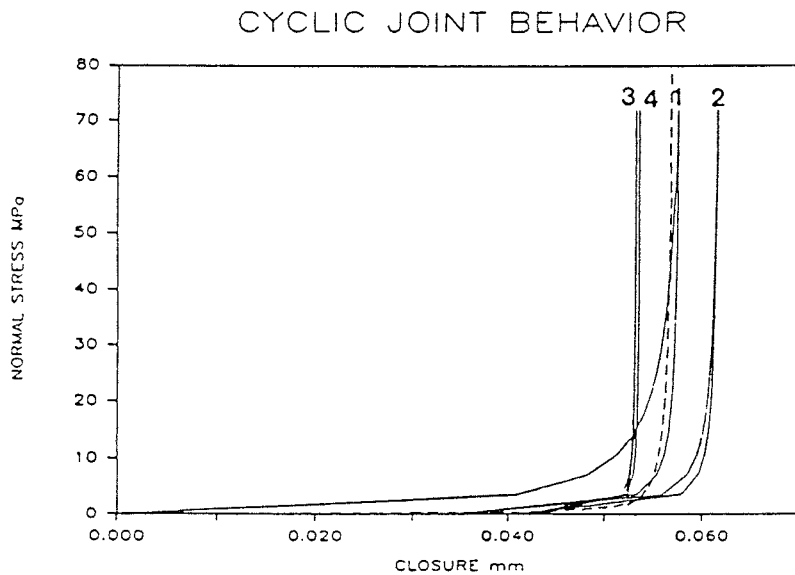


Fig.26 Normal stress vs joint closure. Full lines represent laboratory results, while dashed line represents UDEC approximation used in this investigation

The following values for the in situ principal stresses at 4 km depth were assumed, based on Rummel's equation:

$$\begin{aligned}\sigma_x &= 75 \text{ MPa} \\ \sigma_y &= 110 \text{ MPa}\end{aligned}$$

The far field was modelled with boundary elements using the following values for the elastic properties:

$$\begin{aligned}\text{Youngs modulus} &= 25 \text{ GPa} \\ \text{Poissons' ratio} &= 0.28\end{aligned}$$

When a state of primary equilibrium was arrived at for the respective location of the VDH hole relative to the fracture system, the excavation was simulated by substituting the stresses in the borehole interior by 52 MPa hydrostatic pressure, exerted by the 4 km drilling mud with 1.3 g/cm^3 density. The results regarding aperture changes for the three cases are shown in Figs.27, 28 and 29. Fig.30 shows the stresses for the case chosen for further, thermomechanical analysis.

Tentative conclusions are that the aperture of steeply oriented 4th order fractures that interfere with the hole are vanishingly small and that the change in stress field will have an insignificant effect on the hydraulic conductivity (7). Wedges will be pressed against the rock and mud entering through channels in the fractures forming the wedges will tend to be sealed. However, by this the mud pressure in the fractures may lead to separation of the wedges from the host rock, and this has two effects. Firstly, the

wedges will be completely embedded by mud, which does not have a negative effect on the overall hydraulic conductivity, and secondly, the nearfield stress situation will be changed when the wedges come loose, which may lead to activation of closely located 5th order fractures that may not be sealed by the mud, enhancing the conductivity in the axial direction of the hole.

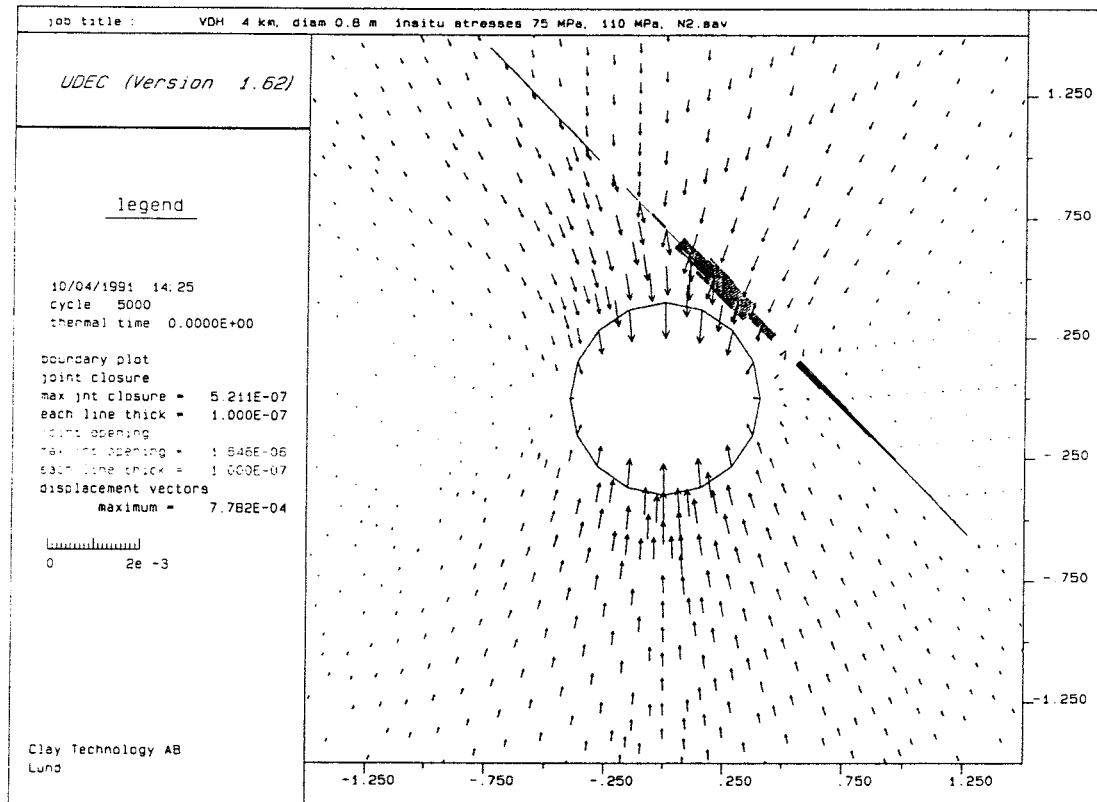


Fig.27 Change in aperture of nearfield 4th order fractures, Case I. Maximum joint opening $2 \mu\text{m}$, and maximum inward displacement of wall $780 \mu\text{m}$

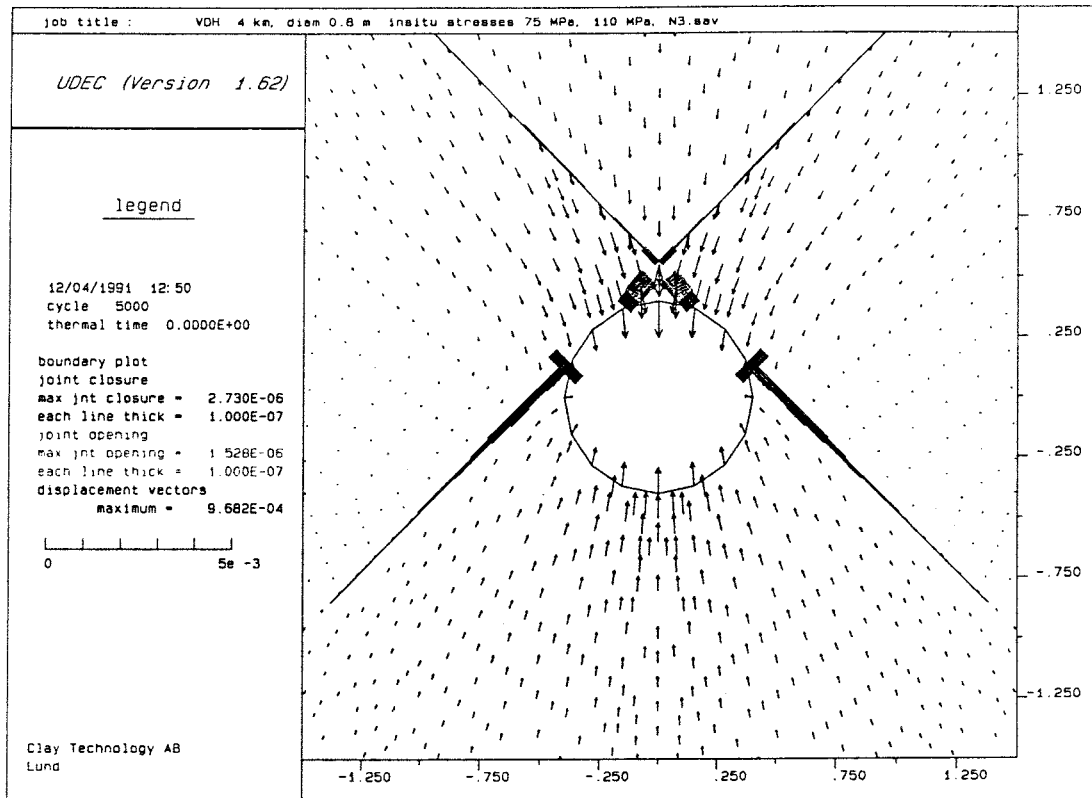


Fig.28 Change in aperture of nearfield 4th order fractures, Case II. Maximum joint opening about 2 μm

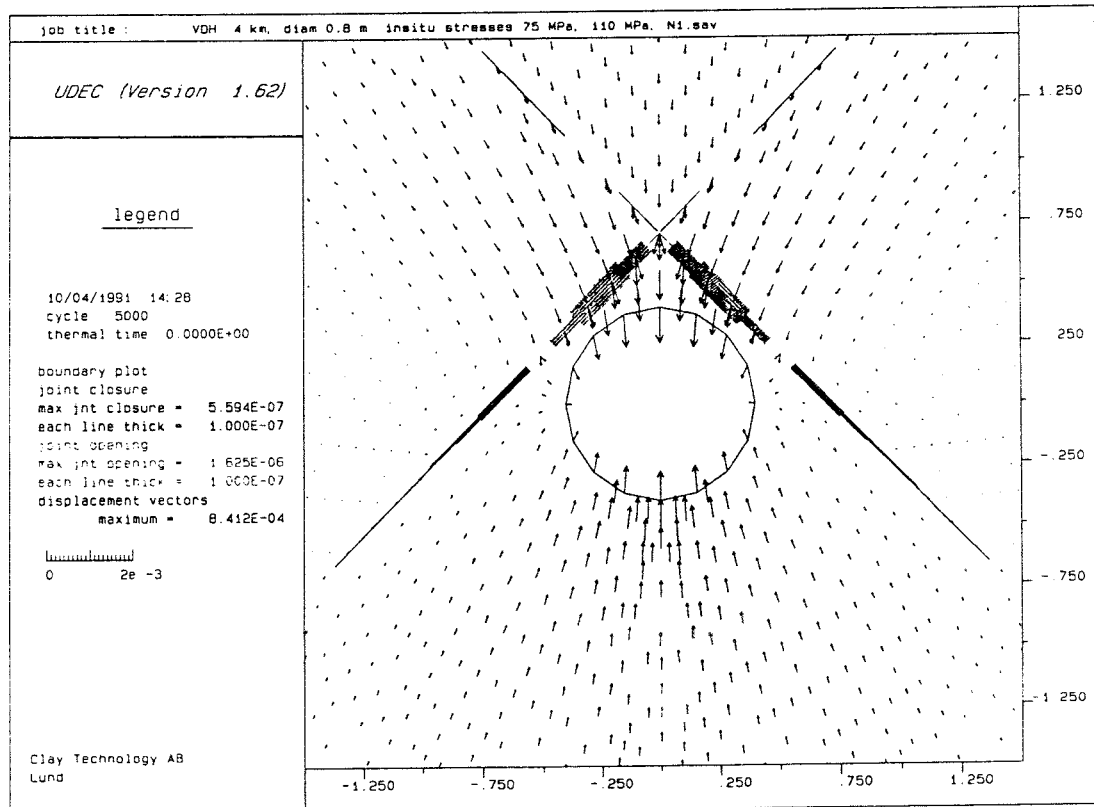


Fig.29 Change in aperture of nearfield 4th order fractures, Case III. Maximum joint opening about 2 μm

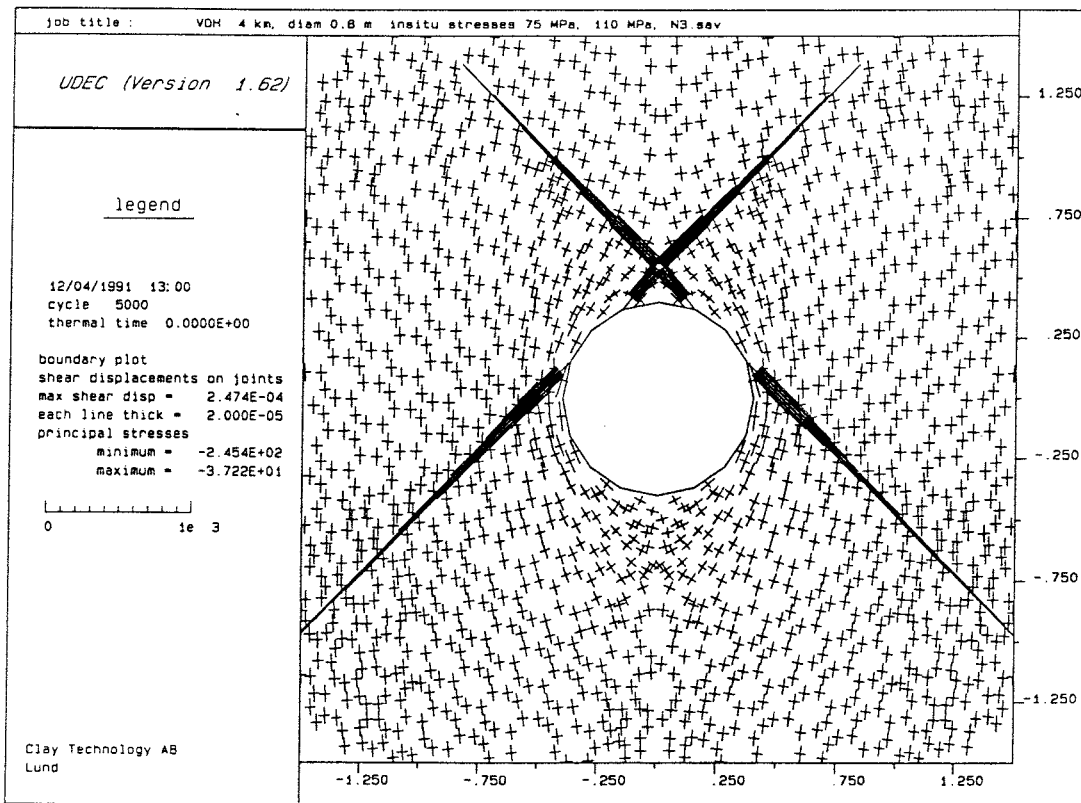


Fig.30 Stresses and shear strain in Case II. Maximum shear displacement 250 μm

3.3.3.2 Fracturing

It is concluded that the shear strain along the discrete 4th order fractures in the nearfield rock is so small, i.e. less than about 250 μm (cf. Fig.25), that the material is largely maintained in the elastic region. However, we see from the stress distributions that the hoop stress is raised to more than 200 MPa when the hole is located within less than about 1 m from neighboring fractures and this will probably activate 5th order "latent" fractures, and generate growth of critically oriented 6th order discontinuities. Hence, it is estimated that although the 52 MPa mud pressure will prevent spalling, rich

fissuring will take place within at least 0.1 m distance all around the hole periphery, i.e. about 10 % of the diameter, and 5th order fractures will be activated to within at least 1 m distance.

Considering first the activated 5th order discontinuities, the generated strain is expected to lead to opening of channel-type passages of varying width and aperture. Taking, for the sake of simplicity and lack of reliable data, the channels to be of "standard" type, i.e. consisting of cross-shaped rectangular openings with a width of 1 cm and an aperture of 100 μm , and to be formed at the intersection of activated 5th order fractures, the system of channels will be one of cubical symmetry with an average spacing of 0.5 m according to the general model. This would correspond to the network in Fig.23 although with 100 times higher frequency of channels, yielding an average bulk conductivity that is two orders of magnitude higher, i.e. about 10^{-9} m/s if the conductivity of the virgin rock is 10^{-11} m/s. Depending on the strain pattern such disturbance may yield isotropic or anisotropic conductivity.

The other effect, i.e. that of fissure growth, is estimated to be one of schistosity, yielding the earlier described regular pattern with an assumed spacing of 5 cm of activated 6th order fissures with 10 μm aperture, and - close to the periphery of the hole - a loosened crystal matrix. The estimated axial hydraulic conductivity to within roughly 10 cm from the periphery would thus be around 10^{-8} m/s and about 10^{-7} m/s within the first 2-5 cm as discussed in Ch.2.4.2.3. These figures may be somewhat conservative for normal rock temperatures while they are probably very plausible for the actual heating phase, which is treated below.

3.3.3.3 Thermomechanical effects

The UDEC code was applied for calculating heat-induced strain and stresses. The thermal properties of the intact rock are given below:

Linear thermal expansion coeff. = $8.3 \times 10^{-6} \text{ K}^{-1}$
Specific heat = 0.8 kJ/kg,K
Thermal conductivity = 3.0 W/m,K

The initial power of the VDH canister was set at 100 W per m of borehole length. This power was distributed uniformly over the borehole cross section area, i.e. the canister itself was not modeled. The power data were specified to account for the decay characteristics of 40 year old BWR fuel. The boundaries, which geometrically coincide with the mechanical boundaries, were adiabatic.

For the borehole interior a constant pressure material model was used. The following thermal data were used:

Linear thermal expansion coeff. = 0
Specific heat = 1.6 kJ/kg,K
Thermal conductivity = 1.5 W/m,K

Heat generation was modeled for one of the cases presented above, i.e. Case II. Thermal and mechanical calculations were closely interlaced, i.e. when the temperature change in any location in the model exceeded 1°C, the thermally induced stresses were allowed to equilibrate before the thermal calculations were continued. Ten years of heat production were simulated, yielding the aperture changes and rock displacement shown in Fig.31. Stresses and joint shear displacements are shown in Fig.32.

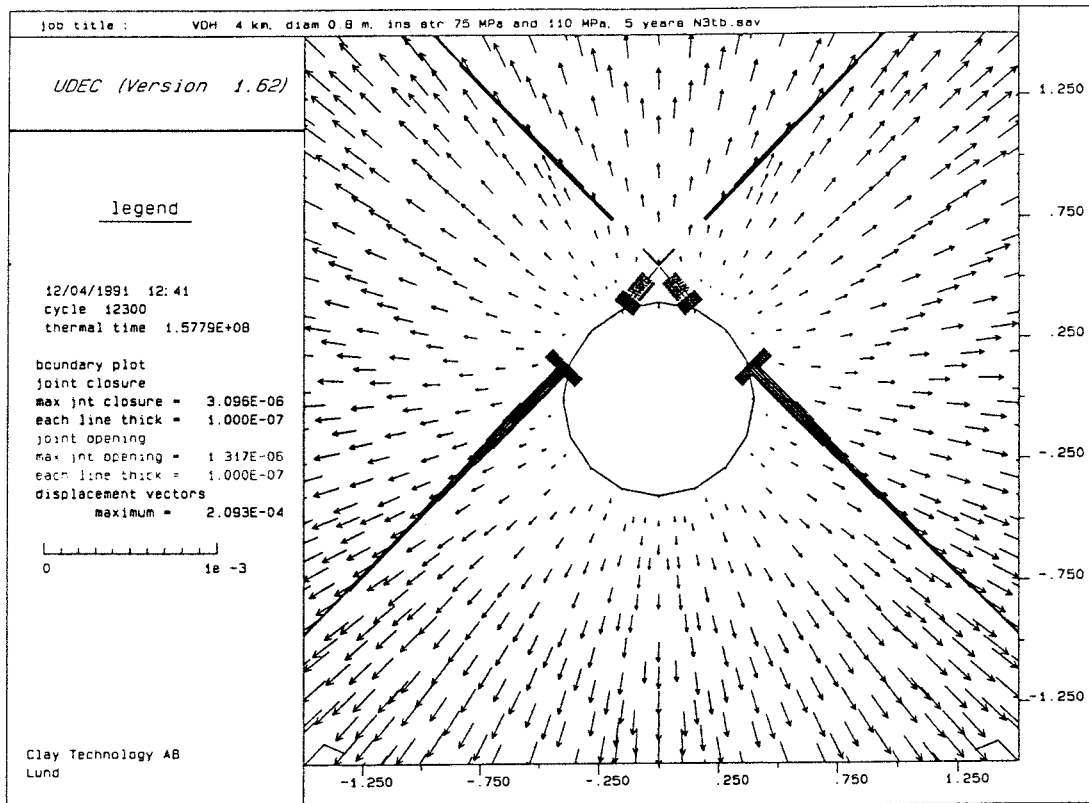


Fig.31 Change in aperture of nearfield 4th order fractures, Case II. Maximum joint opening less than 2 μm

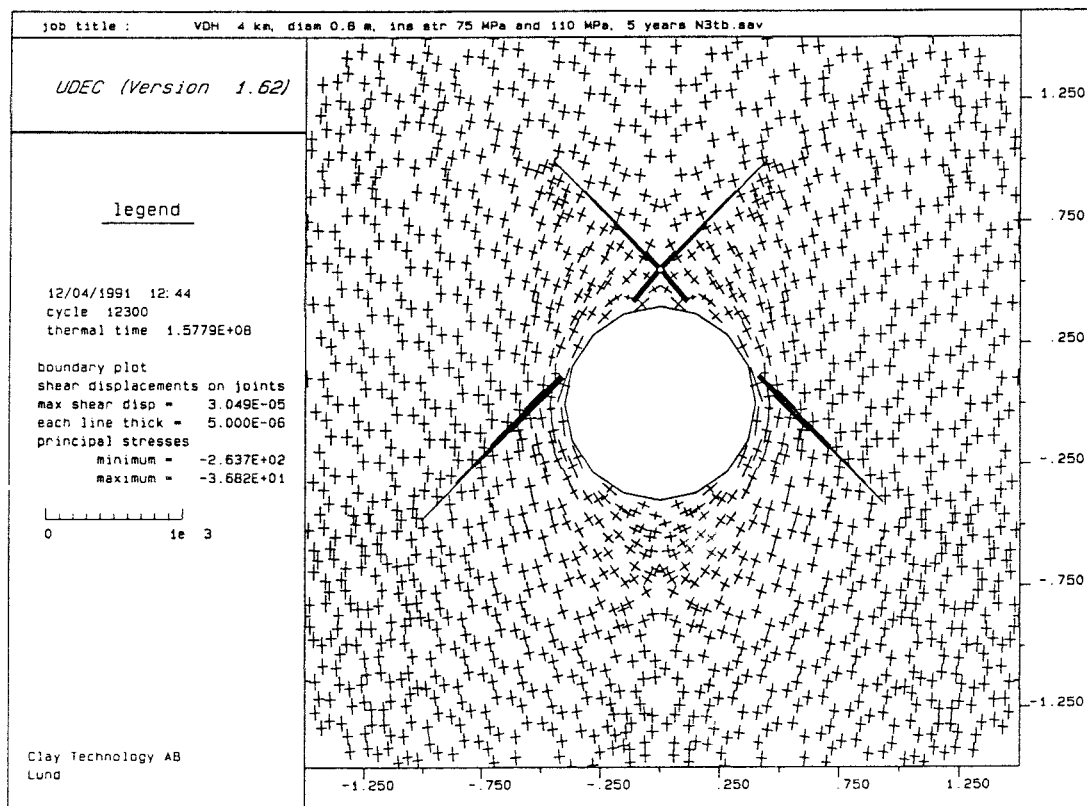


Fig.32 Stresses and shear strain in Case II on superimposing heat effects. Maximum shear displacement 30 μm

A tentative conclusion respecting the effect of heating is that the fracture apertures are not significantly changed from the non-heated state and that the net effect of stress relief from excavation and from superposing a heat pulse of this moderate significance is negligible from the point of hydraulic conductivity (7).

3.4 *Structural model of VDH nearfield rock as influenced by disturbances*

3.4.1 **Basic pattern**

The basic pattern of conductive passages of virgin rock is assumed to have the form of an orthogonal system of cubical symmetry consisting of 4th order fractures with an average spacing of 5 m, a measure that may vary by 50 % in practice. Integrated in a "fractal"-type manner in this system is a corresponding network of 5th order fractures with an average spacing of 0.5 m but this subsystem is not active in transferring water in undisturbed granite. In the nearfield rock that has undergone sufficient strain by stress redistribution or heating, the 5th order fractures are assumed to have been activated.

3.4.2 **"Fine-rock structure"**

Introduction of the various disturbances that will affect the basic, virgin granite structure results in the generalized model of Fig.33, which represents a

unit section of a 80 cm diameter, vertically oriented VDH hole. One finds that, with the various applied simplifications and approximations, a simple tentative picture of the nearfield rock would show an inner annulus of strongly fissured rock with 0.1 m thickness and with an approximate axial bulk hydraulic conductivity of 10^{-8} m/s, the innermost 2-5 cm having an isotropic conductivity of around 10^{-7} m/s, these inner zones being surrounded by a 1 m wide concentric annulus characterized by activated 5th order fractures with cross-shaped channels of 0.5 m spacing and a width and aperture of 1 cm and 100 μ m, respectively. This annulus has an axial conductivity that is 2 orders of magnitude higher than that of the surrounding virgin, undisturbed rock, which is estimated to have an average hydraulic conductivity of 10^{-11} m/s at 4 km depth.

The channels that are exposed in the hole, and at least a shallow part of the innermost fissured zone may be sealed by the drilling mud but at this stage this effect should not be introduced in the model.

3.4.3 Interaction with large structures

For the VDH concept, the interaction between large-scale structures and the generalized "fine rock structure" needs to be considered in particular, and it is suggested here to do this by applying the basic "fractal" type system of discontinuities of different scales. Thus, 3rd order discontinuities, which are taken here to be characterized by fracture zones with 50 m spacing, 0.2 m thickness and a conductivity of 10^{-8} m/s (cf. Chapter 2.2.4) can be integrated in the system. As indicated in the preceding text it is reasonable to assume that they represent an orthogonal-type system that is largely conformous with that of the 4th and 5th order fractures. If the undulation

mode of the latter system also characterizes 3rd order zones, the most critical condition would be the interference with VDH holes that is shown in Fig.34, which implies that the holes intersect one steep continuous 3rd order discontinuity at 100 m intervals, and sets of flatlying 3rd order discontinuities at 50 m intervals. It is concluded that this is a more critical case than if the holes intersect a set of large structures dipping more than about 45° .

As to discontinuities of lower order it appears reasonable to believe that steeply oriented 1st and 2nd order discontinuities can be avoided, i.e. the ones that are assumed to have 3000 and 500 m spacings, respectively, and that the deployment zones can be located so that they will not be intersected by 1st order structures. However, flatlying 2nd order structures, with an assumed average spacing of 500 m, will intersect VDH holes as indicated in Fig.34.

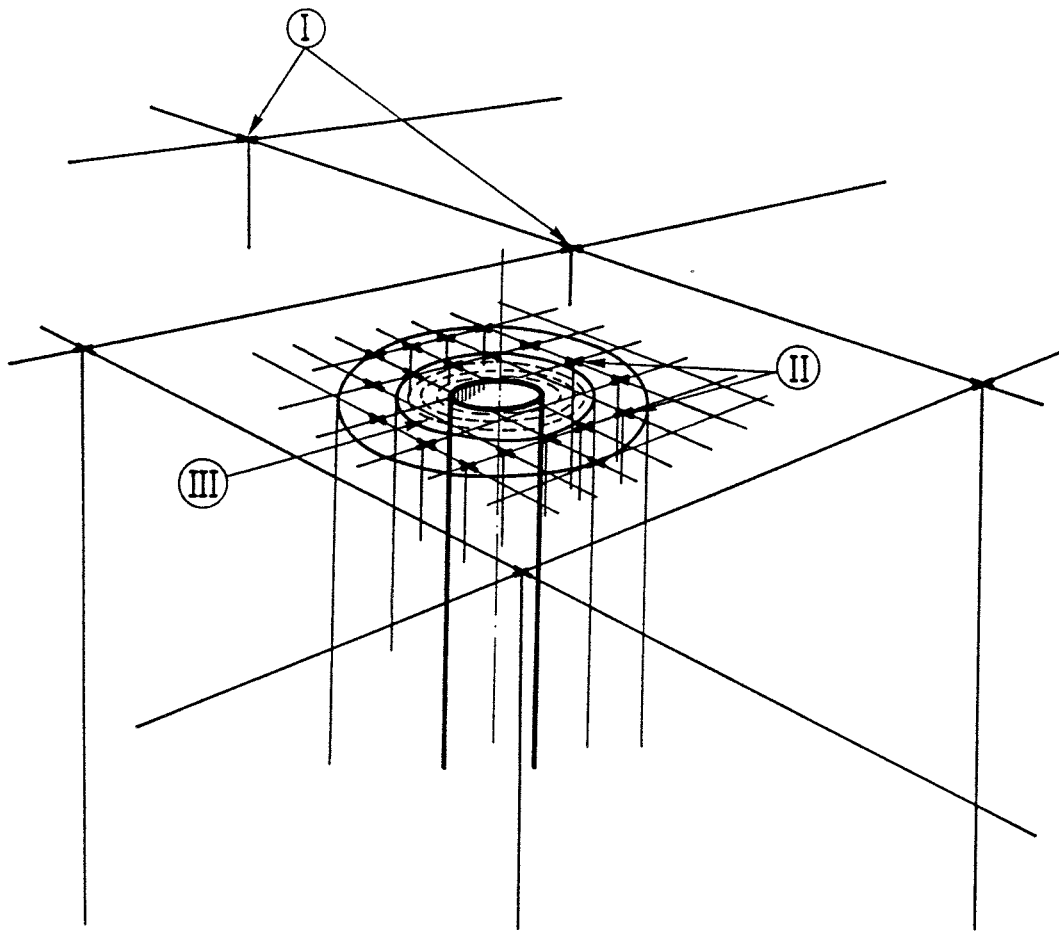


Fig.33 View of generalized nearfield structure of mud-filled VDH hole. I) vertical channels formed at the intersection of steep sets of 4th order fractures (5 m spacing, bulk conductivity 10^{-11} m/s). II) Vertical channels formed at the intersection of activated 5th order fractures (0.5 m spacing) forming an outer 1 m thick annulus with a bulk conductivity of 10^{-9} m/s. III) 0.1 m thick annulus of steeply oriented fissures with a bulk hydraulic conductivity of 10^{-8} m/s except for the innermost 2-5 cm which has a conductivity of 10^{-7} m/s.

The channels form orthogonal patterns all of which are not shown

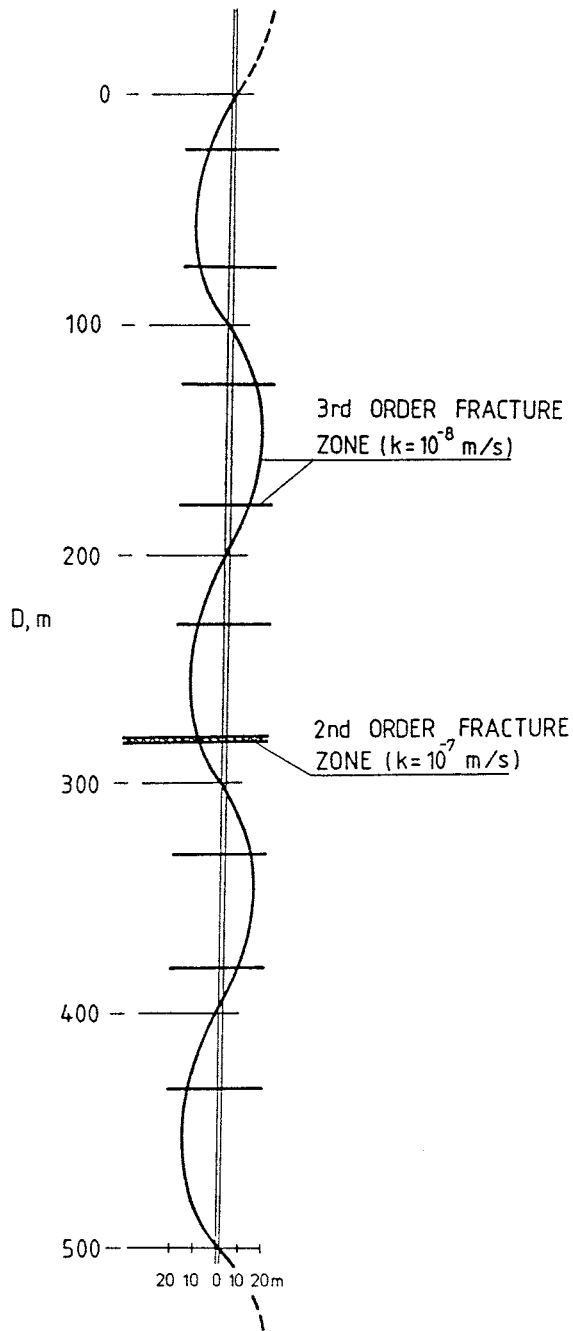


Fig.34 Generalized 500 m section of the deployment zone of a VDH hole interacting with one step 3rd order discontinuity, and being intersected by flatlying, regular sets of 3rd order structures and one flatlying 2nd order structure

4.1 *General*

The main features of the KBS3 concept can be described as sets of parallel blasted tunnels with a spacing of about 25 m at one or two levels, and with 1.5 m diameter and 7.5 m deep deposition holes drilled from the floor of the tunnels. The concept was outlined some 10 years ago and forms the basis of repository design in several countries. In contrast with VDH it is supposed to be constructed at 500 - 1000 m depth, which means that no rock stability problems are expected. A major difference is that blasting is applied for the tunnels, which means that the upper part of the deposition holes will be located in the disturbed zones surrounding the tunnels, which will have a width of approximately 4 m and a height of around 5 m.

We will use here, for characterizing the rock, the same basic structure model as in the preceding discussion of the VDH concept.

4.2 *Influence of excavation on the rock conductivity*

4.2.1 **Blasting of tunnels**

As described earlier in the report blasting will cause expansion and formation of fractures along a large part of the blasting holes, while significant fracturing will take place at their tips. This is estimated to increase the axial bulk hydraulic conductivity within at least a few decimeters distance from the periphery of blasted tunnels to 10^{-9} to 10^{-6} m/s. This enhancement may not be effective over long distances, however, since the continuity of the disturbed zone is very much dependent on the natural

rock structure as demonstrated in the subsequent paragraph. Still, it can be assumed that the degree of continuity is high in the floor and that the net bulk hydraulic conductivity down to almost 1 meter depth in the central part of the floor is 10^{-8} to 10^{-7} m/s.

4.2.2 Fragmentation by drilling of deposition holes

The mechanical impact when the drillbits of a rotating cutting-head shear off and break up the crystal matrix is known to cause fissuring by activating 6th and 7th order discontinuities. Assuming that full-face-type drilling is applied, mechanically and heat-induced defects are expected to appear within 10 cm distance from the borehole wall, yielding an average hydraulic conductivity of presumably about 10^{-8} m/s. Some more intense microfracturing is expected within the first 2-5 cm distance, where the conductivity may be raised to 10^{-7} m/s.

4.2.3 Stress redistribution of rock around tunnels

4.2.3.1 Tunnels

As in the VDH case one can identify several types of stress influence on nearfield rock that affect the porosity and thereby its hydraulic conductivity. The larger size of the KBS3 tunnels means that strain-induced changes in aperture and extension of the hydraulically active part of existing, natural fractures - mainly of the 4th order type - will be more obvious than in nearfield VDH rock. It is appreciated that the high stresses that are generated in the moment of blasting will cause activation of 5th order fractures that were hydraulically inactive fractures in the virgin rock, and create new fractures of the 6th order.

While the relative block movements around VDH:s will be insignificant one can imagine the manner in which they take place in KBS3 nearfield rock, which allows for more freedom to move in the form of rotational and translatory displacement of rock blocks yielding opportunities for considerable changes in aperture of the joints (Fig.35). A second effect is that the hoop stress increases considerably, by which the rock close to the periphery becomes exposed to high uni-axial stresses leading to growth of 6th and 7th order discontinuities ("schistosity"). Such effects lead to softening of the shallow rock, which alters the stress conditions deeper into the rock. We will consider this phenomenon by regarding first unaltered strength conditions and subsequently the case of mechanically degraded shallow rock.

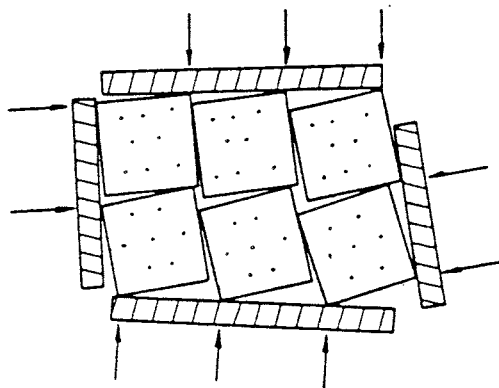


Fig.35 Exaggerated picture of rock block movement on changing the stress state (After Goodman)

Unaltered rock properties

The primary rock stress conditions at 500 m depth are characterized by a major principal stress of 15 to 25 MPa, operating horizontally, and a more or less vertical minor principal stress of around 13 MPa. This can be taken as a basis for estimating the distance from tunnel and borehole peripheries within which

there is significant influence on fracture apertures and hydraulic conductivity by stress changes. The outcome of such calculations will be referred to here.

Various numerical analyses based on 2D and checked by 3D stress/strain calculations have been made for calculating changes in axial hydraulic conductivity due to stress redistribution (7,8,9). A slightly different fracture pattern than the basic one was applied in order both to consider the influence of disturbance by excavating a rather large tunnel and to fit structural mapping data of the drift where the so-called Buffer Mass Test (BMT) in the Stripa mine took place Fig.36. They can be taken to represent 3 superimposed networks of 4th order fractures of orthorhombic symmetry with an average spacing of 2 to 9 m, that are differently oriented in reality but having the same strike in the 2D analyses.

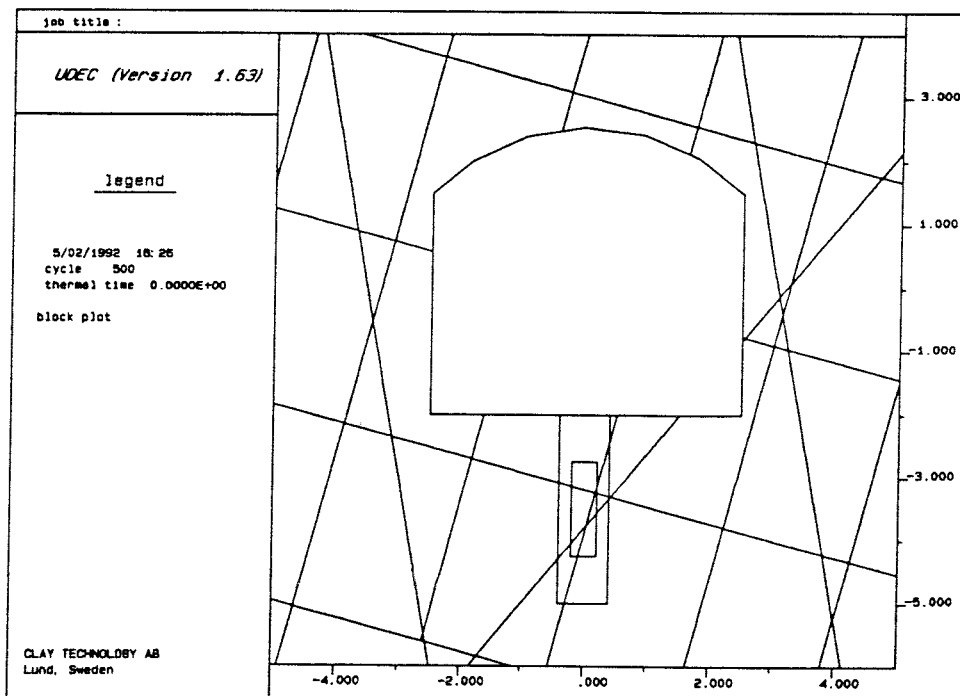


Fig.36 Schematic fracture pattern assumed in 2D and 3d calculations of the BMT nearfield

The smaller average fracture spacing than in the VDH case was compensated for by ascribing to the KBS3 rock a higher Young's modulus (70 instead of 50 GPa of the VDH rock) and a lower Poisson's ratio (0.20 instead of 0.30 of the VDH rock), by which the results are expected to be comparable.

Qualitative and semiquantitative estimates of changes in conductivity have been obtained and they appear to be in reasonable agreement with experimental data (9, 10). If due attention is paid to actual restraints to block movements as implied by the limited extension and undulation of axially oriented fractures, one finds that changes in aperture are negligible beyond a distance from the tunnel periphery corresponding to one tunnel diameter.

Within 1 m distance from the periphery the net effect of stress redistribution on fracture apertures can be interpreted as an increase in axial conductivity by 2 to 3 orders of magnitude, while the increase is estimated at 1 - 2 orders of magnitude for the rock zone extending from this outer zone to 1 tunnel diameter distance from the periphery. The structural changes generated by stress redistribution can be assumed to have the form of activation of 5th order fractures in the outer disturbed zone. Using the simplified model of transport paths in the form of standardized channels along the lines of intersection of fractures, one finds that the number of channels is increased by 100 times by activation of all 5th order fractures, which would correspond to an increase in hydraulic conductivity of 2 orders of magnitude. The actual disturbance in the outer zone is naturally stronger within the first few meters from the tunnel periphery than closer to it.

The combined effect of dynamic loading by blasting and very high hoop stresses in the moment when the room is created, causes overstressing and formation of a shallow, fissured zone by growth of 6th order discontinuities. It contributes to the increased axial conductivity of the blasting-affected peripheral zone, but its practical importance depends very much on the orientation of the tunnel with respect to the strike of the major steep fracture sets.

In the roof, which is usually more or less aligned with the ubiquitous sets of flatlying fractures, the effect of high hoop stresses may yield a particularly strong increase in axial conductivity in the shallow rock due to rock disintegration by intergrowth and expansion of 6th and 7th order discontinuities. The disturbance depends on the shape of the tunnel and on the rock structure as indicated by the displacement vectors shown in the example given in Fig.37. One finds by applying reasonable rock strength values that the roof may deflect by up to 2 mm over the central 2 m part and that associated movements in the rock mass can extend to about 2 m from the periphery. These figures can be interpreted in the form of widening of 3 natural flatlying 5th order fractures by 800 μm each, or by the growth and expansion of 20 6th order discontinuities to an aperture of 100 μm . The first example would yield a net hydraulic conductivity of a $2 \times 2 \text{ m}^2$ rock element at the crown of the tunnel of about 10^{-3} m/s , while the same element would have a conductivity of around 10^{-5} m/s in the second example. Similar effects may also appear in the upper parts of the walls.

A more suitable, arched shape of the crown would minimize the risk of instant development of a very conductive roof zone but it is estimated that the high stresses generated in the roof may then induce time-dependent displacements that will cause progressive failure and fall of blocks if the support of

the tunnel backfill is not sufficient. Hence, the net effect of stresses in the roof may range from the aforementioned increase in conductivity by 2 orders of magnitude within 1 m distance from the periphery, to a state with an increase to as much as 10^{-3} m/s.

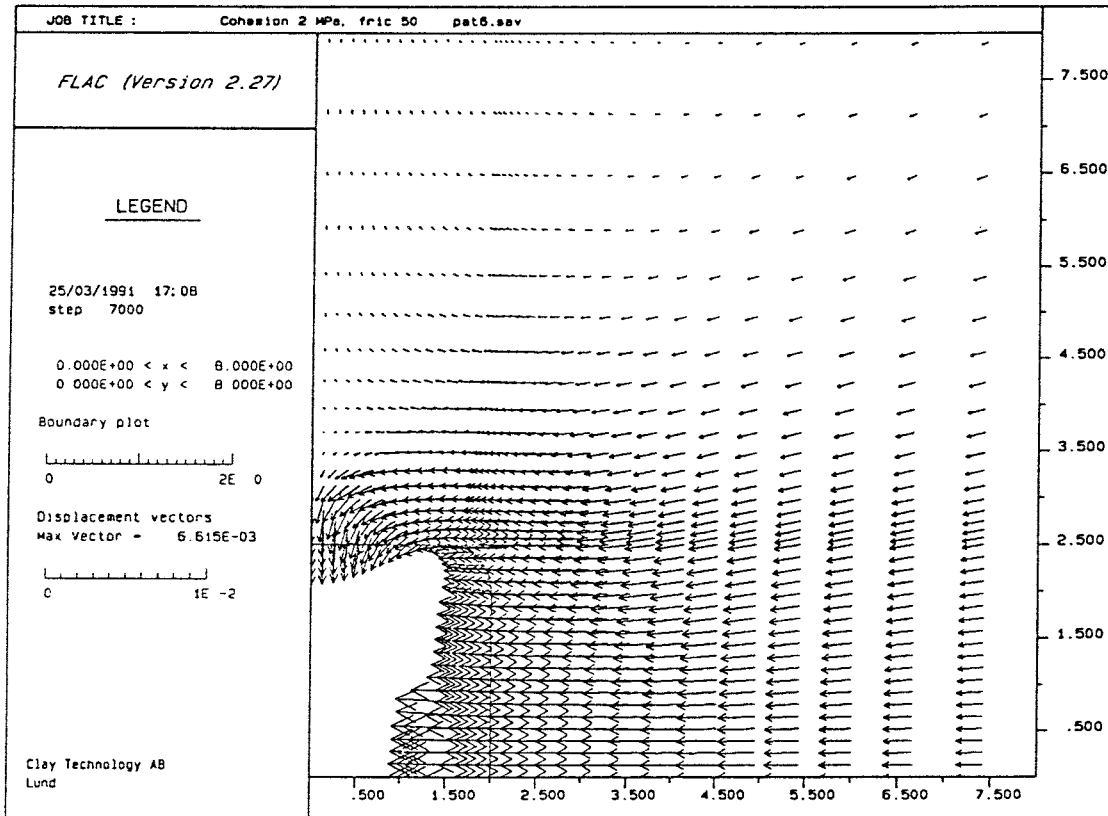


Fig.37 Possible displacement pattern in the upper part of KBS3 tunnels. One half of the tunnel is depicted (Cohesion 2 MPa and angle of internal friction 50°)

Altered rock properties

The disturbance of the shallow rock around a blasted tunnel due to the combined effect of high hoop stresses and gas pressure at the moment of detonation, results in an increased porosity and reduced

rock strength. The latter is expected to depend on the frequency and orientation of blasting-induced fractures and on the virgin rock structure, and it is therefore probable that the intensity in disturbance varies along the tunnel periphery and with the distance from it. For the sake of simplicity this was not considered in the attempt that has been made in the present study to quantify the loss in strength, but it may well be considered in a deeper analysis.

The study was made by applying the FLAC code (Fast Lagrangian Analysis of Continua), considering the disturbed rock to be Mohr/Coulombian with reduced cohesion and internal friction within 0.3 or 0.5 m distance from the periphery of a tunnel with circular cross section. The diameter was taken to be 2.4 m for making the analysis applicable also to the VLH concept.

The following criteria and conditions were chosen for the study, which concerned 2D conditions:

Model:

Dimensions 25x25 m with quadrant symmetry and roller boundaries and the grid shown in Fig.38

Primary stresses:

1. Anisotropic conditions with

$$\sigma_h = 25 \text{ MPa}$$

$$\sigma_v = 10 \text{ MPa}$$

and

2. Isotropic conditions with

$$\sigma_h = \sigma_v = 17.5 \text{ MPa}$$

Material properties:

Young's modulus $E = 38 \text{ GPa}$

Poisson's ratio $\nu = 0.21$

Density 2.63 t/m^3

Condition of disturbed zone (0.3 or 0.5 m):

Cohesion 0.5, 1, 2, 4, 6, 8, 10, 15, and 20 MPa

Angle of internal friction 50 or 65°

Dilatancy 0 or 15°

Mode of procedure:

1. Assume perfectly elastic conditions in the excavation phase
2. Redefine the material in the disturbed zone so that Mohr/Coulombian failure can take place and ascribe cohesion, friction and dilatancy to the disturbed zone
3. Reduce the cohesion stepwise and run calculations for equilibrium at each step

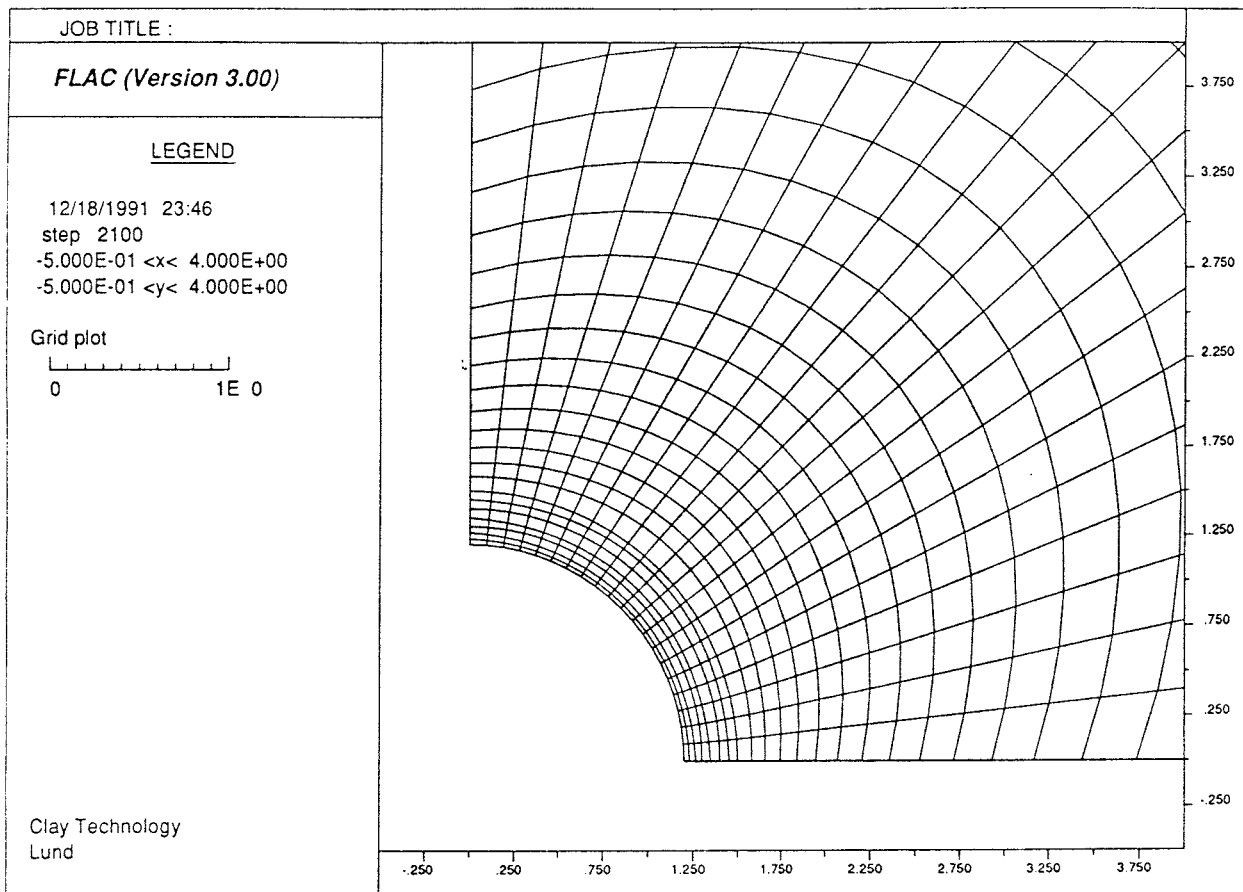


Fig.38 Grid net for the FLAC study

The following major results were obtained from the study of displacements and stress relaxation in the disturbed zone which plasticizes, as well as of the influence on the hoop stress in the rock beyond this zone:

Displacements:

- * Where anisotropic primary stress conditions of the present order prevail, radial movements are inwards except from about 0.5 m above the crown where upward displacement take place (Fig.39). This observation applies also in the case of a completely elastic material and is in agreement with analytical solutions

- * The crown region is sensitive to shear strength reductions because the primary stress anisotropy causes the major stress to be tangential to the tunnel periphery, yielding a strongly deviatoric stress state. This is not the case at the springline where the initial stress anisotropy is counteracted by stress redistribution

- * The actual magnitude of the radial expansion of the disturbed zone depends on all the Mohr/Coulomb parameters. At cohesions higher than about 8 MPa the expansion is less than 150 μm at the crown and floor, while it is 200-700 μm at 2 MPa cohesion, and up to 1100 μm at 0.5 MPa cohesion and 50° friction angle and 15° dilatancy (Fig. 40). This points to the same effect as demonstrated in Fig.36, namely a strongly increased axial conductivity in the roof and floor.

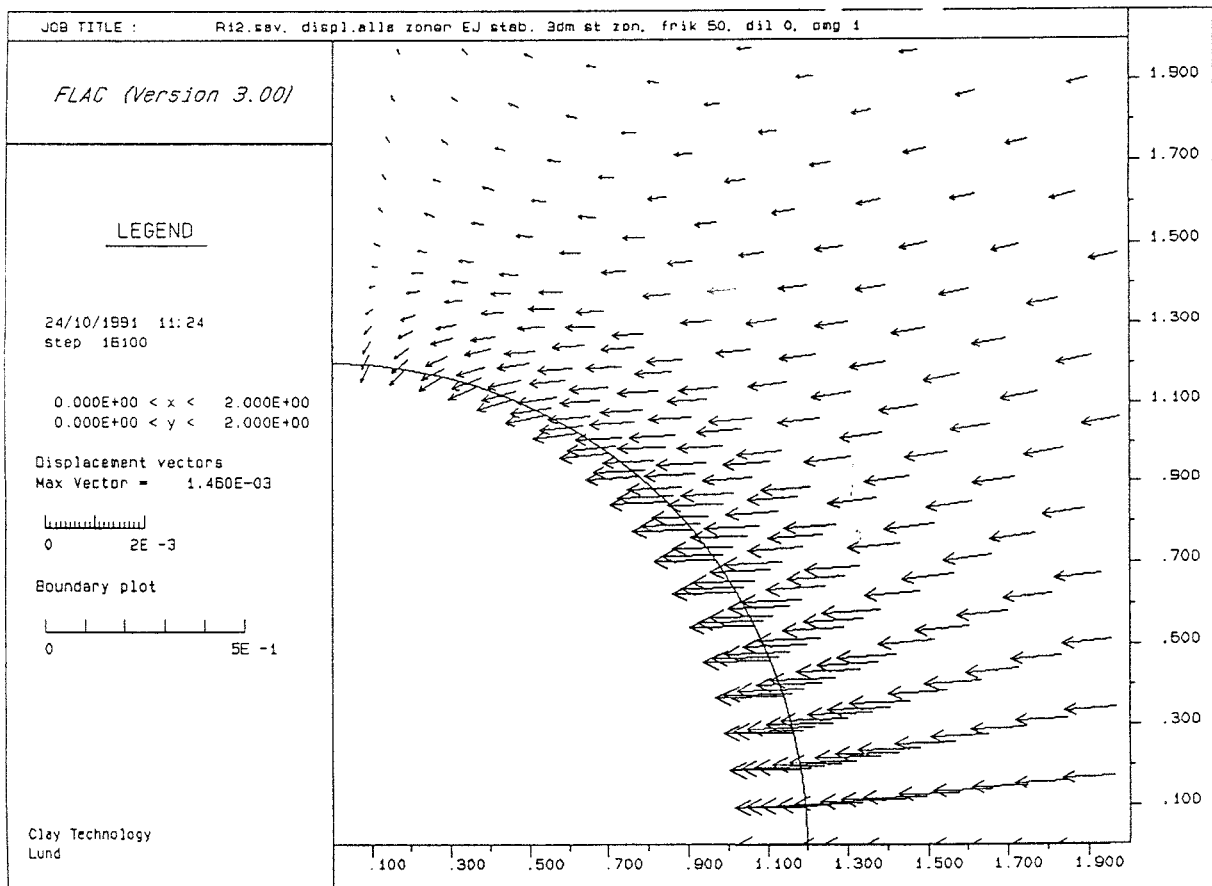


Fig.39 Displacement vectors for 0.3 m disturbed zone

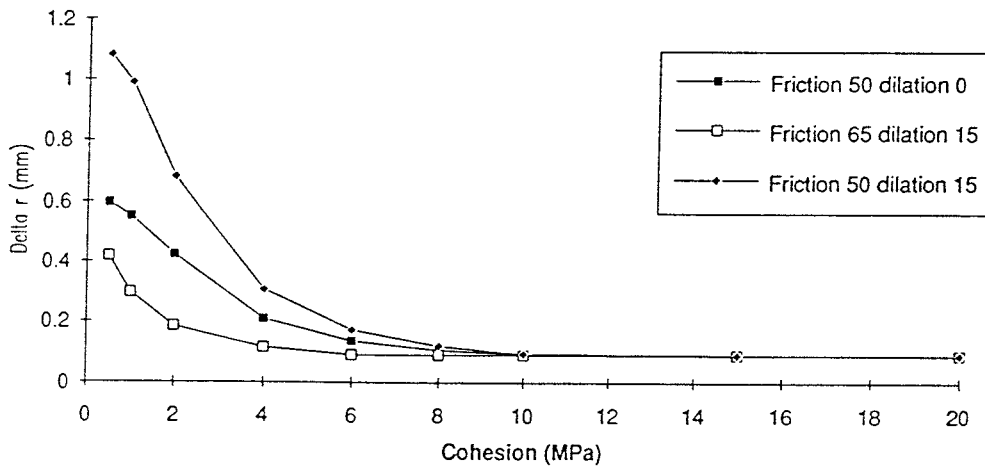
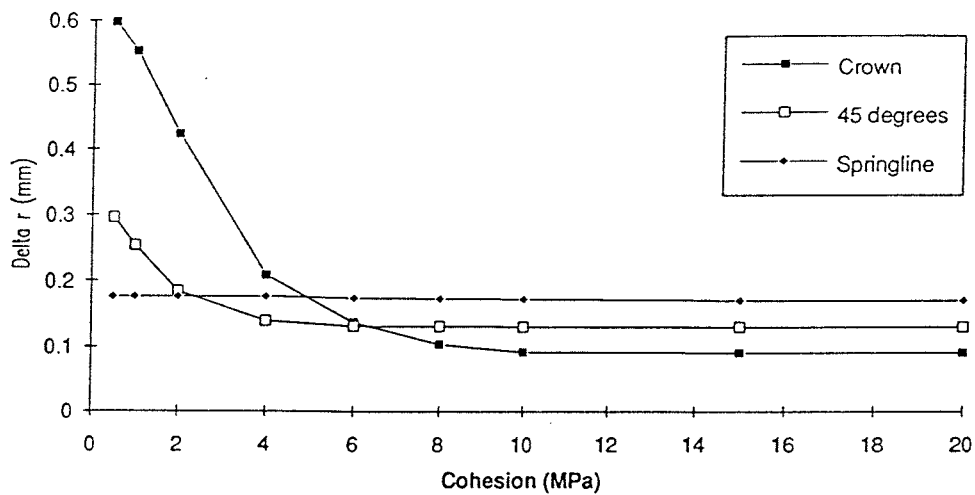


Fig.40 Expansion of the disturbed zone. Upper: Influence of cohesion. Lower: Effect of friction and dilatancy at the crown

Hoop stresses:

* The stress relaxation in the disturbed zone is very small at cohesions higher than about 8 MPa, while it is very significant at 2 MPa cohesion for which the hoop stress at the periphery is only about 15 % of the theoretical case of completely preserved elasticity (Fig.41). This

means that the peak hoop stress is moved to just beyond the outer boundary of the disturbed zone while the stress is still considerable in its outer part. For disturbances leading to 0.5 MPa cohesion, the entire disturbed zone undergoes very considerable stress relaxation associated with expansion. This is what one expects when applying normal blasting

* The influence of even strongly disturbed zones with a radial extension of 0.5 m is very moderate at larger distance from the periphery than twice the radius of the tunnel (Fig.42)

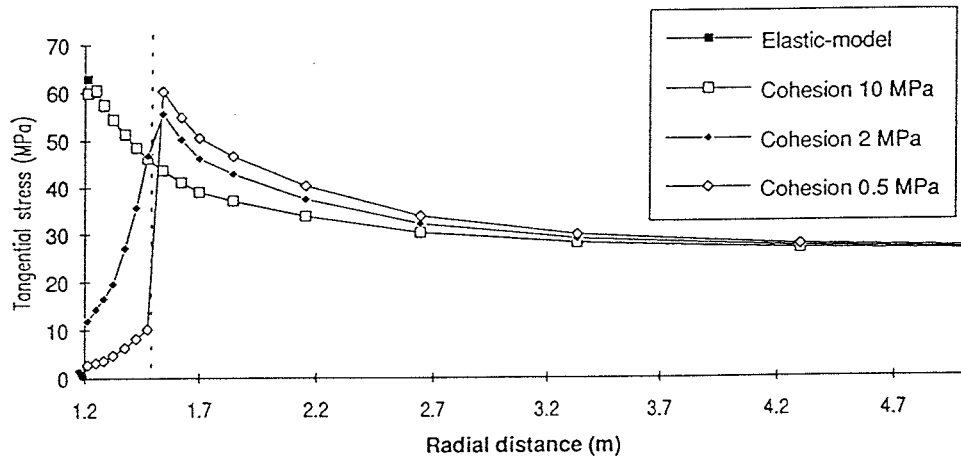


Fig.41 Influence of the cohesion on the hoop stress

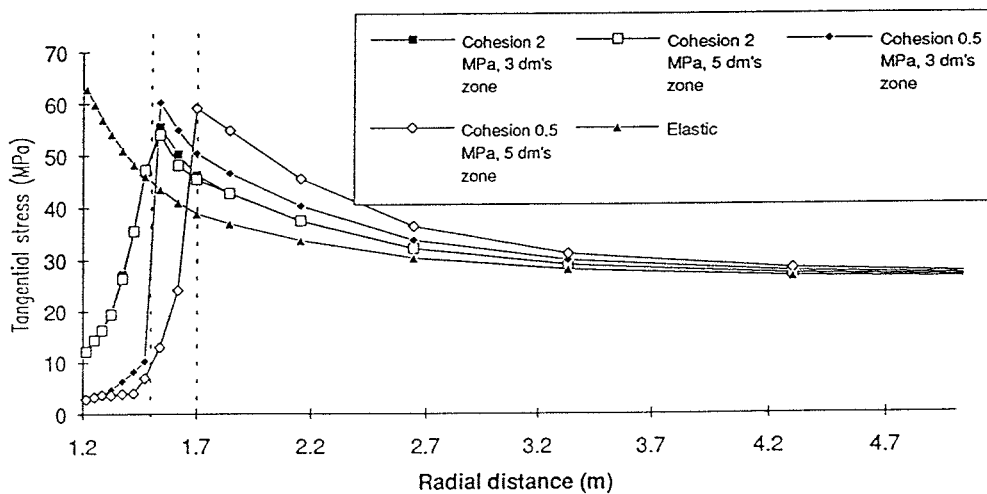


Fig.42 Effect of depth of disturbed zone and its cohesion

General stress state:

- * The stress-distributing effect of shallow zones of disturbance and their cohesion is illustrated by the contours of the principal stress fields (Fig.43). When the disturbance is small, like when very careful blasting is applied, the entire surrounding rock mass is strongly engaged in carrying the rock stresses. In this case creep effects yielding time-dependent shearing of joints is expected to be more pronounced than in the case of strong disturbance caused by normal blasting

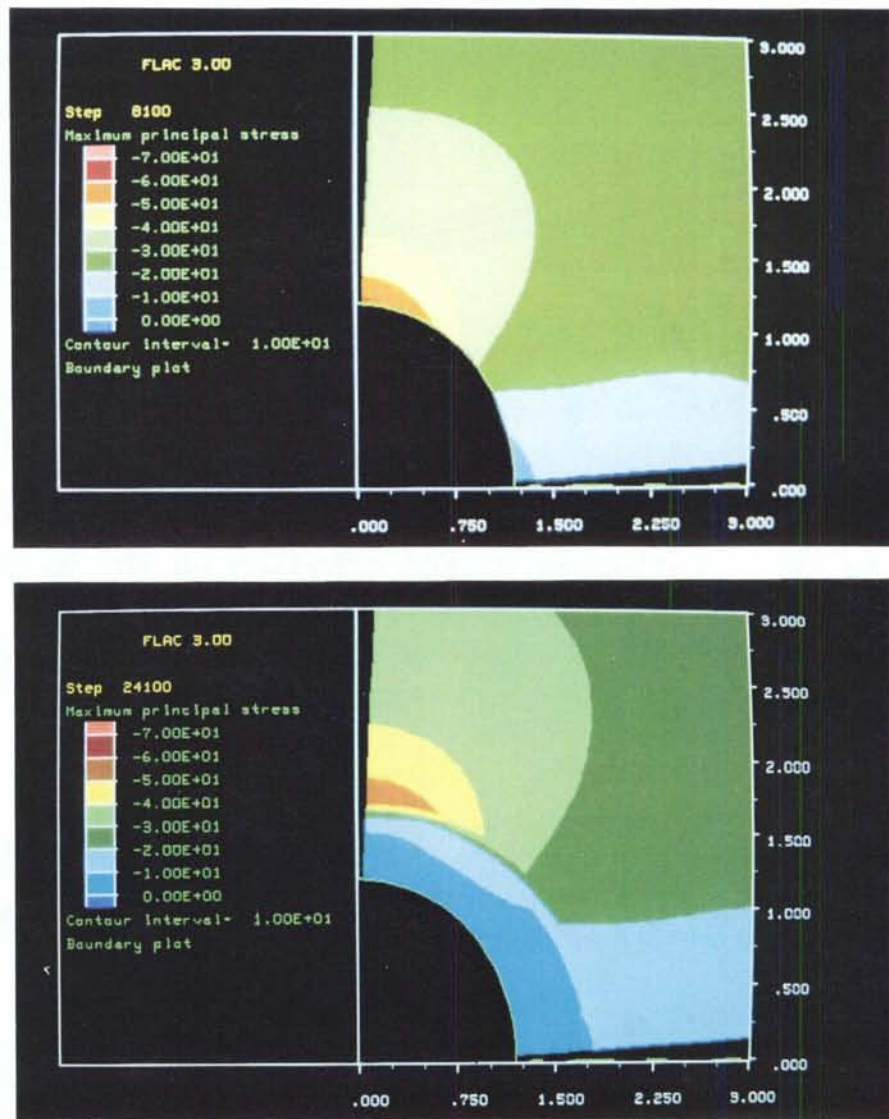


Fig.43 Contours of major principal stress. Upper: 0.5 m zone 10 MPa cohesion. Lower: 0.5 m zone, 0.5 MPa cohesion

4.2.3.2 Deposition holes

Using characteristic fracture patterns and 2D analyses of rock movements around drilled holes one concludes that shear displacements along natural fractures will probably not exceed a few hundred microns, meaning that the system will behave almost completely elastically. The apertures of natural fractures of the 4th order type are insignificantly altered and although some 5th order fractures may be activated they will probably not contribute much to the conductivity of the rock mass. However, it is clear that since the radius of influence of the stress redistribution caused by the tunnel excavation reaches down to about half the depth of the deposition holes, their upper half will be located in structurally altered rock with enhanced conductivity in the axial direction of the tunnels. The influence on the hydraulic conductivity of the surrounding rock of the up to 10 MPa high swelling pressure on the walls of the holes is insignificant.

The hoop stresses will be less than 100 MPa, which means that the rock crystal matrix will stay intact, except for the close vicinity of the hole peripheries, where some microstructural breakdown will take place in the course of the drilling.

4.2.4 Influence of location and orientation of tunnels and deposition holes with respect to structural features

4.2.4.1 General

The 2D- and 3D-based investigations referred to in Ch.4.2.3.1 included estimation of the influence of tunnel orientation on the change of aperture of certain major critical fractures in the BMT drift by

applying the numerical code 3DEC (9). The study had the form of a rather comprehensive investigation with the aim of investigating also the importance of the implicate assumptions made in 2D analysis.

4.2.4.2 Tunnels

Fig.44 illustrates displacements in different parts of the BMT rock. The influence of orientation of the tunnels on the fracture aperture was found to be very important at reorientation of the oblique set termed 1 in the figure, i.e. the set with the largest spacing, which yields considerable block movements in the lower right corner. Fig.45 gives the relationship between the orientation of this set and the maximum aperture of all major fractures and it indicates that a larger angle than 15° between the strike of Set 1 and the direction of the tunnel axis reduces the influence on the apertures very significantly.

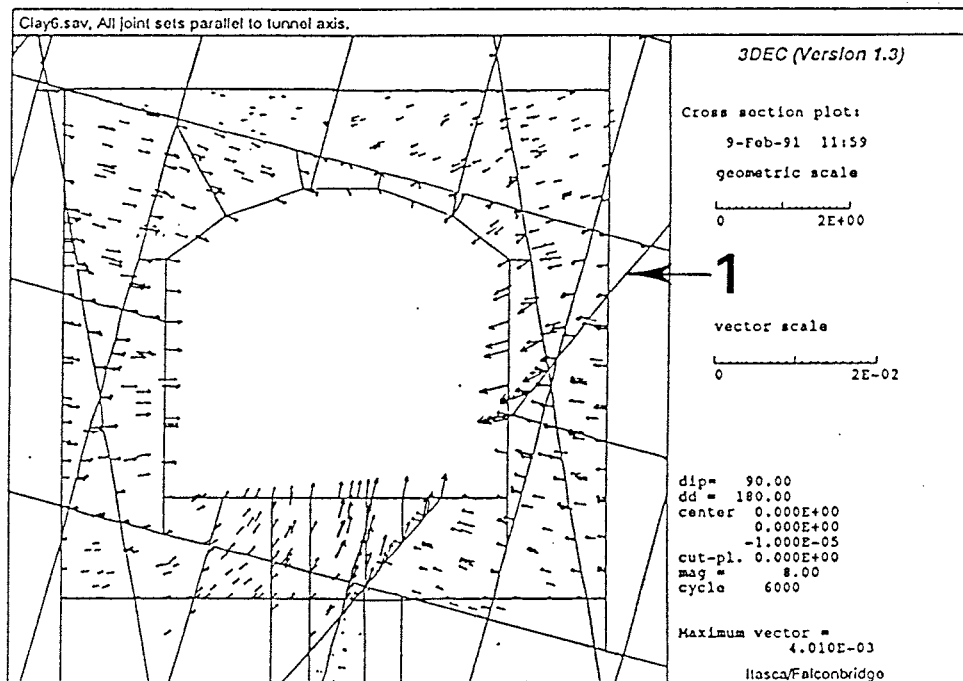


Fig.44 Displacements around KBS3 tunnel in BMT-type rock

It is concluded from the 3D-analyses and from 2D-calculations assuming restricted lengths of the fractures that the orientation of tunnels with respect to the prevailing major fracture sets is most important for the axial hydraulic conductivity of the nearfield of KBS3 tunnels. Hence, if the tunnels strike approximately parallel to major 3rd or 4th order discontinuities, there will be maximum chance of long-range passages for axial water flow. Figs.46-48 serve to illustrate the difference in flow path length and connectivity when varying the angle between the tunnel axis and the strike of major steep discontinuities from 0 to 30°. The radial flow in the shallow zone of activated 5th order breaks would also normally be enhanced according to the model.

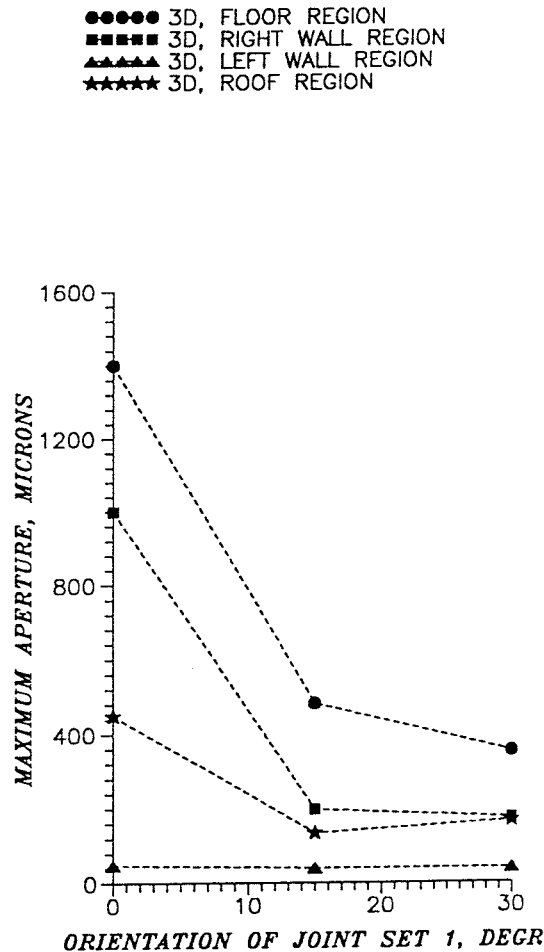


Fig.45 Influence of orientation of Set 1, with respect to the tunnel axis, on the maximum joint aperture. All other joints are taken to be parallel to the tunnel

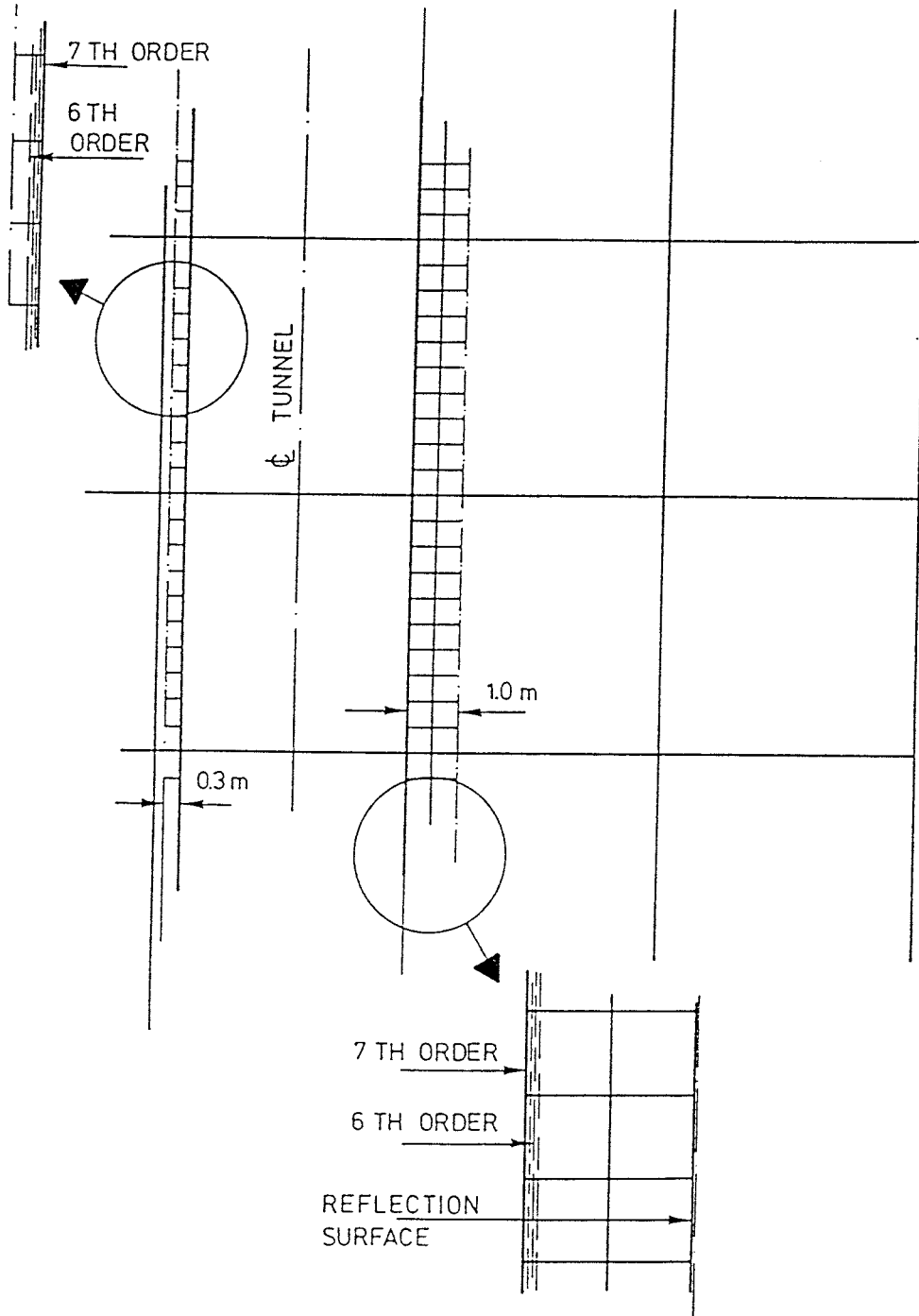


Fig.46 Schematic picture of KBS3 tunnel with its axis parallel to the strike of one major steep fracture set

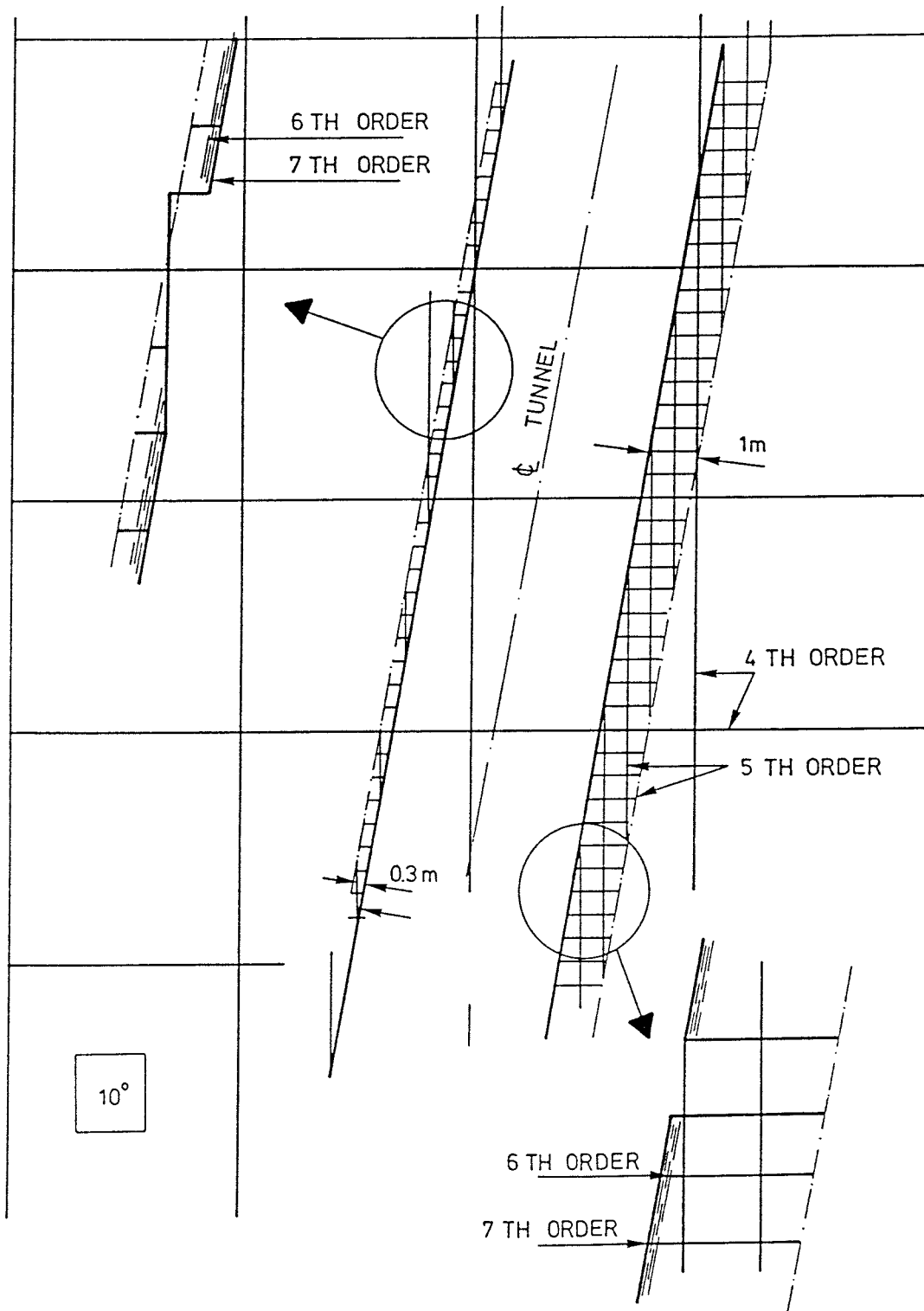


Fig.47 Schematic picture of KBS3 tunnel with its axis deviating 10° from the strike of one major steep fracture set

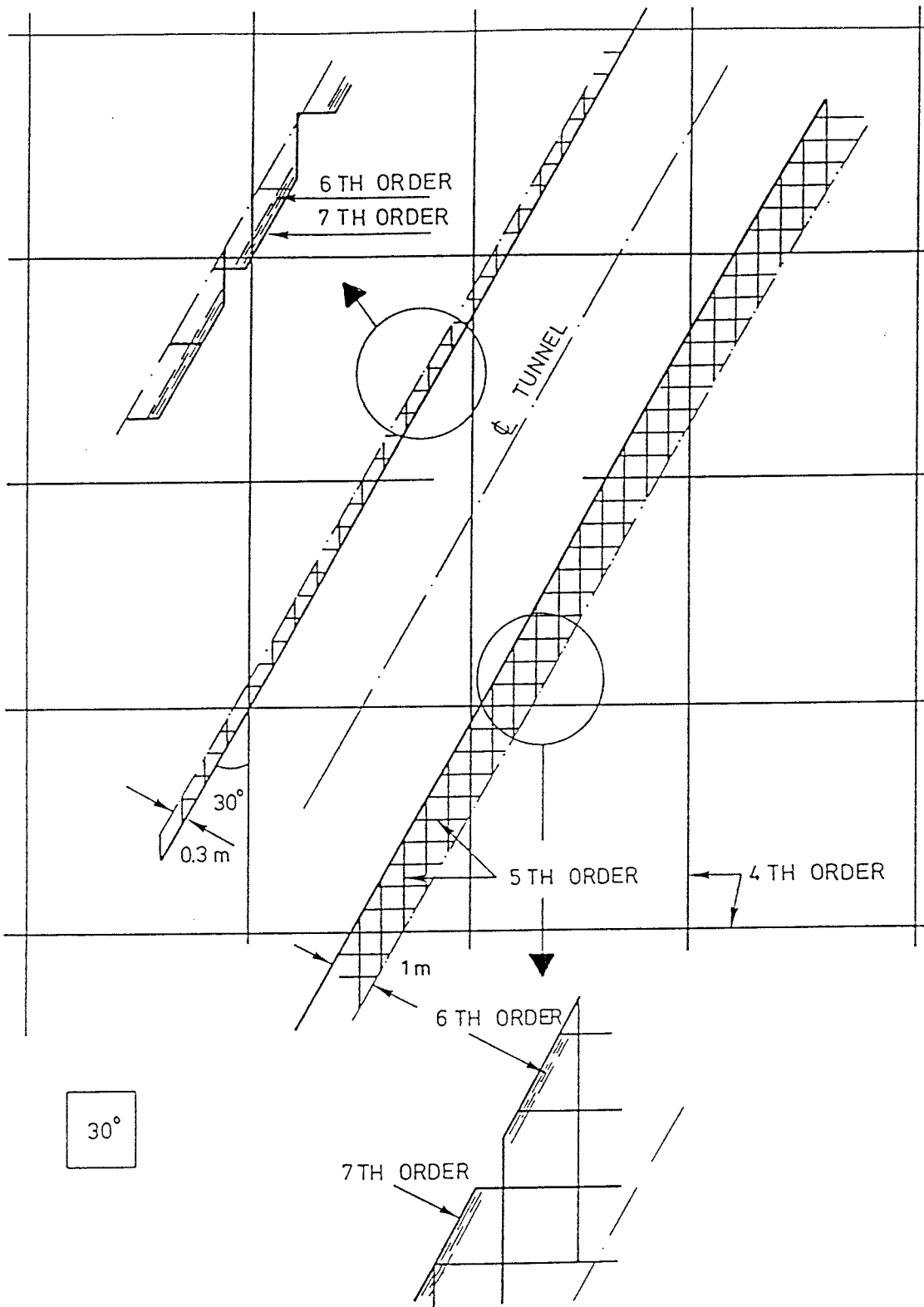


Fig.48 Schematic picture of KBS3 tunnel with its axis deviating 30° from the strike of one major steep fracture set

Theoretically, 45° - corresponding to N/S orientation of the tunnel axis - would be ideal in large parts of Sweden, but considering the actual strike undulation, indicated in Fig.17, one still has to accept that straight tunnels will be locally parallel or almost parallel to major discontinuities over a considerable part of their total length. The diagram in Fig.43 illustrates that if no respect is paid to proper orientation of the tunnels, the fraction of the total tunnel length where the angle between the strike of the tunnel axis and that of major steep 4th order fracture sets is less than $10-15^{\circ}$ can amount to 35 %. Since large-scale undulation of major structures in other areas may be different from that derived from the Stripa study, the conditions may be more critical and there are reasons to assume that this percentage may be higher. At any rate it is clear that the axial hydraulic conductivity along tunnels can be effectively minimized by orienting them in a suitable way with respect to the geological structures.

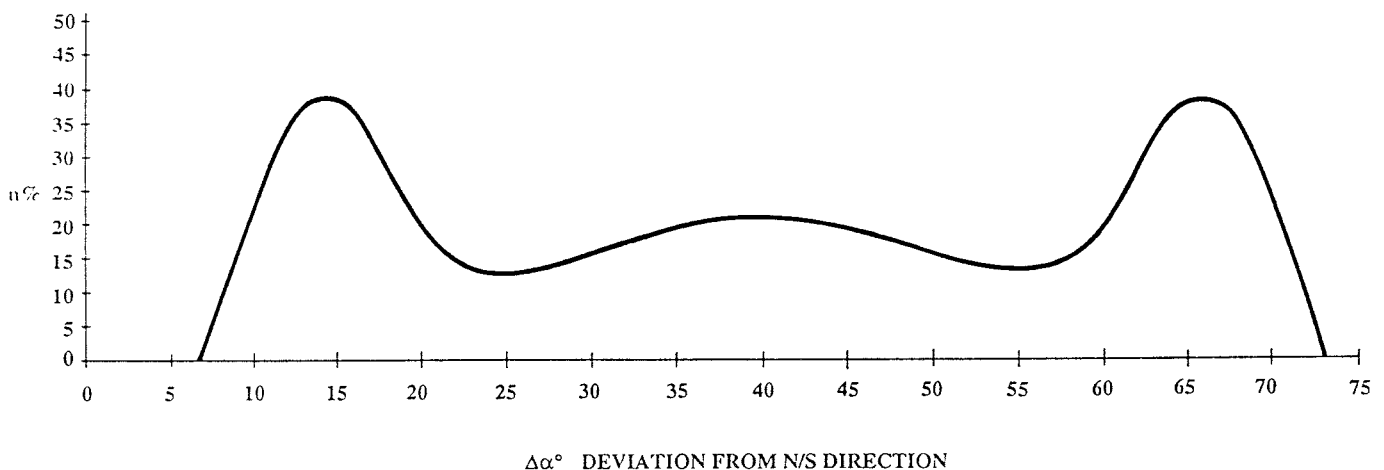


Fig.49 Fraction (n%) of tunnel length where the deviation between strikes of tunnels and steep fracture sets is less than $10-15^{\circ}$

The effect of tunnel orientation indicated in Figs. 46-48 is actually very well illustrated by the features seen in tunnel walls in the Stripa mine as illustrated by Figs.50-57. In these figures, which refer to the eight locations indicated in Fig.14, the result of mapping of $2 \times 10 \text{m}^2$ areas of the rock wall are given with respect to:

1. Exposure of major intersecting fractures (3rd, 4th and 5th order)
2. Exposure of blasting holes
3. Presence and frequency of schistosity
4. Frequency of open fissures (6th order)
5. Profile of rock wall
6. Strike of major fractures and of tunnel

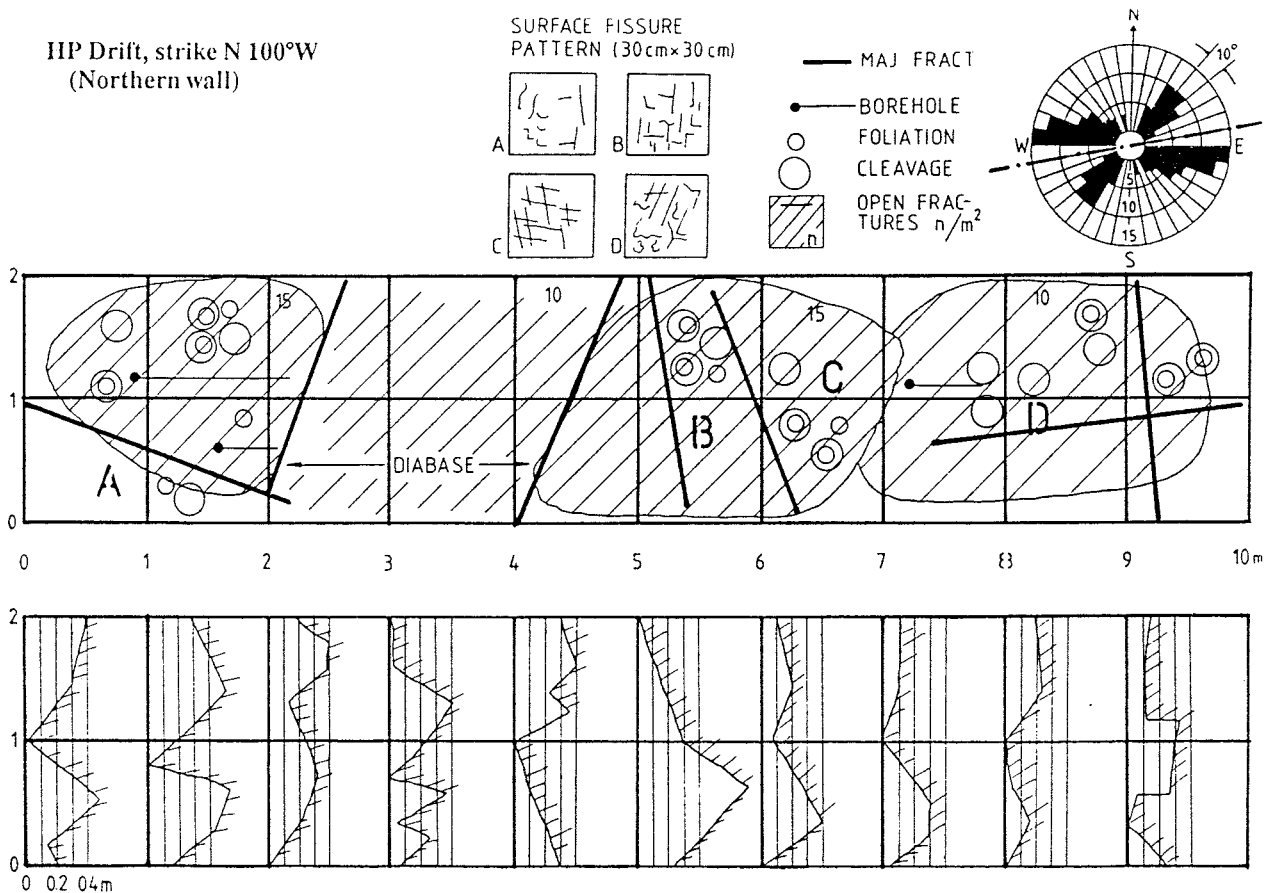
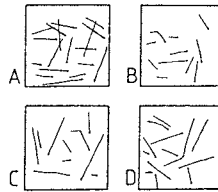


Fig.50 Mapping of tunnel wall in the Stripa mine (A in Fig. 14). The spacing of steep 4th order fractures is small (2m) due to diabase intrusion (2 m)

Extensometer drift (addit), strike N 5°W
(Eastern wall)

SURFACE FISSURE
PATTERN (30cm×30cm)



— MAJ. FRACT.

● BOREHOLE

○ FOLIATION

○ CLEAVAGE

▨ OPEN FRACTURES n/m^2

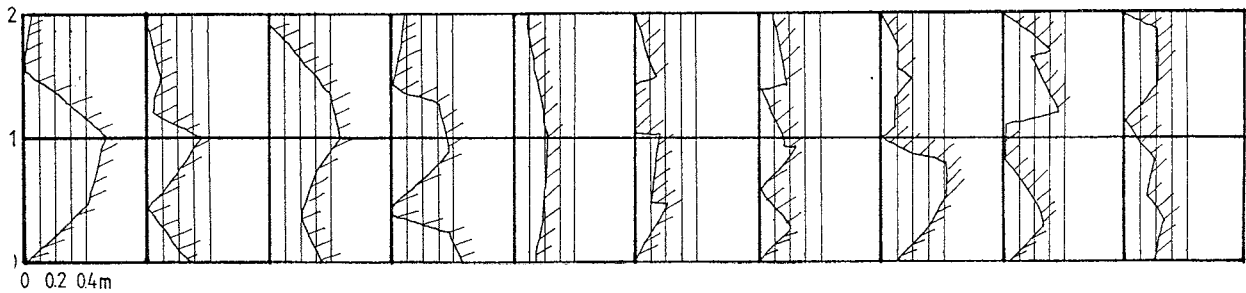
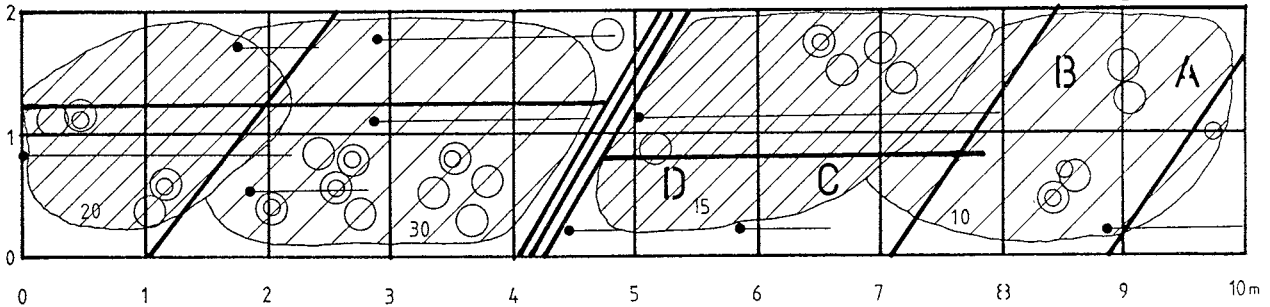
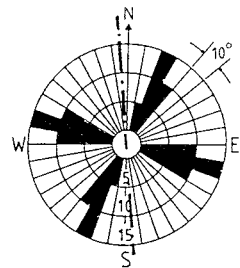
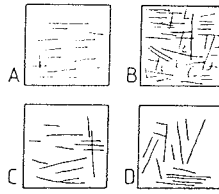


Fig.51 Mapping at site B. One 3rd order fracture (zone) in the center. Spacing of major steep 4th order fractures about 4 m. Very irregular profile due to 25° deviation of tunnel axis strike from strike of major (NNE) fractures. Schistosity and foliation very moderate

Extensometer drift, strike N 50°E
(Northern wall)

SURFACE FISSURE
PATTERN (30 cm×30 cm)



— MAJ FRACT.

● BOREHOLE

○ FOLIATION

○ CLEAVAGE

▨ OPEN FRACTURES n/m^2

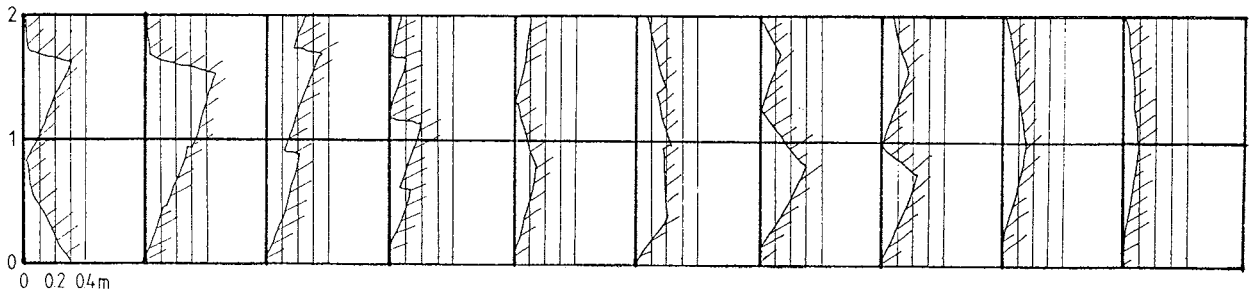
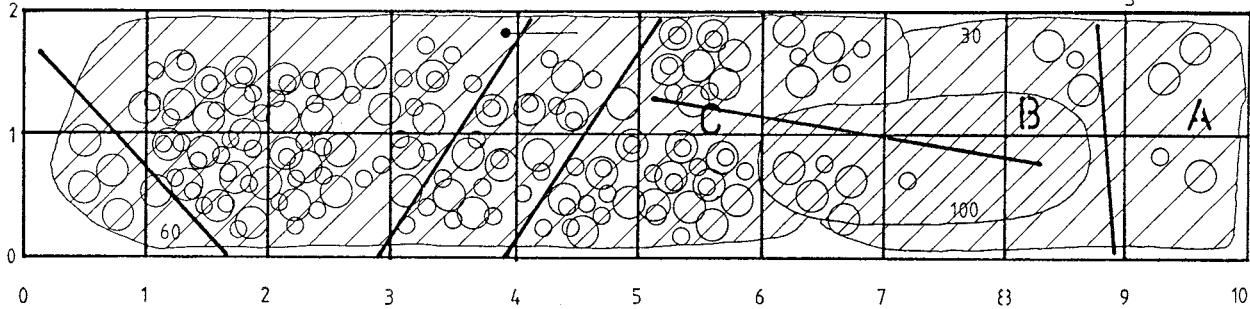
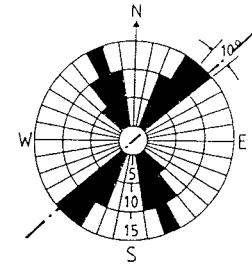


Fig.52 Mapping at site C.
Spacing of major
steep 4th order
fractures about 5
m. Rather plane
profile and very
strong "schisto-
sity" because the
wall is parallel
to major NE frac-
ture set

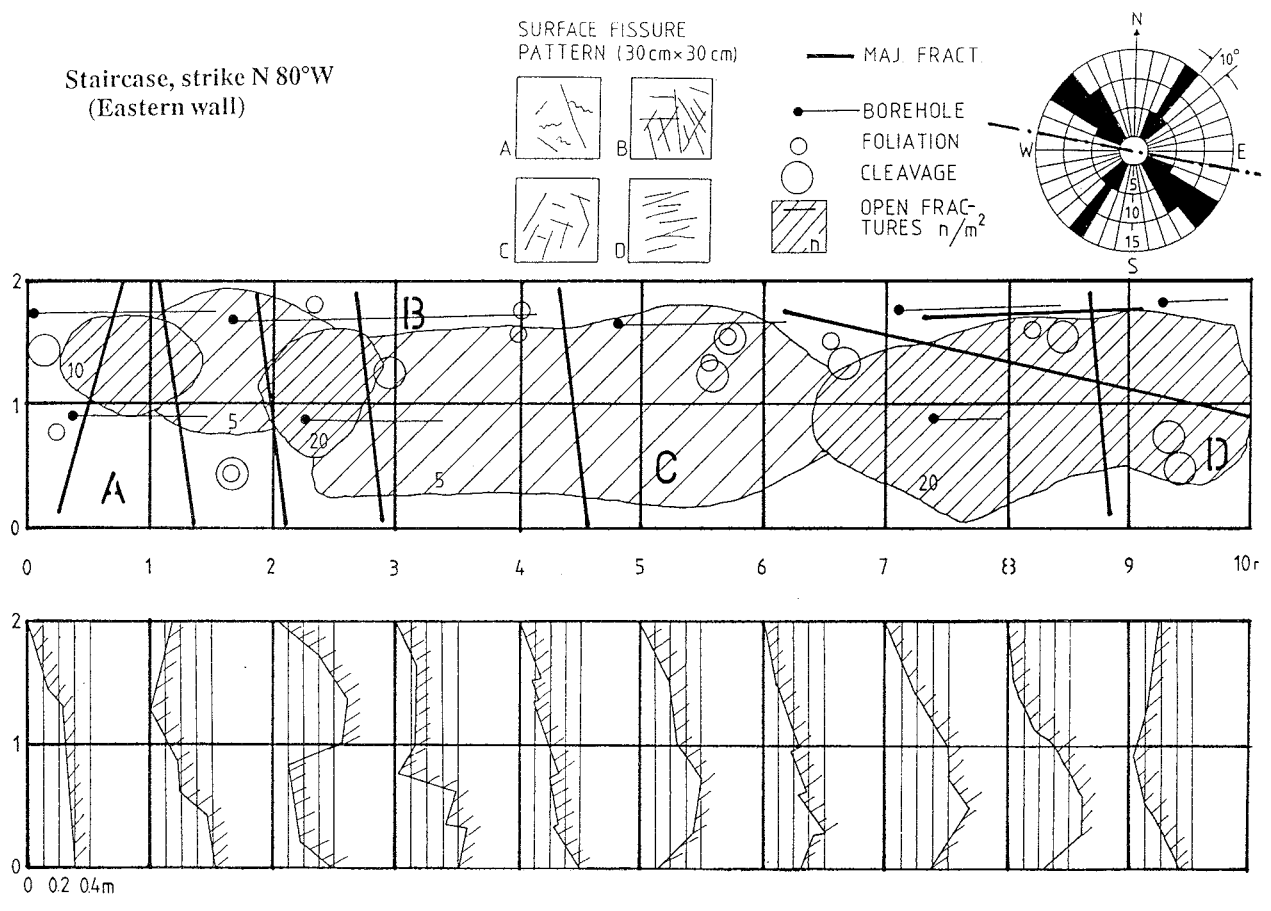


Fig.53

Mapping at site D. Three 4th order fractures (1-3 m on scale) form one set. Average spacing of 4th order fractures about 3 m. Very irregular profile and short boreholes due to 25° deviation of tunnel axis strike from strike of major (NW) fractures. Foliation very moderate

Photo shows regular flatlying set of 6th order fractures

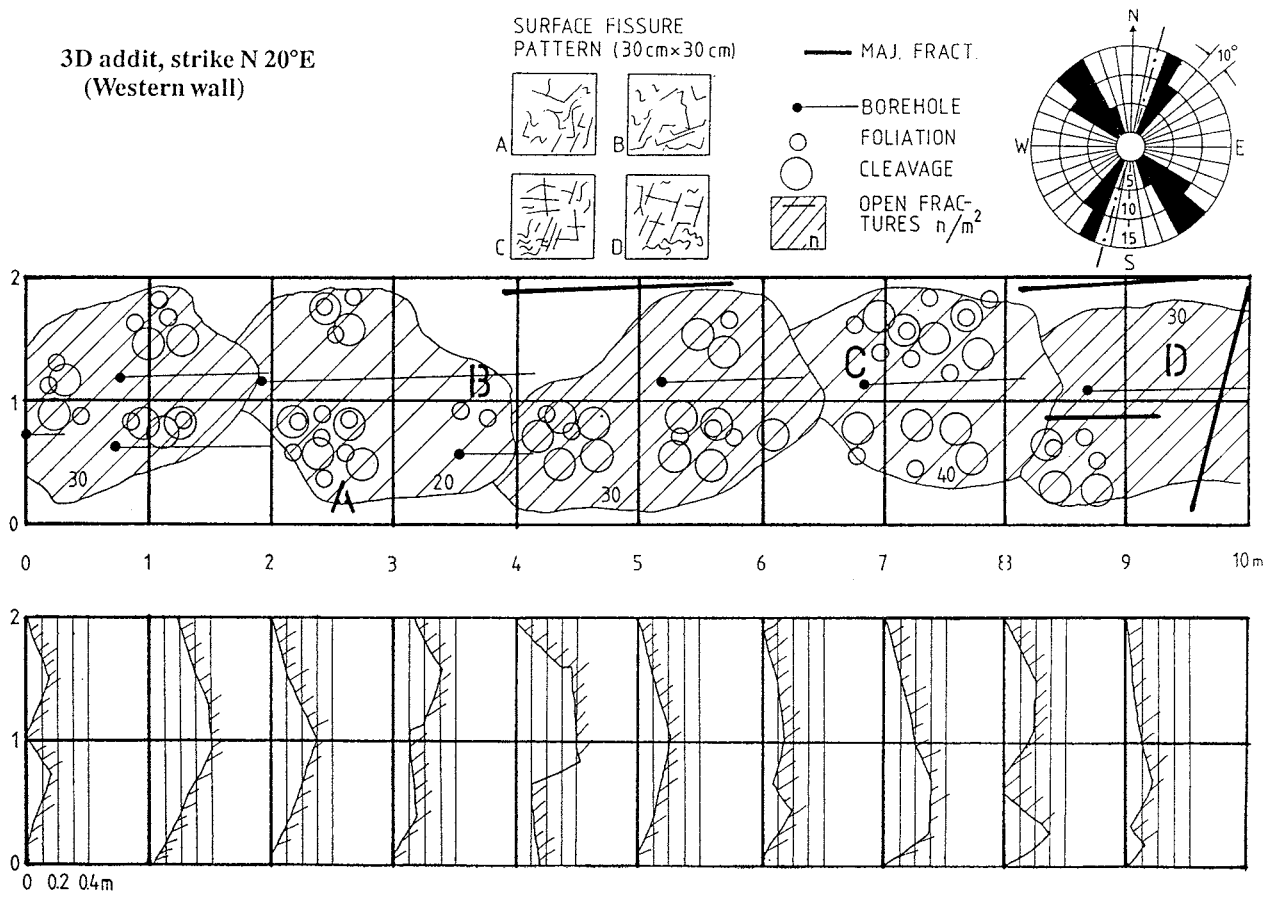


Fig.54 Mapping at site E. Average spacing of steep 4th order fractures 5-10 m. Rather plane profile and relatively rich foliation due to near parallel tunnel axis and strike of major (NNE) fractures (10° deviation)

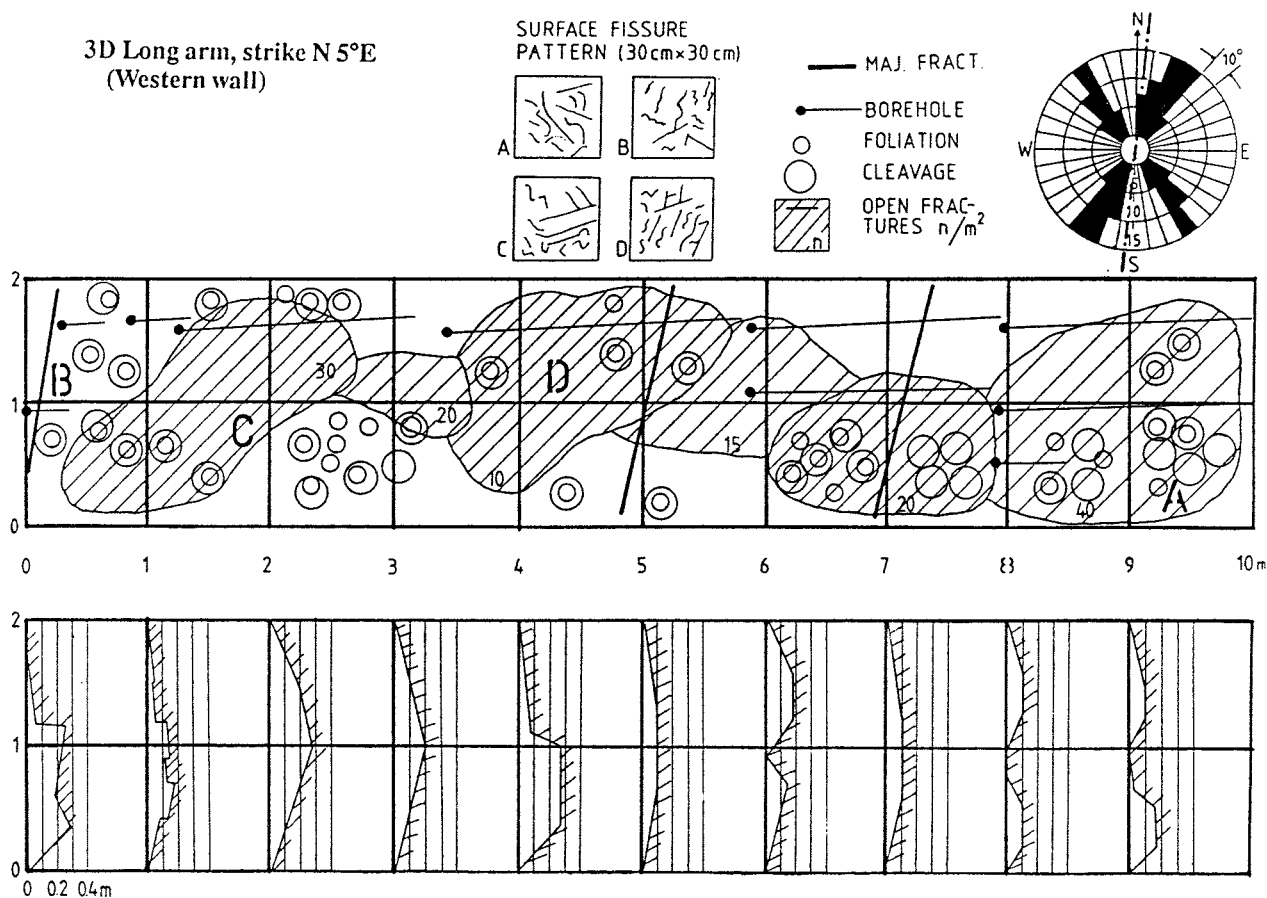


Fig.55 Mapping at site F. Similar observations as at site E are logical since the orientation of both tunnels was almost the same with respect to the strike of major steep 4th order fractures

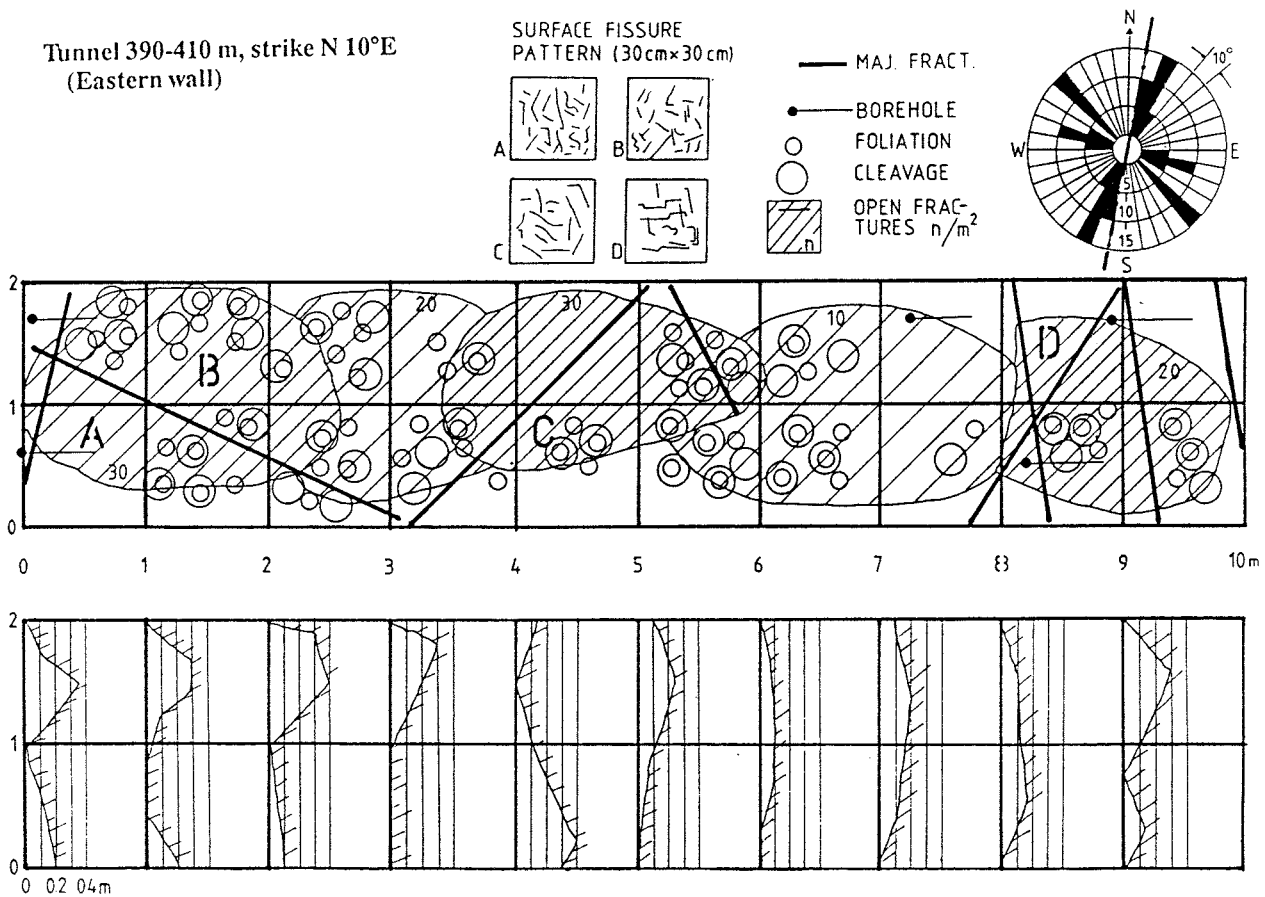


Fig.56 Mapping at site G. Average spacing of (sets) of 4th order fractures about 4 m. Rather plane profile and relatively strong schistosity due to near parallelism of tunnel axis and strike of major steep (NNE) fractures. Very few blast-holes due to foliation and trimming as in Fig.52

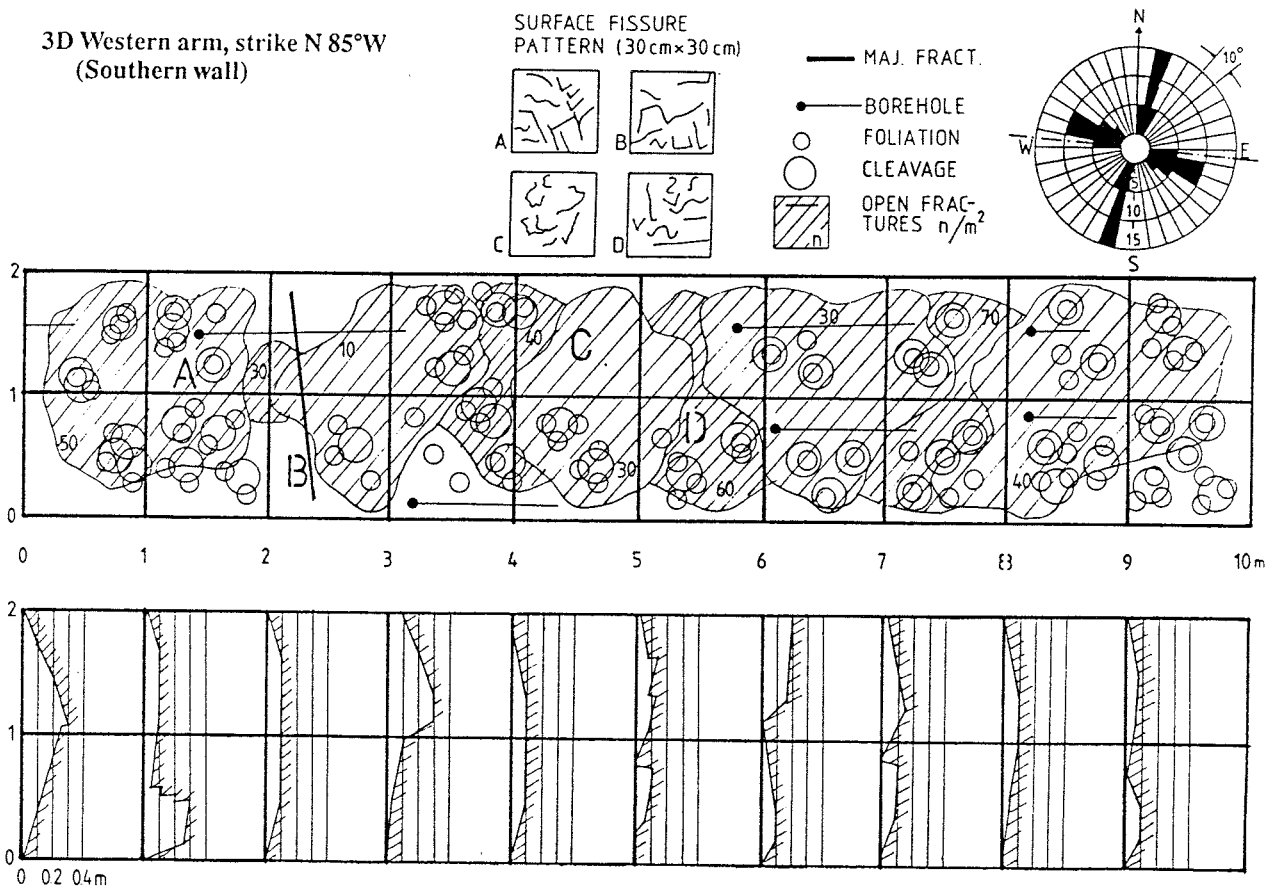


Fig.57 Mapping at site H. Average spacing of 4th order fractures 5-10 m. Very plane profile, few blast-holes and strong schistosity due to almost parallel tunnel axis and strike of major steep (WNW) fractures

The major outcome of the field observations at Stripa can be summarized as follows:

1. If the strike of the tunnel deviates by more than about $10 - 15^{\circ}$ from the strike of one of the steeply oriented fracture sets, there is a low degree of interconnectivity of natural water passages and of induced passages by blasting and stress changes close to the walls
2. The fact that horizontal or nearly horizontal tunnels are largely parallel to the system of flatlying fractures that is always present, the interconnectivity of flow passages in the floor and roof should be high independently of the strike of the tunnel
3. A very typical effect of "overstressing" the rock at the periphery of tunnels due to the combined effect of high static hoop stresses and the impact of blasting, is shallow foliation. Its practical implication is very important: *The high number of very thin fractures can not be effectively sealed by grouting or by backfilling, while they are wide enough to yield a significant axial hydraulic conductivity.*

The foliation, which is richly developed and produces schistosity when tunnels are nearly parallel to the strike of major fracture sets, is very clearly illustrated by the higher frequency of 6th order fractures in the first few decimeters from the tunnel periphery than deeper into the rock. Thus, Fig.58, in

which data from Stripa drill cores are compiled, shows that the number of "disc-type" fractures increases from 3-4 in the first 2 decimeters to 1-3 in the next 3 decimeters, while it drops to 1-2 per meter at more than 2 m distance from the free surface.

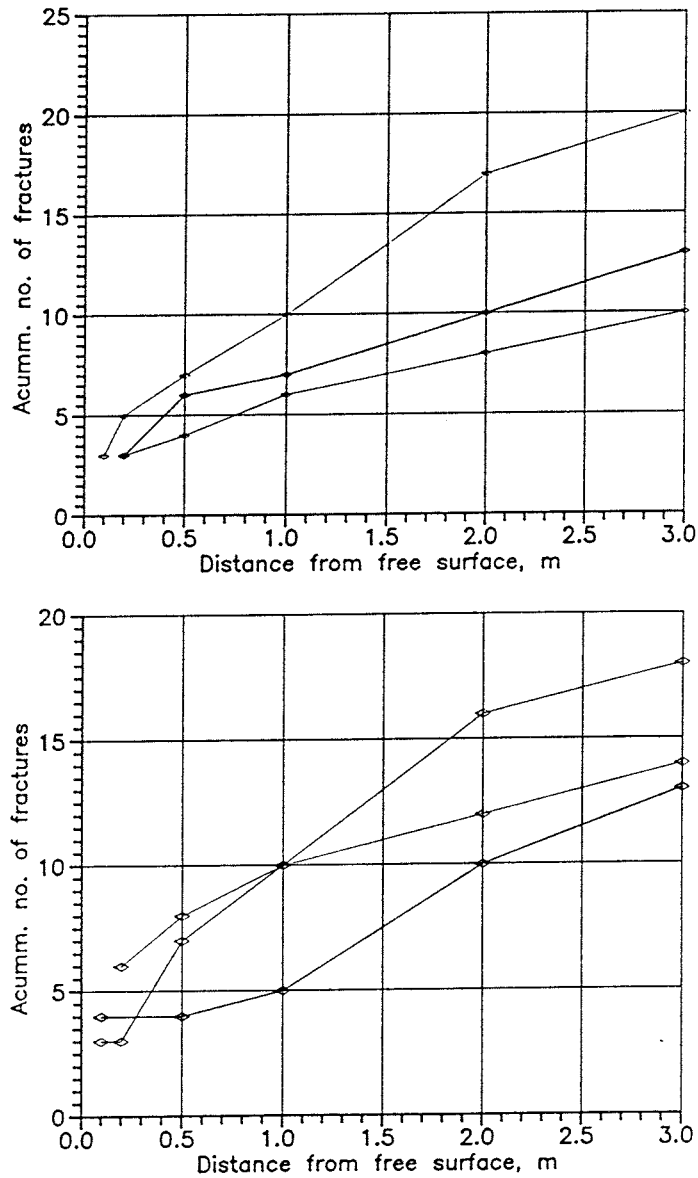


Fig.58 Diagrams from Stripa showing frequency of "disc-type" fractures in cores as a function of the distance from the free wall surface. Upper diagram represents non-parallel tunnel and strike of major fractures, while the lower diagram represents parallelity

4.2.4.3 Deposition holes

A special effect of stress redistribution is caused when the holes are located so that rock wedges are formed (Fig.59). Since the spacing of 4th order fractures is almost the same as that of the deposition holes it is realized that wedges will appear in a large fraction of the holes in a repository although there is a reasonable chance of minimizing it by proper location of the individual holes. The change in aperture of the fractures forming the boundaries of wedges that can become completely separated from the "host rock" can only be roughly estimated by use of numerical methods since unstable conditions will prevail. 3D calculations are required for reasonably accurate calculation of aperture changes of stable wedges but 2D analyses using reasonable rock stress and joint properties serve to indicate the order of magnitude of fracture expansion as illustrated by a simple study reported in Fig.60. It refers to the case of long 1.5 m diameter holes with parallel fractures at different distance from the periphery for simulating a rock wedge and suggests that local fracture widening by a few tens of micrometers will take place over the larger part of steep wedges except where unstable conditions prevail (upper picture). Where the fractures are exposed in the holes, bentonite clay may enter and help to seal them and they will also tend to be compressed and partly closed by the swelling pressure exerted by the canister-embedding dense clay.

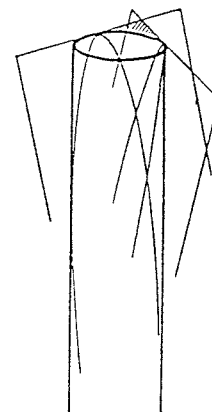
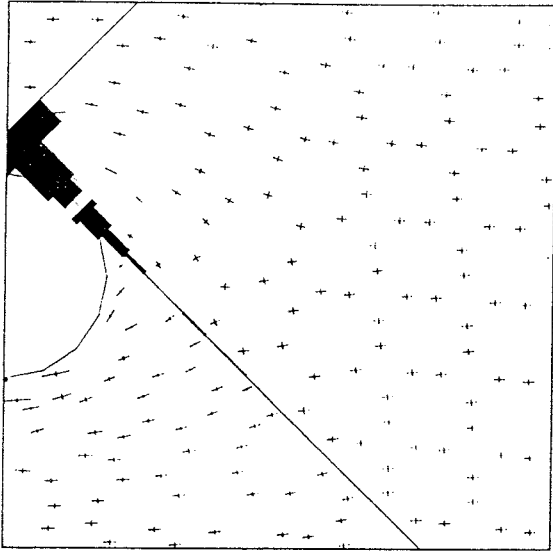
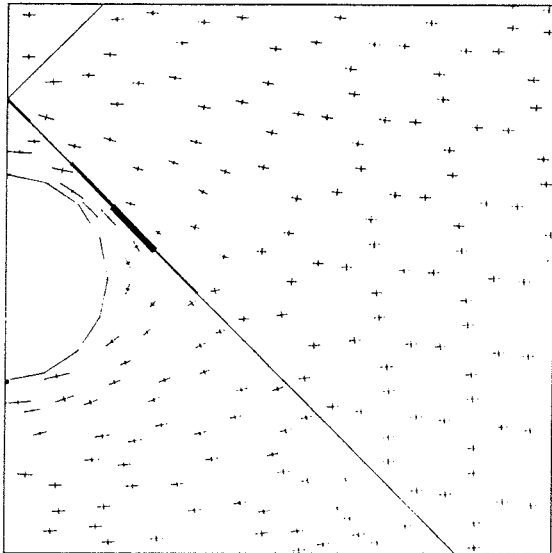


Fig.59 Rock wedge formed in deposition hole



Max. hoop stress 53 MPa
 Max. apert. exp. 430 μm

Detached block makes
 apert. cal. uncertain



Max. hoop stress 49 MPa
 Max. apert. exp. 38 μm

Max. hoop stress 46 MPa
 Max. apert. exp. 29 μm

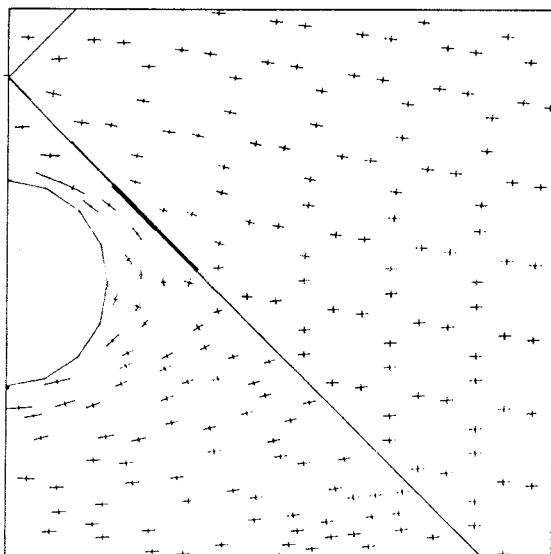


Fig.60

Stresses and estimated changes in aperture along wedge boundaries as simulated by 2D analysis of parallel joints at different distances

4.3 *Thermomechanical effects*

4.3.1 General

Propagation of a heat front from the deposition holes will induce successive expansion of rock blocks by which strain is caused that alters the aperture and extension of hydraulically active fractures and activates previously sealed ones. The influence on fracture apertures can be calculated by use of the aforementioned computer codes as indicated below.

4.3.2 Tunnels

Calculations using the aforementioned 2D computer codes suggest that, in the early heating phase when high thermal gradients prevail close to the deposition holes, the induced displacements in the floor of KBS3 tunnels may be on the same order of magnitude as those caused by excavation. As a rough estimate one can assume that the net effect of thermally induced changes in aperture may yield an increase in average hydraulic conductivity by one order of magnitude during this initial phase of the heating period. Later, the effect on the conductivity is expected to be much less, while the subsequent cooling will lead to some residual fracture expansion. A rough estimate, which needs to be confirmed by 2D and 3D analyses of the entire heating/cooling cycle with due respect to rock creep effects, is that the net effect of excavation and heating and subsequent cooling is taken into consideration by applying the aforementioned rule that the average axial hydraulic conductivity is increased by 2-3 orders of magnitude within 1 m distance from the periphery and by 1 to 2 orders of magnitude within the distance of the tunnel diameter (p.63). This appears to be in fair agreement with the results of large-scale flow tests being part of the Stripa Rock Sealing Project. These tests had the form of driving

water from an inner borehole gallery along the BMT drift, which had been exposed to 40°C, to an outer gallery as illustrated by Fig.61 (3). The tests were conducted in a host rock with a hydraulic conductivity of 3×10^{-11} to 10×10^{-11} m/s such that the axial flow along the drift and also the piezometric pressures could be measured at different locations along the drift and in the surrounding rock.

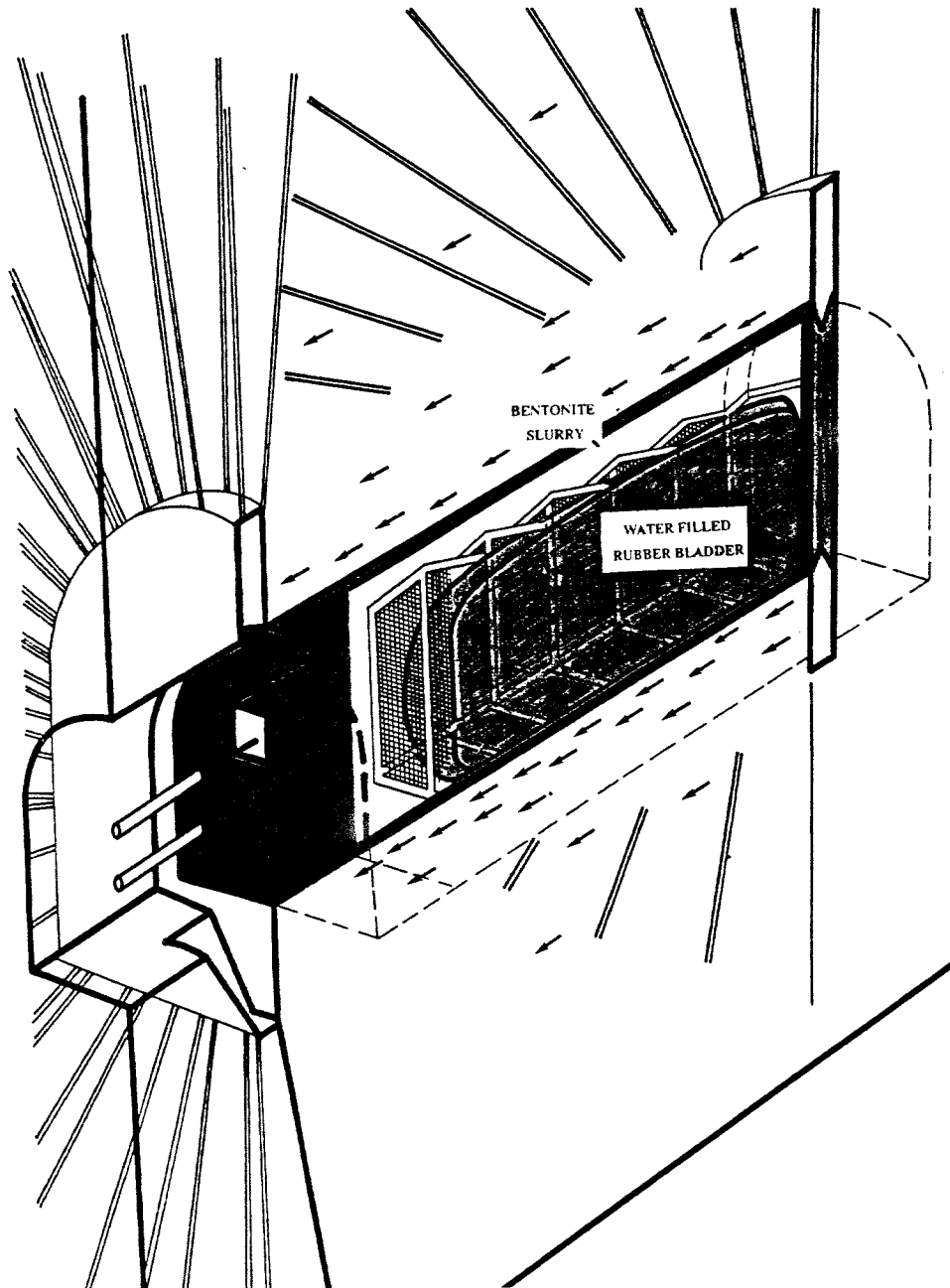


Fig.61 Perspective of the test arrangement at Stripa for measuring the conductivity of nearfield rock. The right, inner slot and borehole gallery were pressurized by which water was driven to the left end

The results from a number of different pressure constellations and flow recordings were satisfied by a FEM model that implied that the disturbed zone within 0.8 m distance from the periphery had an average isotropic hydraulic conductivity of 10^{-8} m/s, and that the conductivity may be as high as 10^{-7} m/s in the most shallow 1-2 dm deep part. The model also implies that stress changes affect the circumscribing rock zone that extends to about 3 m from the periphery such that the axial conductivity is increased by 1 order of magnitude while the radial conductivity is decreased to 1/4 of the original value.

The rock mechanical calculations as well as the field tests (10) show that heating to 80-100°C yields significant upward movement of the rock around the upper half of the deposition holes, which suggests that associated activation of 5th order breaks causes an increase also in *radial* and *tangential* conductivity in the outer disturbed zone below the tunnel floor. Here, the conductivity can therefore be assumed to be more or less isotropic.

4.3.3 Deposition holes

The effects of a heat pulse on the fracture system in the tunnel floor region have been investigated by use of the 3D distinct element code 3DEC applied to the BMT rock structure (10). Fig.62 shows the temperature field after 60 days operation of a 1500 W heat source in the heater hole. All fractures except the one that intersects the lower right tunnel corner were parallel to the tunnel axis. The horizontal fracture, labeled 2, which expanded by about 250 μm during the tunnel excavation phase, was closed approximately by 100 μm during the heating phase. The residual effect of a complete heat cycle was a separation of about

200 μm at maximum for this fracture. The residual effect on the steeply oriented fracture that intersects the heater hole and terminates in the tunnel floor (labelled 1), was a separation of about 20 μm . At the end of the heating stage, parts of this fracture had become closed by about 10 μm .

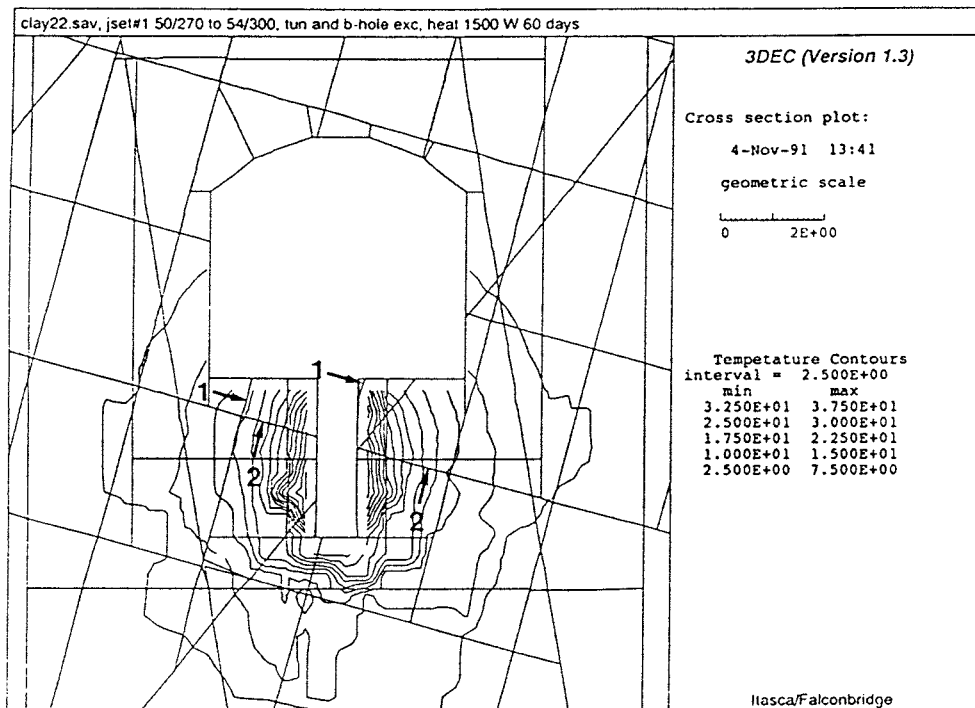


Fig.62 3D analysis of temperatures after 2 months of heating of KBS3 deposition hole (10). Contour interval 2.5 $^{\circ}\text{C}$

The heating is concluded to increase the hoop stresses considerably, i.e. by almost 100 %, which yields pressures of more than 100 MPa, but this is still only about 50-75 % of the figure that would yield spalling. A swelling pressure of at least a few MPa

exerted on the walls by the maturing canister-embedding clay helps to stabilize the rock.

Stripa tests shed some light on this matter as well, since one of the major field tests comprised heating of the large core-drilled holes in the BMT drift in conjunction with an attempt to seal the rock around the holes, which had a depth of around 3 m and a diameter of 0.76 m (10). The hydraulic conductivity was measured before the grouting, and after grouting and heating the holes to a temperature of 100°C with subsequent cooling. The initial conductivity was 4×10^{-7} m/s to somewhat more than 10^{-6} m/s from the tunnel floor down to 0.75-1.0 m, 6×10^{-9} to 6×10^{-8} m/s down to 1.25-1.5 m, and 3×10^{-10} to 2×10^{-9} m/s down to 2.5 m depth. After grouting, the conductivity was reduced by 3 to 1000 times, while heating caused a raise to only somewhat less than before the grouting due to activation of fracture channels that were not hydraulically active before the heating and which had not been sealed by grouting. The increased frequency of major, blast-induced fractures down to about 1 meter depth is exemplified by Fig.63.

An interesting fact is that the total number of leaching points that were visible in the holes before grouting was 31 to 41 distributed over an average of 8 fractures with a total length of around 10 m length, yielding a mean spacing of the channels of around 0.05-0.1 m down to a few dm depth and around 0.5 m deeper down. This is in good agreement with the generalized structure model which implies channel spacings of 0.5 m in the stress-disturbed zone with activated 5th order fractures, and a fissure spacing of the observed type in the most shallow rock that was "overstressed" by high hoop stresses in conjunction with the blasting.

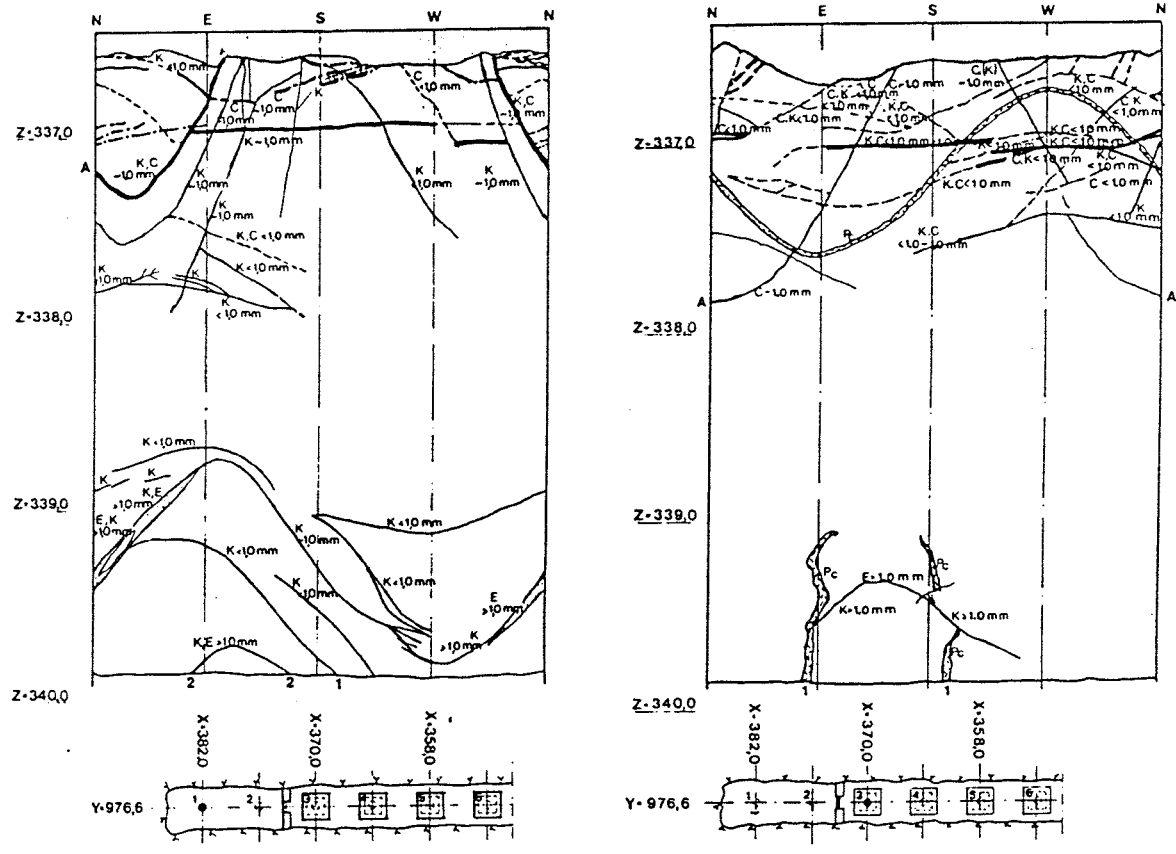


Fig.63 Fracture mapping in large core-drilled holes in the BMT drift. Thick lines in the graphs, which show the entire periphery of two holes, represent strongly water-bearing fractures. Lower pictures show the location of the holes

4.4 Structural model of KBS3 nearfield rock as influenced by disturbances

4.4.1 Basic pattern

We will apply the same basic pattern of discontinuities in the virgin rock as in the VDH case, meaning that the model with "fractal-type" systems of orthogonal discontinuities is assumed to be valid. As in

that case, the system of 4th order, hydraulically active breaks is of major importance for water and radionuclide migration but the very significant impact of blasting and the large size of the tunnels give quite different transport conditions of the nearfield.

4.4.2 "Fine-rock structure"

The integrated effect of the various disturbing factors results in a general model that has different features depending on the orientation of the tunnels with respect to the strike of major fracture sets. Close to the tunnel periphery, the effect of blasting and high hoop stresses is manifested by a shallow zone of expanded, intergrown 6th order fissures. It is assumed to extend to 0.2 to 0.4 m from the periphery.

4.4.2.1 "Conservative" case

Tunnel

The most conservative case corresponds to the 2D plane strain version that has been investigated in most of the computer analyses. In this case, which is illustrated in Figs 46 and 47, the tunnel is almost parallel to one of the steeply oriented fracture sets. With some generalization, and approximating the tunnel section to be circular, one finds the distribution of the hydraulic conductivity in the axial direction to be the one in Fig.64, taking the average hydraulic conductivity of the undisturbed, virgin granite to be 10^{-10} m/s. Referring to the preceding deductions it is possible that the hydraulic conductivity within 1 m from the periphery is three orders

of magnitude higher, i.e. 10^{-7} m/s, with the exception of the roof where the net average hydraulic conductivity can be up to 10^{-3} m/s due to splitting up and blast-disturbance. The most shallow 0.2-0.4 m part of the floor is also expected to be very pervious, a probable maximum hydraulic conductivity being 10^{-6} m/s including heat effects and blasting damage.

A conservative interpretation of the numerical calculations concerning stress- and heat-influenced changes in fracture apertures for the considered case with the tunnel oriented parallel to major fracture sets, implies that the hydraulic conductivity of the circumscribing disturbed zone, which extends to about 1 diameter distance from the periphery, is increased by two orders of magnitude, i.e. to 10^{-8} m/s.

The lower picture in Fig.64 shows a schematic channel network corresponding to the average axial hydraulic conductivity of the respective zones. The assumption that the channel network forms an orthogonal pattern implies that the hydraulic conductivity is isotropic in the disturbed zones, which is conservative but in line with the logical assumption that variations in normal pressure can not alter the geometry of channels located at the crossing of fractures significantly.

Naturally, the model implies that if the average hydraulic conductivity of the virgin rock is lower, e.g. 10^{-11} m/s, the conductivity of the disturbed zone within 1 meter from the periphery will be 10^{-8} m/s, and that of the outer stress-disturbed zone 10^{-9} m/s. However, the most shallow part extending from 0.2-0.4 m from the periphery may still have a maximum conductivity of 10^{-6} m/s.

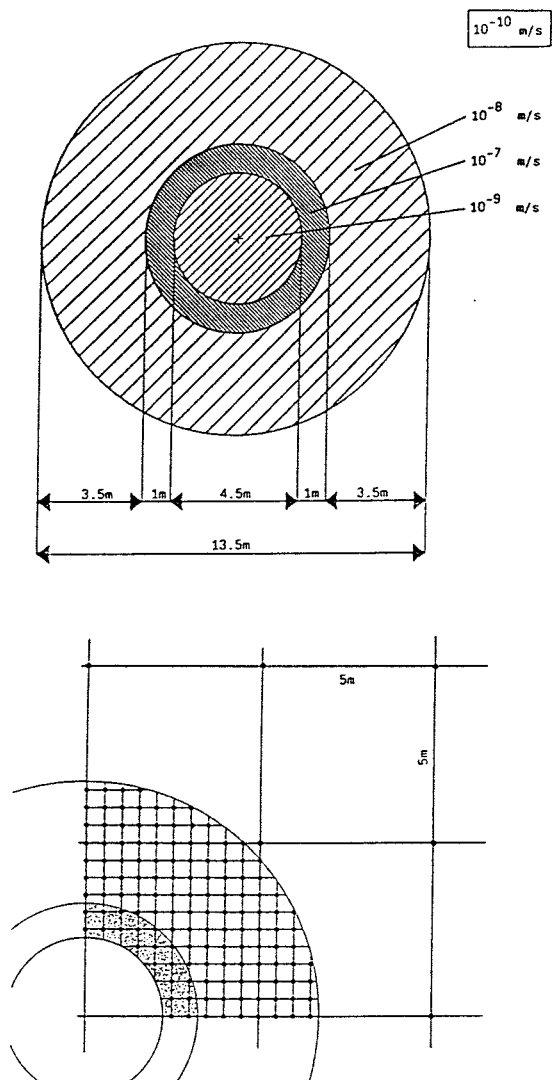


Fig.64 Cross section of KBS3 tunnel, "conservative" case. Upper: Generalized zonation with respect to the hydraulic conductivity. Lower: Crosses in the 4.5 m zone of disturbance representing channels at the points of intersecting, activated 5th order discontinuities. The most shallow zone of disturbance is not shown

Deposition holes

The uppermost 1 m length of the deposition holes is located in the blasting-disturbed rock zone with an average hydraulic conductivity of 10^{-7} m/s, except for the upper 0.2-0.4 m shallow zone to which an average hydraulic conductivity of $k=10^{-6}$ m/s is ascribed in the conservative case (Fig.65).

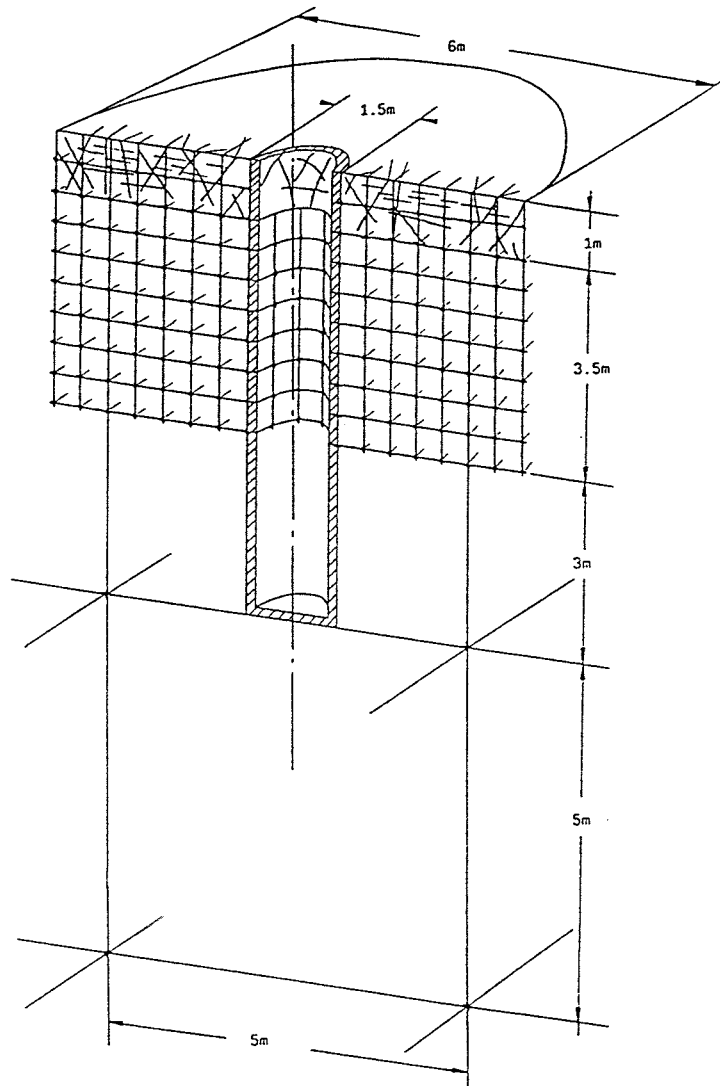


Fig.65 Deposition hole in the "conservative" case. The hole is surrounded by disturbed rock with $k=10^{-7}$ m/s to 1 m depth, the upper 0.2-0.4 m having $k=10^{-6}$ m/s. Down to 4.5 m under which the stress- and heat-affected rock has $k=10^{-8}$ m/s due to activated 5th order breaks. Lower down the rock has $k=10^{-10}$ m/s except for the shallow zone with $k=10^{-9}$ to 10^{-7} m/s (hatched)

From 1.0 to 3.5 m further down, the holes are located in rock affected by stress redistribution caused by the tunnel excavation and by heating and here the hydraulic conductivity is around 10^{-8} m/s for the considered case with an average hydraulic conductivity of the virgin rock of 10^{-10} m/s. In the lowest 3 m part of the holes the rock is practically undisturbed and maintains its original, virgin hydraulic conductivity, i.e. 10^{-10} m/s, except for a shallow zone caused by fragmentation at the drilling. If TBM drilling or raise-boring is applied for drilling the holes, the model implies that the disturbance in this zone will yield an average conductivity of 10^{-8} m/s within 10 cm from the periphery, and 10^{-7} m/s within the first 2-5 cm. If core-drilling and presumably also water-jet cutting is applied, the fragmentation is assumed to cause disturbance only within 2-5 cm depth where the conductivity is assumed to be around 10^{-9} m/s.

4.4.2.2 "Standard reference" case

A sort of standard, normally achievable case is assumed to be one where the tunnel axis deviates by more than 15° from the strike of one of the major, steeply oriented fracture sets. This case implies different properties of both the blasting-disturbed zone and the outer zone affected by stress redistribution and temperature. The first-mentioned one will not comprise a continuous zone of intense fissuring close to the periphery and it is therefore assumed that the average axial conductivity may not exceed 10^{-8} m/s within 1 m distance from the periphery irrespective of the conductivity of the virgin rock. The axial hydraulic conductivity of the outer zone that extends 1 tunnel diameter from the inner blast-affected zone, is estimated to be only one order of

magnitude higher than that of the undisturbed virgin rock, i.e. 10^{-9} m/s for the assumed value 10^{-10} m/s of the undisturbed rock. However, also in this case the roof zone may reach a very high conductivity depending on how effectively the rock is supported.

4.4.2.3 Water-flow paths, channeling

While the models of the nearfield rock is presented in the form of zonation with average hydraulic conductivities, it is possible to visualize in schematic form also the flow passages in the form of channels. Taking - for the sake of simplicity and lack of detailed information on the character of water-bearing fractures - the channels to be located at the crossing of intersecting fractures, Fig.65 offers a way of depicting the passages. Referring to the description of the VDH case, virgin granite rock with 1 channel per 25 m^2 square-shaped section yields a gross conductivity of around 10^{-11} m/s (p.39), while activation of "latent" 5th order fractures mobilizes 100 times more channels causing an average conductivity of 10^{-9} m/s. A conductivity of virgin rock of 10^{-10} m/s would correspond to somewhat wider channels or to a smaller spacing of the 4th order fractures. Hence, assuming a standard rock structure with 5 m spacing of these fractures, and assuming that stress- and heat-induced strain causes activation of 5th order fractures, the resulting average conductivity would be 100 times higher, or 10^{-8} m/s, i.e. the data given in Figs.64 and 65.

Naturally, the actual pattern of channels may be much more complex especially since the activation of initially non-associated discontinuities is strain-dependent and therefore not uniform in the stress-disturbed zones, and also because channels may be formed in other parts of the discontinuities than

where they intersect. This is believed to be the case when shearing associated with dilatancy of fractures takes place although it is logical to believe that the intersection of major fractures still represent the most important channels. One further point should be mentioned concerning the influence of shearing and that is the disintegration of fracture coatings, like chlorite. Thus, it is felt that even very small shear strain leads to such disintegration by which very fine-grained debris is produced, forming silty clay fillings that tend to clog fractures and undergo mineral alteration to smectitic forms by which self-sealing may become significant. Such debris is concluded to strongly reduce the possibility of grouting fine fractures.

4.4.2.4 Aspects on the applicability of the models

Real rock structure patterns

A matter of great significance is of course how close to real conditions that the simple orthogonal, "fractal"-type structure model adapts. It appears that the agreement is usually rather good although the structure often, like in the BMT case, has the character of 2 or even 3 superimposed structures. They may represent different generations formed under different regional stress conditions or tectonic events and their importance with respect to the contribution to hydraulic conductivity caused by rock excavation is controlled by their orientation and ease in getting activated, as well as by their interaction.

Choice of bulk hydraulic conductivity of virgin rock

The choice of the hydraulic conductivity 10^{-10} m/s of the virgin, undisturbed granite is not critical to the use of the models. Thus, assuming this figure to be 10^{-9} m/s, which is a commonly used value for rock located at 100-500 m depth, the "conservative" and "standard" cases would yield 10^{-7} m/s and 10^{-8} m/s, respectively, for the axial conductivity of the stress-disturbed zone, while the figure 10^{-11} m/s for undisturbed rock would yield the figures 10^{-9} and 10^{-10} m/s, which is more or less what one finds for the Stripa granite.

4.4.3 Interaction with large structures

A matter of practical importance is the natural undulation of the strike of the fracture sets discussed earlier. In summary, one finds that - for conditions like the ones in Stripa - a deviation of the main tunnel orientation from the (ideal) N/S direction by less than about 7° would mean that no part of a several hundred meter long tunnel will yield the "conservative" case, i.e. when the tunnel walls become parallel to the strike of one major steep fracture set. If the deviation is $\pm 15^{\circ}$ from the N/S direction about 35 % of the tunnel length will correspond to the "conservative" case, while the percentage drops to 15 to 20 when the deviation is in the range of $\pm 20 - 40^{\circ}$ from the N/S direction. Although this idealized model would make it theoretically possible to completely avoid the "conservative" case, it will probably still be met with over at least about one fourth of the total tunnel length in practice.

Interaction of the tunnels with 3rd order structures, which are taken to be fracture zones with 50 m spacing, 0.2 m thickness and a conductivity of 10^{-8} m/s, is inevitable whatever direction the tunnels are given, while it should be possible to avoid locating deposition holes in such structures. A favorable and probably achievable hydraulic situation is the one in which steeply oriented 3rd order structures intersect KBS3 tunnels at an angle of $20-45^{\circ}$, since it would give a large spacing of the intersections and, applying the "fractal-type" structure model, a possibility to avoid intersection with 2nd order structures, which have a spacing of 500 m in the simple basic model.

Interaction with flatlying 3rd order zones should be possible although the natural undulation may require that the tunnels are given a suitable slight dip. Hence, applying the dip undulation pattern used in the discussion of the VDH concept, one finds that it may be necessary to accept an inclination of 1:20 to keep a reasonable distance to nearby 3rd order zones. Again, it would be a simple matter to avoid structures of lower order.

5 THE VLH CONCEPT

5.1 *General*

The VLH concept has the form of several kilometers long TBM-drilled tunnels with 2.4 m diameter. They may be inclined upwards by a small angle and their orientation can be varied within reasonable limits. The depth may be in the range of 500 to 1000 m, i.e. intermediate to that of the VDH and KBS3 concepts. Rock stability may therefore be an important issue.

We will use here, for characterizing the rock, the same basic structure model as in the preceding discussions of the VDH and KBS3 concepts.

5.2 *Influence of excavation on the rock conductivity*

5.2.1 **Mechanical disturbances**

5.2.1.1 **General**

Full-face drilling intended for producing VLH:s is associated with less but different sorts of mechanical disturbance than in excavating a KBS3 repository. Influence of stress changes due to excavation is intermediate to that of VDH and KBS3. The temperature pulse, or rather the heating/cooling cycle, caused by the radioactive decay, will influence the fracture apertures to a significant extent in a way that is similar to that of the KBS3 deposition holes. In summary, effects on the near field rock are expected from four types of disturbances, namely:

- Disturbances caused by full face drilling of long tunnels (thrust and fragmentation)

- Disturbances caused by stress release that results from the excavation of the tunnel
- Disturbances caused by internal tunnel pressure, i.e. the swelling pressure of the clay barrier.
- Disturbances caused by the heat production of the fuel waste

5.2.1.2 Thrust

A thrust load of about one thousand tons transferred to the front of a 2.4 m diameter tunnel yields an elasto/plastic displacement of the front in the interval 0.1-1 mm. Most of this displacement is assumed to be due to elastic strain of the rock matrix but some of it is caused by permanent, plastic strain in the form of block movements associated with shear along preexisting 4th order fractures, activation of 5th order fractures and creation of new fractures. This latter effect can be assumed to appear in zones a-b indicated in Fig.66, where it contributes to the increased frequency of fine fractures (fissures) that is caused by the high stress concentrations induced at the "corners" of holes of any size in stress fields of high intensity. The extension of the zone affected by unloading at the drilling front is expected to be larger and the intensity of damage stronger in the 2.4 m diameter hole than in the 0.8 m VDH hole although the difference is probably not very significant.

Quantitative estimates of the extension of the zone adjacent to the wall of a full-face drilled tunnel where significant disturbance is expected to take place, have yielded the average figure 10 cm for diameters of about 1.5 m, while it may extend to 20 cm

for the planned 2.4 m diameter tunnels. Like in the VDH case, growth of 6th order discontinuities is assumed to take place in this zone, yielding a net hydraulic conductivity of about 10^{-8} m/s.

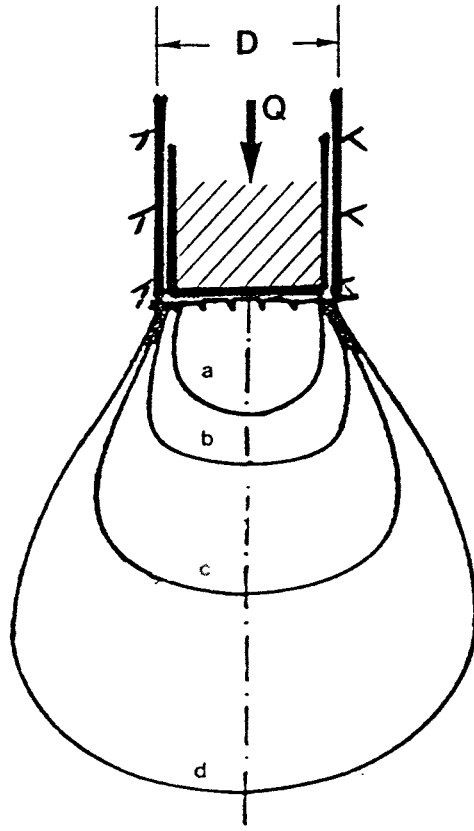


Fig.66 Influence zones of loading within which the generated normal and shear stresses may induce permanent structural changes. a) Strong, b) Moderate, c) Slight, d) Very minor

5.2.1.3 Fragmentation

In addition to the thrust-induced disturbance there will also be mechanical damage caused by the fragmentation process. As referred to in the discussion of

the VDH concept, previous studies of the influence of the size of buttons and of the detailed shear failure leading to successful fragmentation, have indicated that the rock will be rather richly fissured to a depth of 2 to 5 cm depth from the periphery (2). The estimated comprehensive mechanical softening in this shallow zone is expected to yield a hydraulic conductivity of 10^{-7} m/s.

5.2.2 Stress redistribution

5.2.2.1 General

The disturbances caused by stress release, by the swelling pressure of the clay barrier and by canister heat production are discussed below on the basis of results obtained from a series of numerical 2D and 3D simulations (8,9,10).

The numerical simulations presented in this section were performed with the two-dimensional distinct element code UDEC. The basic physical data and the basically orthogonal-type fracture pattern of the rock were the same as in the corresponding calculations of the KBS3 concept. This means that the assumed network of discontinuities was somewhat different for the KBS3 and VLH concepts than for the VDH concept, in the sense that the average fracture spacing was smaller (2-9 m) and that 3 fracture networks were superimposed in line with actual mapping of the BMT drift at Stripa. The same material models and physical data were applied in the KBS3 and VLH cases.

5.2.2.2 Calculations

Excavation of VLH:s by drilling was simulated in three runs for three different locations of the tunnel relative to an assumed fracture system (Fig.67). One of the cases was chosen for further simulations, i.e. pressurization of the tunnel interior and finally heat production in the tunnel. The calculations are described in Table 5.

Table 5 Cases considered

Excavation	Pressure	Heat production
run 1		
run 2	run 2p	run 2t
run 3		

The modeled region was a 100 m diameter circular section with the 2.4 m diameter VLH tunnel in the center. At distances larger than about 15 m from the tunnel, no discontinuities were modeled, (Fig.68). The intact rock material, i.e. the material between joints, was assumed to behave elastically and to be homogeneous and isotropic.

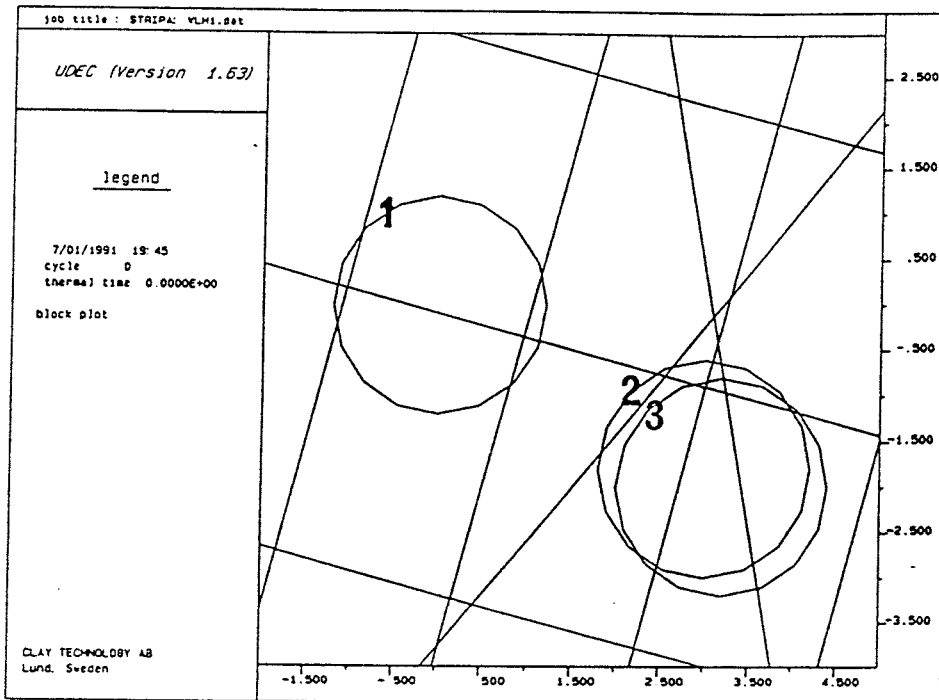


Fig.67 Location of VLH:s in runs 1,2 and 3, respectively

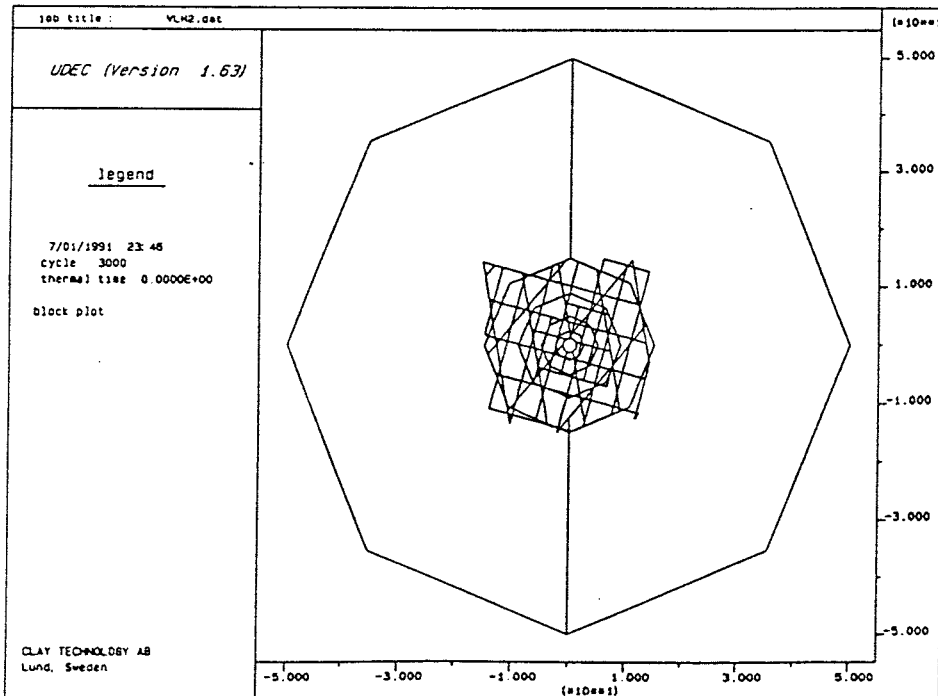


Fig.68 Model region. The octahedral structures and vertical line are artificial and with no influence on the mechanical properties of the model

In all runs except for 2t, a complex joint model, including a non-linear joint closure relation was assumed for all joints (cf. Figs.25 and 26), while a simpler joint model with a Mohr-Coulomb failure criterion and a linear joint closure relation was used for 2t.

While the farfield was modelled with boundary elements for the VDH and KBS3 cases, free-to-move constant stress boundaries were used throughout the calculations for the VLH case. Like in the KBS3 calculations the primary principal stresses were taken to be those recorded at the Stripa BMT drift, i.e. with a lower vertical stress than is normally expected:

- $\sigma_h = 15$ MPa
- $\sigma_v = 6$ MPa

Figs.69, 70 and 71 show joint shear displacements induced by excavation. The plots refer to the results from run 1, run 2 and run 3, respectively. Line thicknesses reflect the magnitudes of joint shear displacements. Shear displacements smaller than 50 μm are not shown. We see that the shear strain in run 1 is sufficiently small to preserve elastic behavior, while much inelastic strain is caused in run 3, run 2 being intermediate to runs 1 and 3. Considering compression and expansion of fractures one finds that run 1 yields only very local and negligible expansion, while runs 2 and 3 yield considerable expansion (Figs.72 and 73). Note that different line thickness scalings apply for joint closures and joint separations.

From figures 69, 70 and 71 it appears that the detailed joint structure around the tunnel, i.e. the location of the tunnel relative to the fracture system, is a determinant of the magnitudes of joint shear displacements and the extent of the region of inelastic behavior.

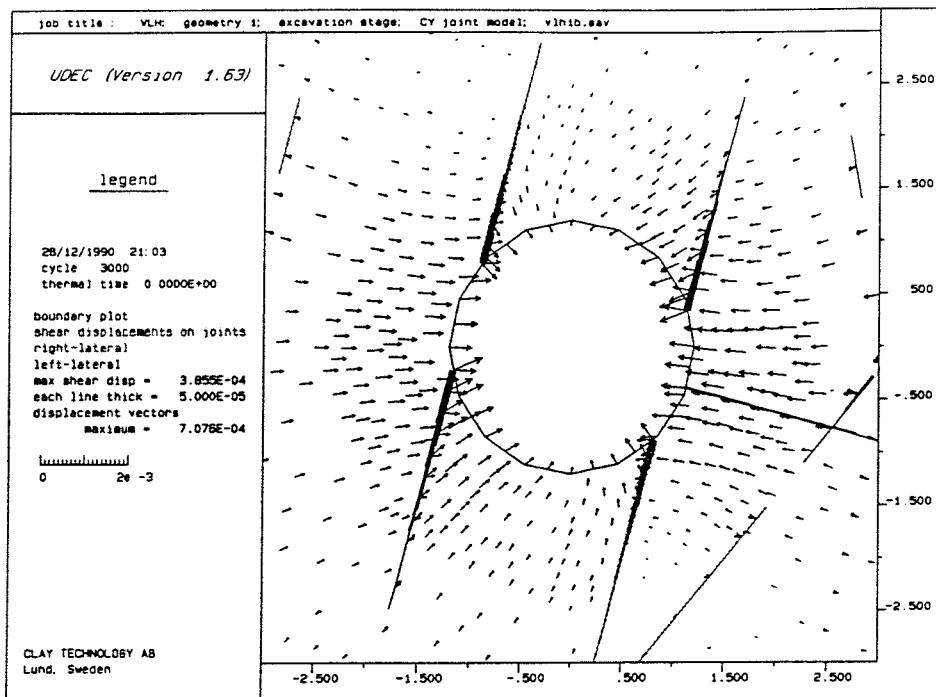


Fig.69 Displacement vectors and joint shear strain in run 1.
 Maximum shear strain about 700 μm

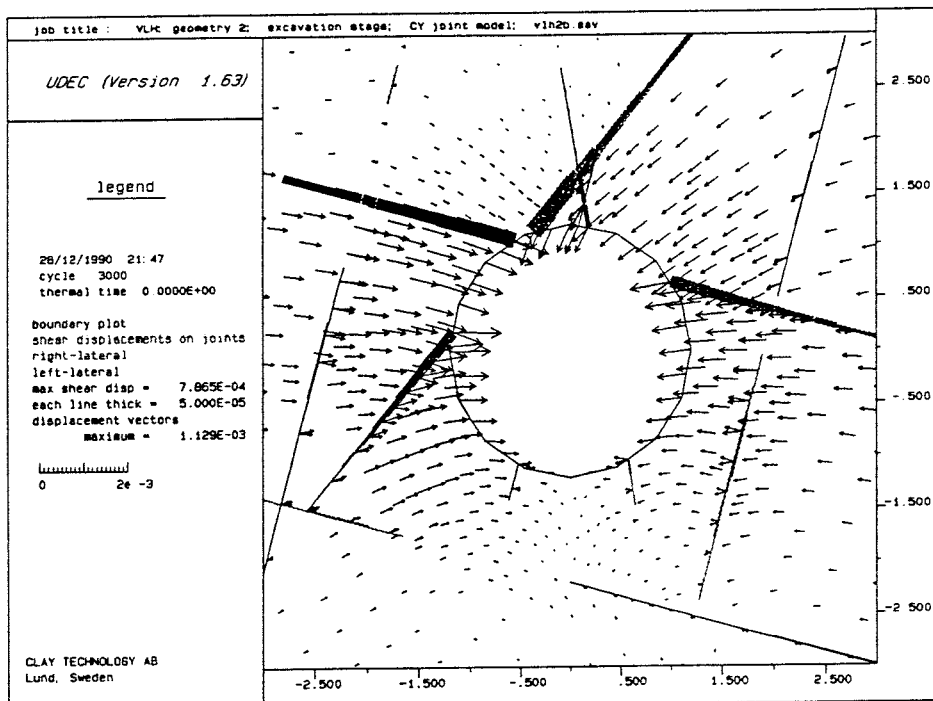


Fig.70 Displacement vectors and joint shear strain in run 2.
 Maximum shear strain about 1.1 mm

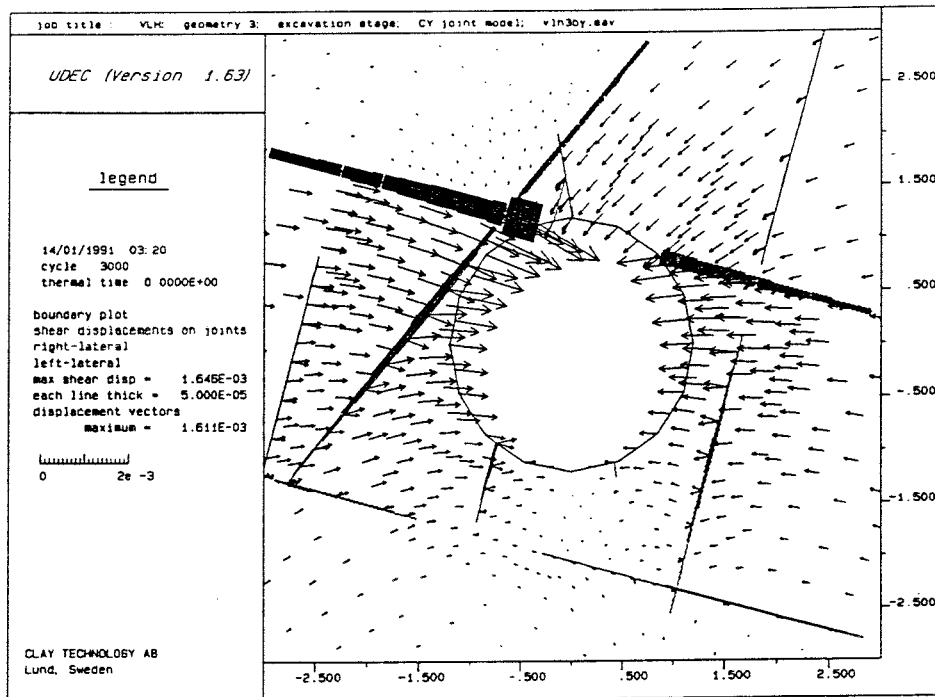


Fig.71 Displacement vectors and joint shear strain in run 3. Maximum shear strain about 1.6 mm

The distribution of rock displacements along the tunnel periphery is, for the nearly elastic case of run 1, more determined by the tunnel dimension and the in-situ stresses than by the detailed joint structure. The maximum inward displacement of the tunnel periphery was 0.71 mm, 1.13 mm and 1.61 mm for runs 1, 2 and 3, respectively.

In run 1 the mechanical aperture changes were very small and it appears that only for joints that intersect the tunnel surface at oblique angles and only for segments very close to the tunnel did the mechanical aperture increase by more than 5 μm . In runs 2 and 3 some joint segments at a distance of almost 2 m from the tunnel surface were expanded by 30-40 μm , while the largest expansion, around 500 μm , was obtained in run 3 and occurred at a distance of a little more than 1 dm from the tunnel surface. Due to the high normal stiffnesses for joints in compression,

joint closures are generally very small, i.e. a few microns at maximum.

The maximum tangential stresses were found to be 44, 51, and 52 MPa for runs 1, 2 and 3, respectively, which means that there would be no risk of spalling for the assumed primary stresses.

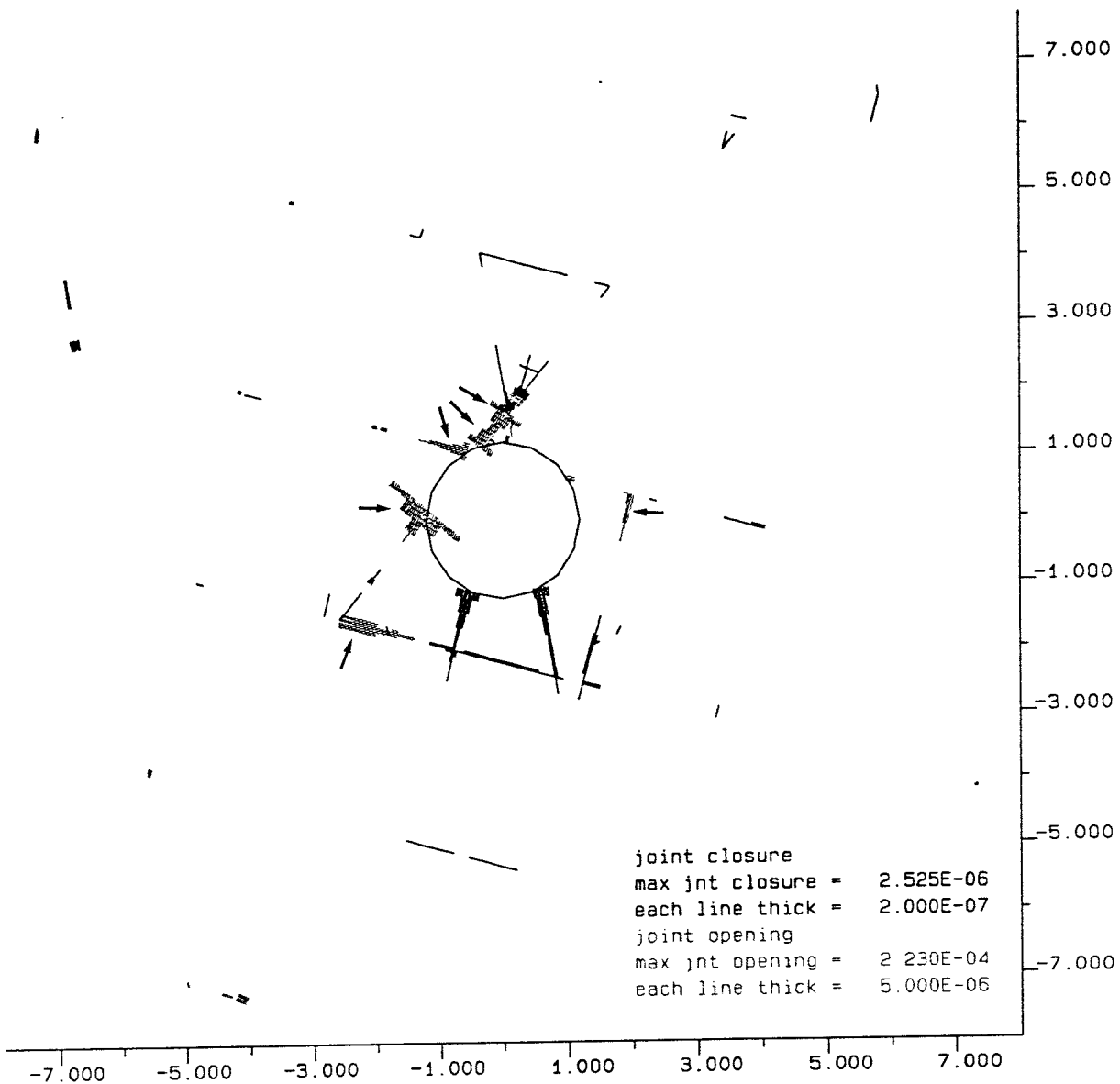


Fig.72 Joint closure and expansion in run 2. Arrows indicate joint separation

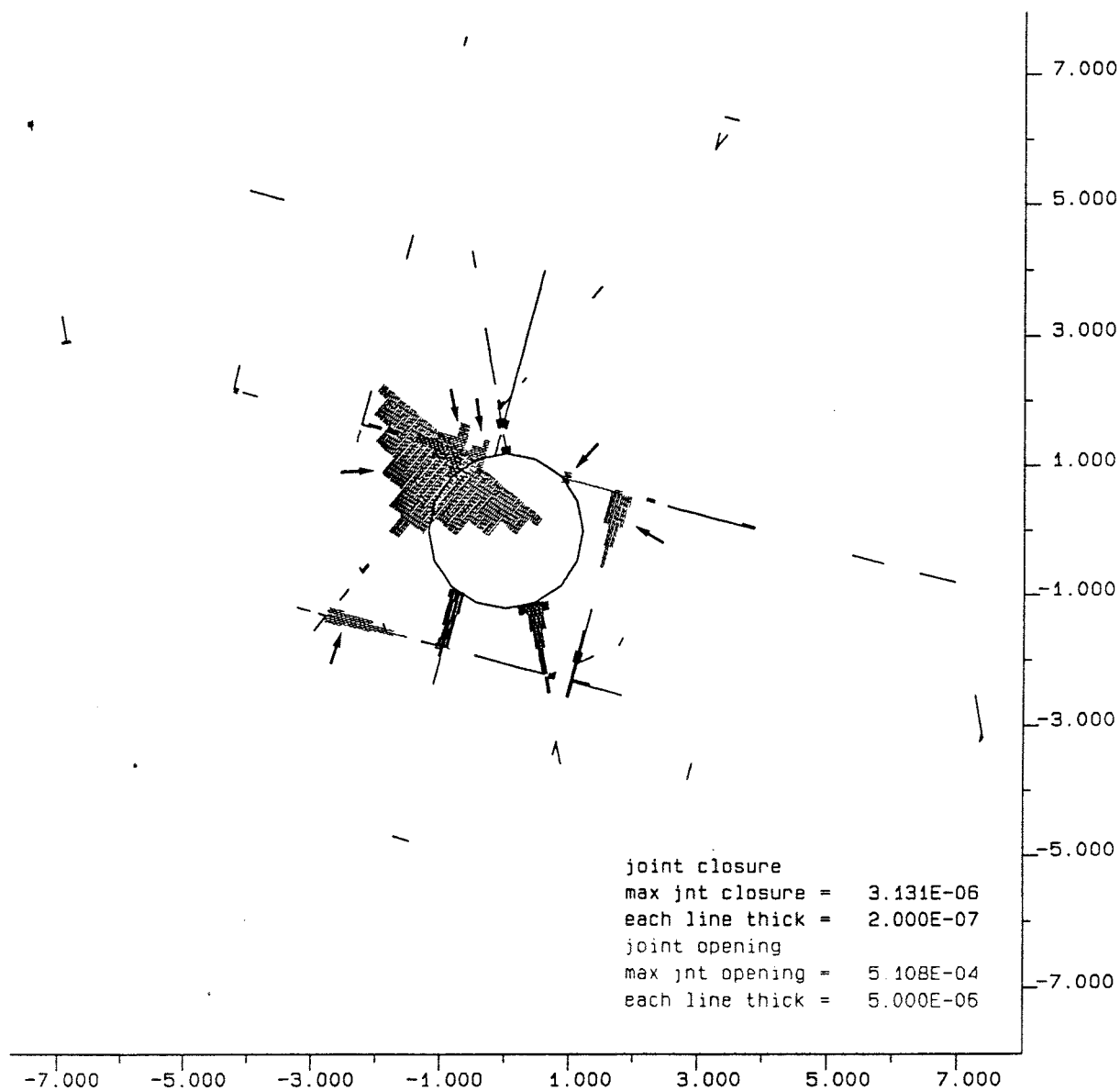


Fig.73 Joint closure and expansion in run 3. Arrows indicate joint separation

While unstable rock wedges in the roof or upper parts of the walls of KBS3 tunnels may certainly appear and require bolting, their contribution to the increase in axial conductivity is masked by the high conductivity of the disturbed zone by blasting. In VLH:s, on the other hand, there are reasons to consider the

wedges because of the close vicinity to the canisters. The general appearance of wedges of possible critical nature is indicated in Fig.74 and wedges are also seen at the crown of the VLH:s in Figs.70 and 71. The wedges in the latter two figures are stable although the fractures that form their boundaries are significantly widened and this is partly explained by the dilatancy on shearing. It is clear that without proper consideration of the rock structure, VLH:s can be unsuitably located by which the axial conductivity may become high.

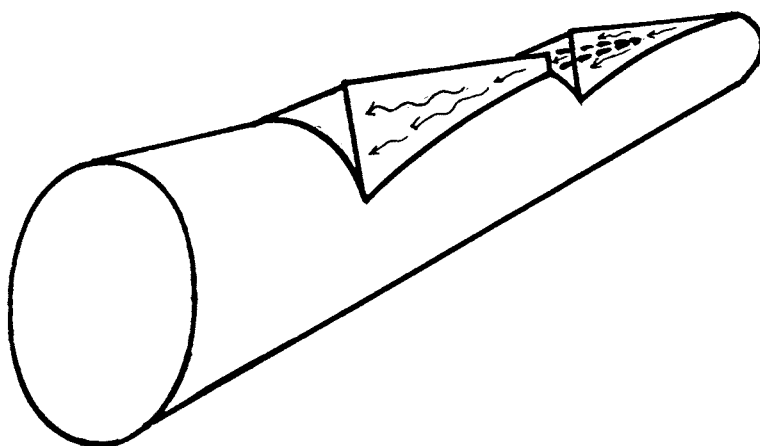


Fig.74 Series of interacting rock wedges by unsuitable location of VLH:s

5.2.3 Internal pressure

The influence of the pressure applied to the VLH periphery by the swelling compacted bentonite, was investigated in the aforementioned run 2p. The mechanical equilibrium stage arrived at in run 2 was used as starting point.

Rock displacements and joint shear displacements calculated in run 2, i.e. in the excavation stage, were reset at zero. This procedure does not affect the

calculations, but is convenient for presentation of results. In this case, for instance, only displacements induced by the pressurization will be displayed in plots. Stresses and mechanical apertures, however, were not reset.

A material model yielding constant pressure was assigned to the tunnel interior. The pressure was applied to the tunnel walls in 1 MPa increments with mechanical equilibrium calculations in between. The final pressure was set at 6 MPa and Fig.75 shows joint shear displacements induced by this pressure. It appears that 6 MPa pressurization has a rather small effect, the maximum joint shear displacement being only about 18% of the maximum value in the excavation stage. The apertures were hardly affected at all. The maximum tangential stress was reduced from 51 MPa to 42 MPa as a result of the 6 MPa pressure.

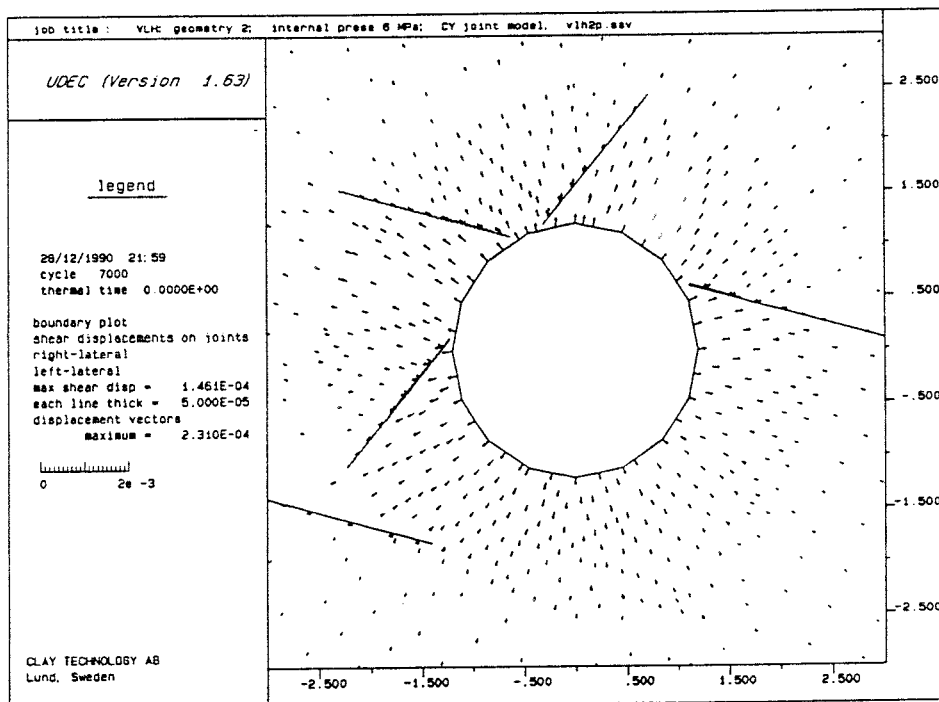


Fig.75 Displacement vectors and joint shear strain in run 2p. Maximum shear strain about 230 μm

5.2.4 Thermomechanical effects

The equilibrium state reached in run 2p, was used as starting point for the thermomechanical calculation in run 2t. Joint shear displacements and rock displacements were reset at zero. The mechanical material model used for the tunnel interior in run 2p was kept intact, i.e. the pressure on the tunnel walls was held constant at 6 MPa. The initial heat production was set at 573 W per m of tunnel length, which corresponds to the case of 24 BWR assemblies per canister and no distance between the canisters. The power was assumed to be uniformly distributed over the tunnel cross section area. The thermal properties used for rock and internal tunnel material are shown in Table 6.

Table 6 Thermal material properties of components

Parameter	Rock	Tunnel int.
Thermal exp. coeff., (K^{-1})	8.3×10^{-6}	0
Specific heat, (kJ/kg,K)	0.8	1.6
Heat conductivity, (W/m,K)	3.0	1.5

8 years of heat production were simulated since it corresponds approximately to the time after deposition when the temperature in the tunnel interior has reached its maximum value. Longer times, e.g. a complete thermal cycle, would require larger models and also that more attention be paid to the thermal and mechanical boundary conditions. Fig.76 shows the temperature field 8 years after deposition.

Operating the complex joint model used in the excavation and pressurization calculations also in the thermomechanical calculation would require a very close interlacing of thermal and mechanical calcu-

lations which was beyond the scope of this investigation. Thus, a simpler joint model with the properties listed below was used.

- Friction angle 25.6 degr
- Angle of dilation 2.0 degr
- Normal stiffness 1000 GPa/m
- Shear stiffness 10 GPa/m
- Cohesion 0
- Tensile strength 0

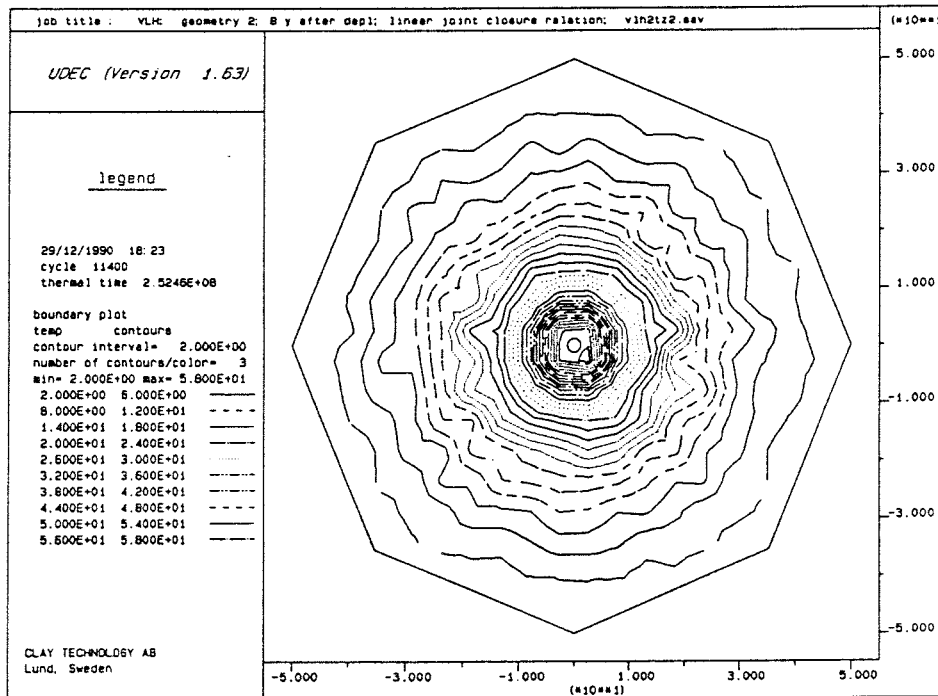


Fig.76 Temperature field after 8 years, the contour intervals being 2°C. The outermost isotherm represents 2°C, while the temperature at the hole periphery is 90°C. The temperature at the center of the tunnel is 115°C

Fig.77 shows the rock displacements and joint shear displacements induced by the temperature increase, while Fig.78 shows the mechanical apertures after 8 years.

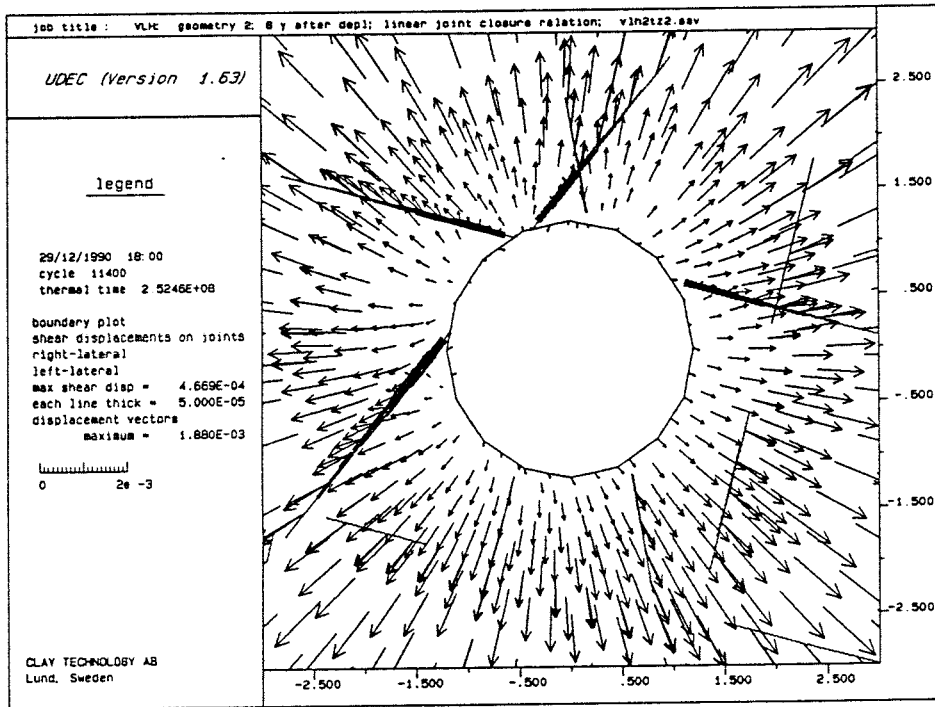


Fig.77 Displacement vectors and joint shear strain in run 2t. Maximum shear strain about 1.9 mm

The maximum tangential stress increased from 42 MPa to 102 MPa. This increase may be underestimated as a result of the use of free stress boundaries. The joint closures in Fig.78 are somewhat overestimated because of the linear joint closure relation.

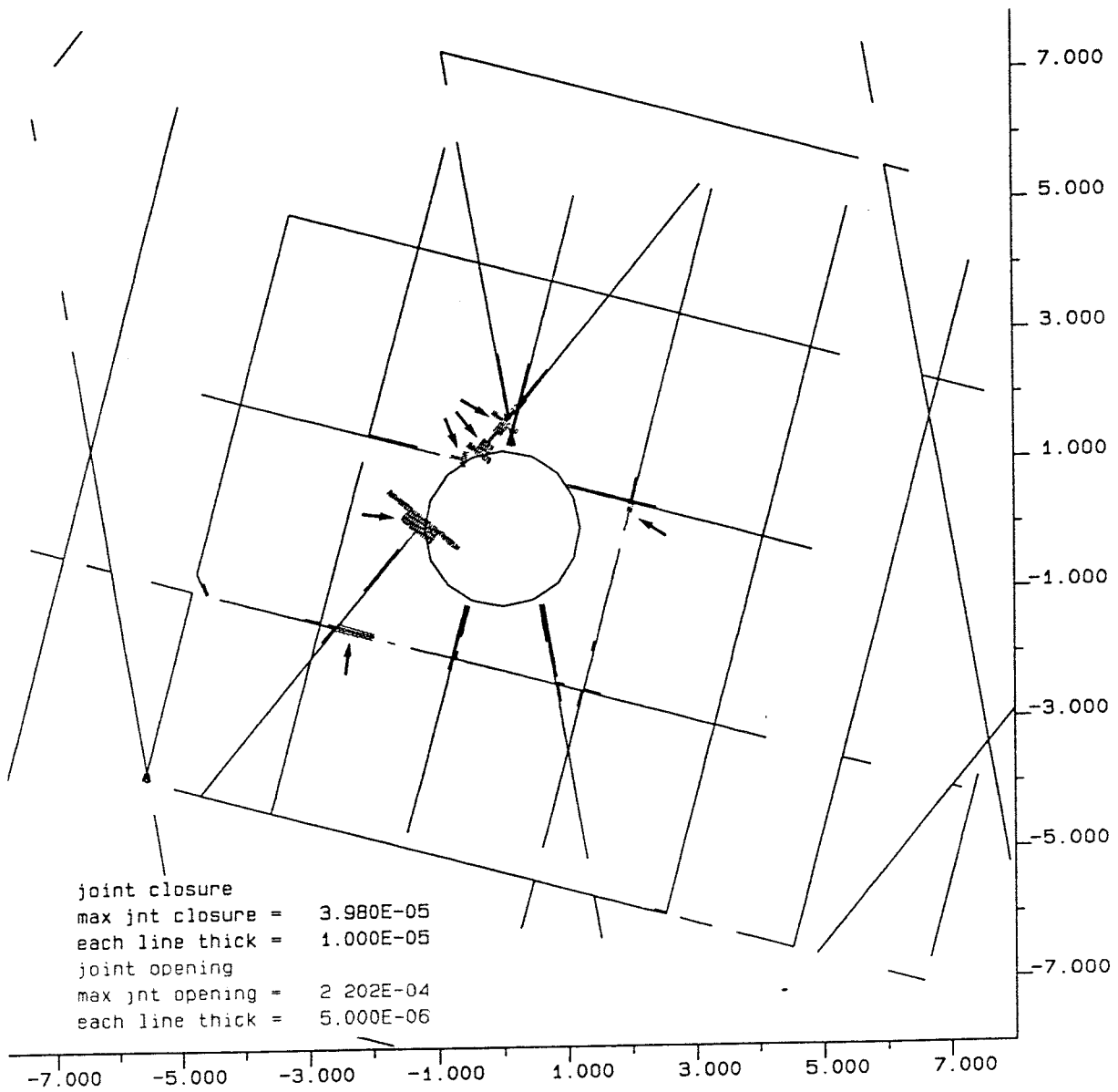


Fig.78 Joint closure and expansion in run 2t. Arrows indicate joint separation

5.2.5 Net effect of the influence of excavation, internal pressure and thermomechanics

The location of the excavation relative to the fracture system is of fundamental importance, as seen from the results of runs 1, 2 and 3. To make proper estimates of the impact of the excavation on the hydraulic conductivity parallel to the tunnel, a detailed investigation of the results with respect to the dependence of aperture changes on the distance to the tunnel would be necessary and can be made by use of the models developed in the present study. However, it would require additional work that is more suitably conducted for the Äspö rock conditions. The values shown in Table 7 are rough estimates of the factors of conductivity increase rather than results from calculations. The estimates are based on the assumption that all joints had 10 μm hydraulic aperture initially and that flow rates are determined by a cubic flow law.

Table 7 Estimates of conductivity increase (times)

Calculation	Distance from tunnel center, m		
	1.2-1.5	1.5-2.2	1.5 - 3.0
run 1	20	0.9	1.2
run 2	500	20	4.2
run 3	20000	30	6.2

Both the pressurization and the heat production calculations show rather small changes in mechanical apertures, probably resulting in a small reduction of the conductivity.

Since the two-dimensional models require that all joints be parallel or almost parallel to the model plane, the results regarding displacements will be overestimated if this condition is not met with, especially if the calculated inelastic displacements are considerable. In addition, the cubic flow law applies to idealized flow through planar slots. The results above should thus not be regarded as predictions but rather as illustrations of the relative importance of different conditions that determine the permeability of the near field rock.

5.3 *Structural model of VLH nearfield rock as influenced by disturbances*

5.3.1 **Basic pattern**

As pointed out earlier the basic rock structure used in the numerical calculations was somewhat different in the KBS3 and VLH cases than in the VDH case, for which the simple basic model was used, but the accordingly adjusted physical parameters of the rock is expected to compensate for this difference and hence to allow for comparison of the rock behavior of the three concepts.

The relatively large spacing of the 4th order discontinuities of the general model means that the frequency of critically oriented wedges will be rather low. Still, it is clear that one can identify cases in which sets of wedges located primarily in the roof may be displaced and cause both an increase in axial hydraulic conductivity and a risk of causing irregularities of the smooth contour of the periphery, which will require adjustment and filling with some suitable substance like special cement.

5.3.2 "Fine-rock structure"

Assuming the same gross hydraulic conductivity of the virgin rock as for the basic KBS3 case, i.e. 10^{-10} m/s, which is reasonable because of the relatively shallow depth in comparison with the VDH case, one finds that the integrated effect of the various disturbances that will alter the basic, virgin granite structure yields the conductivity zonation shown in Fig.78. The rock close to the periphery, i.e. to 0.2 m depth, is concluded to have an average axial and radial hydraulic conductivity of 10^{-8} m/s, except for the most shallow 2-5 cm which is expected to have an average conductivity of 10^{-7} m/s, while the adjacent, circumscribing stress-disturbed zone is taken to have its outer boundary 1.8 m, i.e. 75 % of the hole diameter, from the periphery, and to have an average hydraulic conductivity that is ten times higher than that of the virgin rock, i.e. 10^{-9} m/s.

Applying the simple basic rock structure one can visualize the water flow paths as in the KBS3 case figure by the channels, of which there are 1 per 25 m^2 in undisturbed, virgin granite. The very moderate strain induced in the rock except for the shallow mechanically damaged zone is expected to activate less 5th order fractures than in the KBS3 case, an estimate being that only every second member of these sets is mobilized to become hydraulically active. This would mean that 25 channels become active per 25 m^2 , which would correspond to a net average hydraulic conductivity of about 3×10^{-9} m/s, axially as well as radially. For an average hydraulic conductivity of the virgin rock of 10^{-11} m/s, the corresponding figure would be 3×10^{-10} m/s.

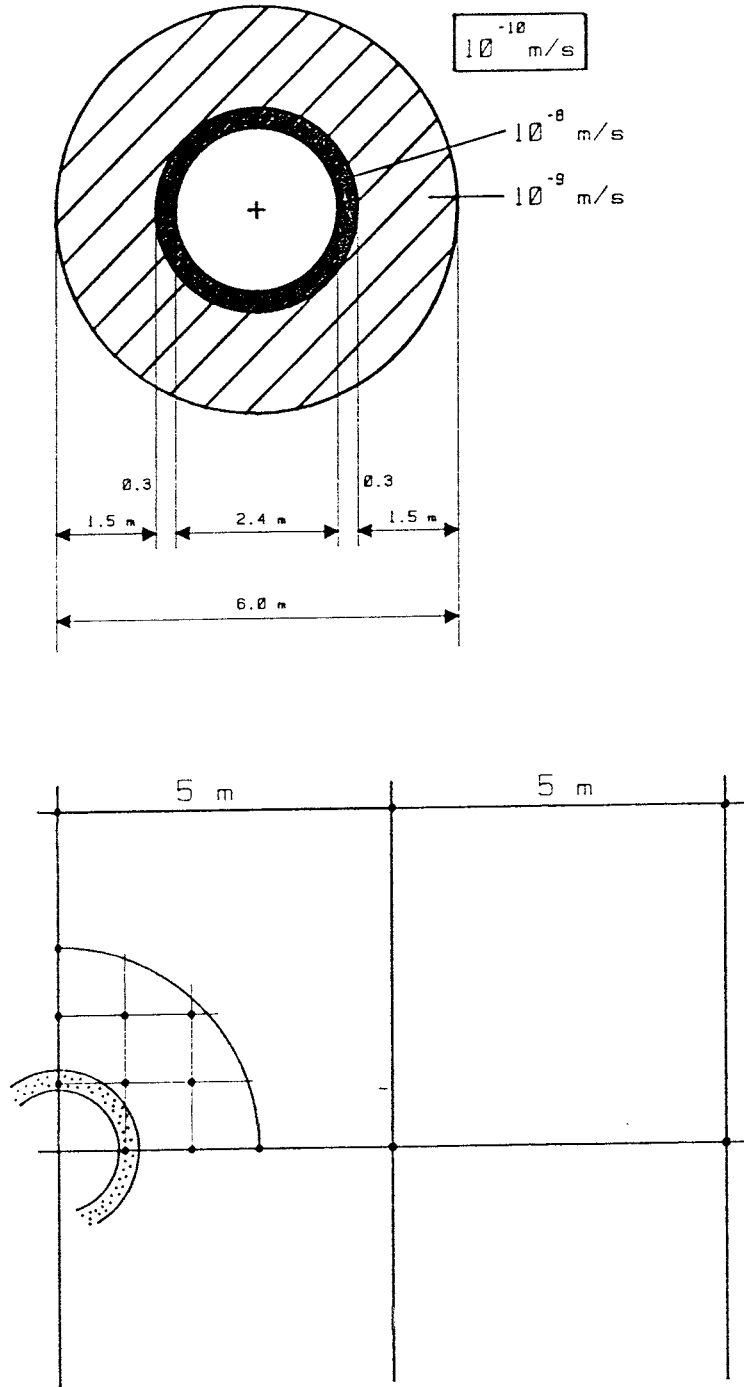


Fig.78 Cross section of VLH. Crosses in the 1.5 m zone of stress-induced disturbance represent channels at the points of intersection of every second 5th order fracture

The widening of 4th order discontinuities that affects the axial hydraulic conductivity, and the possibility of activation of 5th order discontinuities and formation of hydraulically interacting rock wedges are strongly dependent on the orientation of the VLH holes with respect to that of the major structural features. Referring to the discussion of the KBS3 concept, an angle of 0-15° would represent a "conservative" case while a larger angle would correspond to a "standard reference" case also for the VLH concept. The case described here is considered to represent the first-mentioned conditions, for which the angle between the hole and the strike of major fractures is less than or about 15°.

5.3.3 Interaction with large structures

Applying the large-scale variation in orientation of major structural features derived from the observations at Stripa, i.e. sinusoidal undulation with an "amplitude" of about 20 m and a "wavelength" of a few hundred meters, the smaller size of the VLH means that the probability of substantial increase in axial conductivity along more than 20 m intervals is very limited. Like in the KBS3 case it is reasonable to assume that straight VLH:s located in Stripa-type bedrock and oriented N/S will deviate from the strike of major discontinuities by less than 15° over about 25 % of the total length. Still, over the 5 km length of VLH:s, one would expect also higher order undulation patterns that may require some change in axial direction in order not to exceed this percentage. By selecting a suitable inclination it would be possible also to avoid more interference with flatlying structures than with steep ones. This matter needs further consideration, however.

In addition to large-scale effects that have to do with variation in orientation over longer distances, there is also the matter of intersection by low-order structures of very long extension. The interaction with low-order structures is inevitable in the VLH case. Thus, assuming even very favorable orientation of VLH:s, i.e. with 45° deviation of the axis from the strike of major structures, 3rd order zones will be intersected at a frequency of one per 75 m length, and 2nd order zones will be truncated at some 750 m intervals. Although 1st order structures may theoretically be avoided one should still consider intersection by a couple of steep 1st order structures. Interference with flatlying structures will also take place, particularly with 3rd order structures, while it should be possible to avoid practically all flatlying 1st order structures.

6 DISCUSSION

6.1 *Scope*

Major properties of the nearfield rock will be discussed in this chapter with the intention of defining the structure and conductivity, interference with low-order structures, and stability conditions. While this discussion has a bearing on the candidature of the three concepts, the primary aim is to define the nearfield properties for further use in an ongoing performance analysis. The common basis of evaluation of the effects of disturbances by excavation and heat treatment has been the generalized, "fractal"-type rock structure of virgin granite and it is felt that this simple model is sufficiently representative to be used for the present purpose, i.e. to make relative, general qualitative and quantitative estimates of the influence of disturbances on the hydraulic con-

ductivity. It is clear, however, that very significant improvement could be gained by refining the model which is presently used as a pedagogic tool rather than an accurate scientific instrument. Still, a relatively simple standard-type rock structure model is needed for comparative calculations.

6.2 *Summary of nearfield hydraulic properties*

A very important conclusion is that in all the concepts the most shallow parts of the rock in the deposition holes is significantly more pervious than the virgin rock, and this is very beneficial because it will certify uniform access to water of the buffer material and thereby uniform wetting.

Considering the effect of disturbance on the near-field rock by stress changes and heat, it is clear that the radius of influence from the periphery is at minimum for the lower half of the KBS3 holes, small (< 1m) for VDH:s, and largest (about 2 m) for the upper half of the KBS3 holes and for VLH:s. The impact on the axial hydraulic conductivity of the near-field zones is different, however. Thus, the strongest effect appears around the upper half of the KBS3 holes while it is negligible around their lower half. VDH:s and VLH:s give similar and less impact from which one concludes that *the axial flux is lowest for the lower part of the KBS3 holes, next lowest for VDH:s, followed in turn by VLH:s and the upper part of KBS3 holes.*

An important conclusion is that fractures that are oblique with respect to the orientation of the holes (and tunnels) may have a very significant effect on block movements and thereby on the axial conductivity. This is particularly important with respect to the long-extending 4th order breaks and "latent" 5th

order fractures, the connectivity of which is a determinant of the net effect over longer distances. The attempts to attack the problem of evaluating this effect by use of 3D numerical calculations are very promising but much more needs to be made in order to get a more complete view.

6.3 *Interference with low-order structures*

KBS3 is the only concept for which one can completely avoid interference between deposition holes and discontinuities of 1st, 2nd, and 3rd orders. KBS3 tunnels with a length of 400 m will, on the other hand, intersect 5-8 steeply oriented 3rd order structures, while they can possibly be located so that no 2nd order discontinuities become truncated.

The length of VLH:s imply that 1-2 steeply oriented 1st order structures, 5-10 2nd order zones, and 50-100 3rd order breaks will be intersected. Depending on the inclination of the VLH:s, 1-3 flatlying 2nd order and 5-30 3rd order structures will probably be intersected, while 1st order zones can probably be avoided.

The 2 km deep deployment part of VDH:s will intersect around 3-5 flatlying 2nd order zones, while no steeply oriented structures of this type should interfere, and it should be possible also to avoid 1st order zones. 1-2 steeply oriented and 30-50 flatlying 3rd order structures will be intersected.

A general conclusion is that the flexibility of the KBS3 concept, with suitably deepened deposition holes, offers the best possibility of locating the repository in the least permeable bedrock units available in a given area, while it is clear that it is

difficult to locate VDH:s in particularly suitable rock. The VLH concept is intermediate in this respect.

6.4 *Rock stability aspects*

The deposition holes of the KBS3 concept will be perfectly stable in the excavation and canister application phases. By applying careful blasting in the preparation of KBS3 tunnels no stabilization in the form of bolting or grouting will be required since structures of lower order than 3 are not expected to be passed. However, depending on the rock stress situation, some spalling and disintegration associated with widening of flatlying fractures in the roof may take place and a suitable shape of the roof should be found that minimizes these effects.

VLH:s will cause no stability problems except, possibly, for local minor rock fall generated by strong fissuring or clay weathering where 1st and 2nd order structures have to be passed. Local widening and replacement by concrete will be sufficient to support the rock, while grouting can be used to reduce the conductivity of zones with higher conductivity than about 10^{-8} m/s.

The drilling of VDH:s below 1500 m depth is expected to be associated with some rock fall if clay-based muds are used, which is advantageous for self-sealing of fractures. Break-outs may yield roughly elliptical shape of the borehole section with the long diameter being up to 100 % larger than the short one. The difficulty in obtaining good isolating ability of the clay buffer in the holes at significant deviation from circular borehole shape calls for use of drilling muds composed of fibrous components.

The present study of the constitution and hydraulic conductivity of the nearfield rock of the three repository concepts gives a simplified picture that needs to be refined for application in comparative performance analyses. In particular, rock mechanical analyses should be made in order to fully appreciate the influence of 3D effects. Such analyses should include parametric studies of the basic structural pattern. The following issues are recommended for continued investigation:

- * Creation of a number of reference fracture patterns including 3rd, 4th and 5th order breaks and with the type of geometrical arrangement suggested in this report. These patterns should then be employed for predicting the structural variations in the rock along drifts to be excavated in future

- * Establishment of criteria for assigning mechanical properties, e.g. shear strength parameters and joint closure relations, to 3rd, 4th and 5th order fractures

- * Formulation of local three-dimensional numerical models of KBS3 tunnels and deposition holes and of VLH sections using some carefully selected reference fracture patterns. Analyses of all repository processes using these models with the main objective to determine realistic ranges of apertures changes

- * Development of model for relating blasting to the physical state of the blast-disturbed zone, and application of this model for further investigation of the permeability of that zone and of its importance for the stress distribution in the surrounding rock. These relations should then be applied to 2D numerical models

- * Development of model for relating mechanical damage from TBM drilling to the physical state of the affected rock, and application of this model for further investigation of the permeability of that zone and of its importance for the stress distribution in the surrounding rock. These relations should then be applied in 2D numerical models

- * Development of physical model for quantitative evaluation of time-dependent displacements in the roof and upper parts of the walls of KBS3 tunnels and VLH:s by use of mathematical rock creep models (11)

- 1 Gale, J.E. & Witherspoon, P.A. An Approach to the Fracture Hydrology at Stripa: Preliminary Results. Proc. In Situ Heating Experiments in Geological Formations, OCDE/AEN, Ludvika 1978 (pp 161-175)
- 2 Pusch, R. Influence of Various Excavation Techniques on the Structure and Physical Properties of "Near-field" Rock Around Large Boreholes. SKB Technical Report 89-32, 1989
- 3 Börgesson, L., Pusch, R., Fredriksson, A., Hökmark, H., Karnland, O. & Sanden, T. Final Report of the Rock Sealing Project - Identification of Zones Disturbed by Blasting and Stress Release (Tests 2 & 3). Stripa Project, Technical Report 1991 (In press)
- 4 Stanfors, R. Undersökning av Sprängskador i Äspölaboratoriet. Proc. Rock Mechanics Meeting (BEFO) in Stockholm, March 1992. Swed. Rock Engineering Research Found., BEFO, Stockholm, 1992
- 5 Pusch, R., Karnland, O., Hökmark, H., Sanden, T. & Börgesson, L. Final Report of the Rock Sealing Project - Sealing Properties and Longevity of Smectitic Clay Grouts. Stripa Project, Technical Report 91-30, 1991
- 6 Barton, Nick and Vik, Gunnar. Stage I Joint Characterization and Stage II Prediction using Small Core Samples. Stripa project report IR 88-08, NGI, Norway, August 1988

- 7 Hökmark,H. Distinct Element Modeling of Fracture Behavior in Near Field Rock. Stripa Project, Technical Report 91-01, 1991
- 8 Hökmark,H. & Israelsson,J. Distinct Element Modelling of Joint Behavior in Nearfield Rock. Stripa Project, Technical Report 91-22, 1991
- 9 Hökmark,H. VLH - Nearfield Rock Behavior. Clay Technology, Internal Report, June 1991
- 10 Börgesson,L., Pusch,R., Fredriksson,A., Hökmark,H., Karnland,O. & Sanden,T. Final Report of the Rock Sealing Project - Sealing of the Near-field Rock Around Deposition Holes by Use of Bentonite Grouts. Stripa Project, Technical Report 91-34, 1991
- 11 Pusch,R. Mechanisms and Consequences of Creep in Crystalline Rock. Comprehensive Rock Engineering, Pergamon Press, Oxford, 1992

List of SKB reports

Annual Reports

1977-78

TR 121

KBS Technical Reports 1 – 120

Summaries

Stockholm, May 1979

1979

TR 79-28

The KBS Annual Report 1979

KBS Technical Reports 79-01 – 79-27

Summaries

Stockholm, March 1980

1980

TR 80-26

The KBS Annual Report 1980

KBS Technical Reports 80-01 – 80-25

Summaries

Stockholm, March 1981

1981

TR 81-17

The KBS Annual Report 1981

KBS Technical Reports 81-01 – 81-16

Summaries

Stockholm, April 1982

1982

TR 82-28

The KBS Annual Report 1982

KBS Technical Reports 82-01 – 82-27

Summaries

Stockholm, July 1983

1983

TR 83-77

The KBS Annual Report 1983

KBS Technical Reports 83-01 – 83-76

Summaries

Stockholm, June 1984

1984

TR 85-01

Annual Research and Development Report 1984

Including Summaries of Technical Reports Issued during 1984. (Technical Reports 84-01 – 84-19)

Stockholm, June 1985

1985

TR 85-20

Annual Research and Development Report 1985

Including Summaries of Technical Reports Issued during 1985. (Technical Reports 85-01 – 85-19)

Stockholm, May 1986

1986

TR 86-31

SKB Annual Report 1986

Including Summaries of Technical Reports Issued during 1986

Stockholm, May 1987

1987

TR 87-33

SKB Annual Report 1987

Including Summaries of Technical Reports Issued during 1987

Stockholm, May 1988

1988

TR 88-32

SKB Annual Report 1988

Including Summaries of Technical Reports Issued during 1988

Stockholm, May 1989

1989

TR 89-40

SKB Annual Report 1989

Including Summaries of Technical Reports Issued during 1989

Stockholm, May 1990

1990

TR 90-46

SKB Annual Report 1990

Including Summaries of Technical Reports Issued during 1990

Stockholm, May 1991

1991

TR 91-64

SKB Annual Report 1991

Including Summaries of Technical Reports Issued during 1991

Stockholm, April 1992

Technical Reports

List of SKB Technical Reports 1992

TR 92-01

GEOTAB. Overview

Ebbe Eriksson¹, Bertil Johansson², Margareta Gerlach³, Stefan Magnusson², Ann-Chatrin Nilsson⁴, Stefan Sehlstedt³, Tomas Stark¹

¹SGAB, ²ERGODATA AB, ³MRM Konsult AB

⁴KTH

January 1992

TR 92-02

Sternö study site. Scope of activities and main results

Kaj Ahlbom¹, Jan-Erik Andersson², Rune Nordqvist²,
Christer Ljunggren³, Sven Tirén², Clifford Voss⁴

¹Conterra AB, ²Geosigma AB, ³Renco AB,

⁴U.S. Geological Survey

January 1992

TR 92-03

Numerical groundwater flow calculations at the Finnsjön study site – extended regional area

Björn Lindbom, Anders Boghammar

Kemakta Consultants Co, Stockholm

March 1992

TR 92-04

Low temperature creep of copper intended for nuclear waste containers

P J Henderson, J-O Österberg, B Ivarsson

Swedish Institute for Metals Research, Stockholm

March 1992

TR 92-05

Boyancy flow in fractured rock with a salt gradient in the groundwater – An initial study

Johan Claesson

Department of Building Physics, Lund University,
Sweden

February 1992